

The role of canonical and non-canonical regulators of heterotrimeric G protein signaling during *Drosophila melanogaster* morphogenesis

Kimberly A Peters

A dissertation submitted to the faculty of the University of North Carolina at Chapel Hill in partial fulfillment of the requirements for the degree of Doctor of Philosophy in the Department of Biology.

Chapel Hill
2012

Approved by:

Dr. Stephen Rogers

Dr. Kerry Bloom

Dr. Bob Goldstein

Dr. Mark Peifer

Dr. Kevin Slep

Abstract

KIMBERLY ANN PETERS: The role of canonical and non-canonical regulators of heterotrimeric G protein signaling during *Drosophila melanogaster* morphogenesis
(Under the direction of Dr. Stephen Rogers)

Morphogenesis of multicellular organisms requires precise regulation of cell movements and cell shape changes. The first morphogenetic movement to occur in *Drosophila melanogaster* embryogenesis is ventral furrow formation during gastrulation; wherein a subset of presumptive mesodermal cells undergoes cytoskeletal rearrangements to invaginate into the embryo. This process is regulated by a secreted ligand, Folded gastrulation (Fog), that binds a G-protein-coupled receptor (GPCR), which activates Concertina (Cta), a Gα12/13 protein, and triggers a signaling cascade resulting in contraction of the apical actomyosin network to drive cell shape changes leading to internalization of the ventral furrow.

We used an RNAi screen in *Drosophila* tissue culture cells targeting all known and putative GPCRs to identify a receptor required for Fog signaling which we named Mist (Mesoderm Invagination Signal Transducer). We determined that Mist is an essential component of the Fog signaling pathway, and is sufficient to mediate Fog susceptibility in otherwise Fog unresponsive cells. I further identified specific domains within the receptor involved in signal transduction. *Mist* loss-of-function in the *Drosophila melanogaster* embryo revealed a role for Mist in gastrulation, and exhibited defects similar to *Fog* mutants. Ultimately our examination of Mist function within cellular morphogenesis has defined a role

for Mist from its transcriptional regulation, to its function within developmental processes.

I also investigated the role for Ric-8, a conserved cytoplasmic protein, in Cta function. In *Drosophila* tissue culture I used RNAi to show that Ric-8 is necessary for Cta-induced cellular constriction triggered by ectopic Fog application. Biochemical analyses and molecular mis-targeting demonstrated that Ric-8 directly binds to- and localizes Cta, with a much higher affinity for constitutively inactive Cta. Further, I found that Ric-8 modulation directly impacts productive Fog signaling. Finally, by mutagenizing amino acids conserved across species I identified specific residues within Ric-8 required for Cta function and/or establishing a binding interface between the two molecules. These two projects converge to further our understanding of the regulation of G α signaling during gastrulation events by two distinct mechanisms, canonical GPCR activation via Mist signaling and non-canonical modulation of Cta, by the highly conserved cytosolic protein Ric-8.

To Dorothy Mullan, a former educator and ardent supporter of higher education. Your constant, unwavering love and support during my graduate school career was invaluable. I wish you could have been here to see it fulfilled.

Acknowledgements

My advisor Dr. Stephen L Rogers who not only shaped how I think and conduct myself within the lab, but also made it a place I enjoyed being.

My committee members: Dr. Kerry S Bloom, Dr. Bob Goldstein, Dr. Mark Peifer, Dr. Kevin C Slep for making me a better, more well-rounded scientist.

The Rogers, Peifer, Slep, Goldstein, Crews and Siderovski Labs for the collaborations and fun we shared throughout the years. Especially, Paul Giresi, Alyssa Manning, and Dustin Bosch.

Greg Rogers and Tony Perdue for teaching me how to utilize the tools at hand, making it possible to intelligently carry out experiments and interpret data.

The many friends I made at UNC-Chapel Hill that made graduate school so much more fun.

My family for their massive amounts of love and support throughout this process: My mom and dad, Carol and Gregg Peters; My grandmothers, Dorothy Mullan and Agnes Peters; My sister and her husband, Bethanny and Matt Araujo.

My husband, Dan Marston, the most intelligent, patient, and wonderful person I know. There is no way I could have done this without you (and special thanks for reading all one thousand versions of my dissertation).

Thank you all.

Table of Contents

List of Tables	x
List of Figures	xi
List of Abbreviations and Symbols	xiii
Chapter	
I. Introduction	1
The Fog signaling pathway regulates early gastrulation movements in the <i>Drosophila melanogaster</i> embryo.....	1
Canonical activation of G α proteins is driven by G protein coupled receptors.....	3
Ric-8 regulates G α protein signaling during development.....	5
Dissertation Goals.....	8
References	11
II. Establishing the <i>Drosophila</i> tissue culture cell line, S2R+, as a model for studying Fog pathway signaling	17
Preface	17
Introduction	17
Experimental Design	19
Maintenance, transfection and RNAi of S2R+ cells.....	19
Construction of the Fog expression vector and production of ectopic Fog	20
Recapitulation of Fog Signaling events in S2R+ cells.....	22
Materials and Methods	23
Reagents	23
Equipment	23

Equipment Set-up.....	24
Procedures	25
Creating and storing a stable S2 cell line	25
Transient transfection of S2R+ cells.....	26
Harvesting secreted Fog from S2 media	27
Testing the efficacy of concentrated Fog.....	28
Anticipated Results.....	28
References	30
III. Regulation of morphogenesis by intersecting expression patterns of <i>Drosophila</i> Fog and its receptor, Mist.....	36
Preface	36
Abstract.....	36
Introduction	37
Materials and Methods	38
Cell Culture and RNAi.....	38
Production of recombinant Fog protein	40
Immunofluorescence microscopy	40
<i>In Situ</i> Hybridization.....	42
Embryo Injection.....	43
Fly Stocks.....	43
Results	44
Mist acts as a receptor for Folded gastrulation	44
Mist regulates Fog dependent epithelial folding in the imaginal wing disc epithelium	46

	Mist is transcriptionally regulated by Snail in the ventral furrow	47
	Mist regulates ventral furrow formation in the developing <i>Drosophila</i> embryo	48
	Discussion.....	49
	Acknowledgments	50
	References	51
IV.	<i>Drosophila</i> Ric8 interacts with the Gα12/13 subunit, Concertina, during activation of the Folded gastrulation pathway.....	66
	Preface	66
	Abstract.....	66
	Introduction	67
	Materials and Methods	71
	Tissue Culture, Transfection, and RNAi.....	71
	Contractility Assay.....	72
	Molecular Biology	73
	Immunoprecipitation and Immunoblotting	74
	Microscopy.....	74
	Results	75
	Reconstitution of Fog-stimulated cellular contractility in a cultured cell model.....	75
	Ric-8 is necessary for Fog pathway activation in <i>Drosophila</i> S2R+ cells	77
	Ric-8 directly binds Cta and exhibits higher affinity for the inactive form of Cta.....	79
	Ric-8 acts to selectively localize nucleotide-free Cta within the cell	80
	Ric-8 binds to Cta through an interface of conserved residues.....	81
	Discussion.....	84

Acknowledgements	88
References	90
V. Discussion and Future Directions	115
Summary of presented work.....	115
Discussion and Future Directions.....	118
Chapter III	118
Chapter IV	120
Conclusions	125
References	127

List of Tables

Table 3.1 List of genes targeted with dsRNAs in cell culture screen	65
Table 4.1 Summary of data collected from Ric-8/Cta _{GA} binding and contractile assays.....	114

List of Figures

Figure 1.1 Ventral furrow formation in the developing <i>Drosophila</i> embryo.....	15
Figure 1.2 Activation of the Fog signaling pathway drives cytoskeletal changes within the cell.....	16
Figure 2.1 Overexpression of downstream components of the Fog signaling pathway drive cellular constriction in S2 cells.....	32
Figure 2.2 S2R+ cells treated with ectopic Fog ligand respond by reorganizing their cytoskeleton.....	33
Figure 2.3 S2R+ cells treated with dsRNA targeting Rho do not respond to ectopic Fog application, unlike control dsRNA treated cells.....	34
Figure 2.4 Optimization of ectopic Fog collection and application	35
Figure 3.1 Mist acts as a Fog receptor.....	54
Figure 3.2 Proper Mist and Fog expression is required for wing imaginal disc morphogenesis.....	56
Figure 3.3 <i>mist</i> expression is upregulated in the ventral furrow downstream of Snail	58
Figure 3.4 Mist depletion causes defects during VF invagination.....	60
Figure S3.1 Mist is expressed in S2R+, but not S2 cells.....	62
Figure S3.2 Mist is temporally and spatially localized during VF formation	63
Figure S3.3 <i>mist</i> is expressed in embryos depleted of <i>twist</i>	64
Figure 4.1 Recapitulation of Fog signaling in S2R+ cells.....	95
Figure 4.2 Ric-8 regulates the function of Cta within the Fog signaling pathway.....	97
Figure 4.3 Ric-8 and Cta physically interact, and Ric-8 preferentially binds the constitutively inactive Cta _{GA}	99
Figure 4.4 Ectopic localization of Ric-8 drives mis-localization of constitutively inactive Cta, and attenuates the efficacy of Fog signaling.....	101
Figure 4.5 Evolutionarily conserved electrostatic residues are required for binding between Ric-8 and Cta _{GA}	103
Figure 4.6 Individual residues derived from Ric-8 cluster mutants	

comprise key interaction sites for Cta binding and function	105
Figure S4.1 Ric-8 is depleted by dsRNAs directed against the 5'/3' UTR of the gene	107
Figure S4.2 Myc-tagged Cta functions as a proxy for wild-type and constitutively inactive Cta	108
Figure S4.3 Sequence alignment of Ric-8 across taxa reveals evolutionarily conserved residues	110
Figure S4.4 Location of individual point mutants comprising mutant clusters that strongly inhibit Cta _{GA} binding are mapped onto a structural model of Ric-8	111
Figure S4.5 Wild-type and constitutively active Cta exhibit differential binding to Ric-8 cluster mutants as compared to inactive Cta.....	112

List of Abbreviations and Symbols

Abl: Abelson kinase

Arr: Arrestin

C. elegans: *Caenorhabditis elegans*

ConA: Concanavalin A

Cta: Concertina

Ctp: Cut-up

Drosophila: *Drosophila melanogaster*

E. coli: *Escherichia coli*

Fog: Folded gastrulation

G α : G alpha

G β : G beta

G γ : G gamma

GAP: GTPase activating protein

GDP: Guanosine diphosphate

GEF: Guanine nucleotide exchange factor

GDI: Guanine nucleotide dissociation inhibitor

GPCR: G protein coupled receptor

GPR: G protein regulator

GPRK/GRK: G protein-coupled receptor kinase

GTP: Guanosine triphosphate

IP: Immunoprecipitation

Mist: Mesoderm invagination signal transducer

Mud: Mushroom body defects

MWCO: Molecular weight cut-off

Numa: Nuclear mitotic apparatus

OE: overexpression/overexpressing

P-RLC: Phosphorylated regulatory light chain

PMG: Posterior midgut

Pins: Partner of Inscuteable

PDZ: Post synaptic density protein (PSD95), *Drosophila* disc large tumor suppressor (Dlg1), and zonula occludens-1 protein (Zo-1)

RLC: Regulatory light chain

RGS: Regulator of G protein signaling

Rok: Rho kinase

S2R+: S2 Receptors +

SDS-PAGE: Sodium dodecyl sulfate polyacrylamide gel electrophoresis

SOP: Sensory organ precursor cell

VF: Ventral furrow

Wg: Wingless

Chapter I

Introduction

The rearrangement of tissues during development is a fundamentally important process for embryonic viability. One such mechanism of cellular repositioning occurs via apical constriction: wherein a defined set of cells constricts their apical membranes, driving internalization of the cells from an external sheet to an internal tube. Many organisms utilize apical constriction to move and rearrange cells during morphogenetic movements.

Caenorhabditis elegans (*C. elegans*) utilizes apical constriction to internalize endoderm;

Drosophila melanogaster uses apical constriction to internalize mesoderm and endoderm as well as to form various structures, such as the trachea and salivary glands¹; in mammals apical constriction is used during neurulation to drive the invagination of the neural tube².

These examples of morphological events involving apical constriction in varying organisms highlight the ubiquitous nature of this mechanical shape change to drive cellular rearrangement. Interestingly, many of the previously described cellular movements employ similar signaling components.

The Fog signaling pathway regulates early gastrulation movements in the *Drosophila melanogaster* embryo

During the developmental process of gastrulation cells receive instructive inputs to determine their cell fate, and then rearrange to the appropriate positions in the embryo to

establish distinctive germ layers. The first morphogenetic movements that occur in *Drosophila* begin immediately after cellularization with the formation of the ventral furrow. A subset of presumptive mesodermal cells on the ventral side of the embryo constricts their apices to invaginate, as a tube, into the interior of the embryo³ (Figure 1.1).

These cells express the transcription factors Twist and Snail, which confer mesodermal identity⁴. Twist and Snail are essential for mesoderm invagination, as they regulate the transcription of gene products that provide signaling and structural components important for coordinated constriction^{5,6}. Twist drives transcription of the secreted protein Fog in the ventral furrow⁷. Fog is an apically secreted protein^{7,8}, that binds to a putative G-protein coupled receptor (GPCR), to activate the G α 12/13 family member, Concertina (Cta)^{9,10}. Cta activates the guanine nucleotide exchange factor RhoGEF2^{11,12}, which will stimulate the release of GDP from the small GTPase Rho, allowing Rho to bind GTP and be activated. The Rho effector, Rho Kinase (Rok), subsequently phosphorylates and activates non-muscle myosin II, while inhibiting myosin II phosphatase activity, allowing myosin II to bind F-actin and drive apical constriction in the ventral furrow⁸ (Figure 1.2).

The invagination of the ventral furrow is tightly regulated both spatially and temporally. In *Drosophila* embryos mutant for *Fog* or *Cta*, coordinated apical constriction is disrupted leading to a disorganization of cell shape changes and a delay in ventral furrow formation^{7,10}. In embryos mutant for RhoGEF2 or Rok, unlike *Fog* or *Cta* mutants, the cells that make up the ventral furrow lose their basal myosin, but never accumulate apical myosin, and therefore are unable to complete ventral furrow formation, leaving the mesodermal precursors on the outside of the embryo⁸. The effect of *Fog* or *Cta* mutations are much weaker than the mutant phenotypes of RhoGEF2 or Rok in the ventral furrow, indicating

there are additional inputs in the Fog signaling pathway that are important for coordinated constriction. One of these additional inputs is the non-receptor tyrosine kinase, Abelson kinase (Abl), which has been shown to be important for organizing the actin cytoskeleton at the apical domains of ventral furrow cells; Abl mutants exhibit uncoordinated cell constriction and delayed ventral furrow formation¹³. A transmembrane protein, T48, was also found to be involved in successful apical constriction during ventral furrow formation. This protein contains an -ITTEL sequence that binds the PDZ domain of RhoGEF2 to anchor RhoGEF2 at the membrane upon pathway activation. In *Cta* or *T48* mutants RhoGEF2 is still localized weakly at the apical membrane of cells in the ventral furrow. However, when *Cta* and T48 gene expression is depleted in tandem, RhoGEF2 expression is completely abolished in ventral furrow cells⁵. Despite the significant breadth of information describing this pathway, questions still remain. The most obvious of which, being the identity of the receptor that transduces the Fog signal. As the $G\alpha_{12/13}$, *Cta*, has been found to act genetically downstream of Fog⁹ it is likely that the unidentified receptor is a member of the G-protein coupled receptor (GPCR) family of proteins.

Canonical activation of $G\alpha$ proteins is driven by G protein coupled receptors

GPCRs are a diverse class of receptors, comprising one of the largest groups of encoded genes in the human genome and a frequent drug target studied in pharmacological sciences¹⁴. GPCRs relay external signals received by the cell to produce tightly regulated intracellular activation of signaling cascades. GPCRs are composed of 7- α helical domains spanning the membrane, with an extracellular N-terminus and an intracellular C-terminus. Agonist binding to the extracellular domain of GPCRs cause a conformational change in the

cytoplasmic domains of the receptor. This conformational change allows the GPCR to activate its associated $G\alpha$ subunit by facilitating its release of GDP for GTP¹⁵. GPCR signaling is compounded by the fact that GPCRs are capable of binding several ligands and G proteins, and G proteins in turn are able to interact with numerous receptors and intracellular effectors, allowing for highly complicated signaling networks¹⁶.

$G\alpha$ proteins form a heterotrimeric complex with $G\beta$ and $G\gamma$ subunits. The stability of these proteins is dependent on this complex, as the formation of the $G\alpha\beta\gamma$ heterotrimer is necessary for exit from the ER. Post-translational isoprenylation of the $G\gamma$ subunit and fatty acylation of the $G\alpha$ subunits targets the complex to the plasma membrane, where $G\alpha\beta\gamma$ can interact with GPCRs and downstream effectors¹⁷. Activation of the $G\alpha$ subunits by a GPCR triggers exchange of GDP for GTP causing disruption of the heterotrimer, allowing both $G\alpha$ and $G\beta\gamma$ to activate intracellular signaling cascades. Once $G\alpha$ hydrolyzes GTP to GDP, the inactive heterotrimer reforms¹⁸. $G\alpha$ proteins have slow intrinsic GTPase activity, however RGS (regulator of G protein signaling) domain containing family members, including the Fog pathway component RhoGEF2, act as GAPs (GTPase accelerating protein) for $G\alpha$ subunits to potentiate hydrolysis of GTP to GDP¹⁹.

$G\alpha$ subunits fall into 4 major classes: $G\alpha_i$, $G\alpha_q$, $G\alpha_s$, $G\alpha_{12}$ based on their sequence homology. The different classes of $G\alpha$ family members also modulate different sets of effectors. For example Phospholipase-C is activated by $G\alpha_q$, whereas adenylyl cyclase is activated by $G\alpha_s$ and inhibited by $G\alpha_i$ ¹⁶. The $G\alpha_{12}$ family, which includes the molecules $G\alpha_{12}$ and $G\alpha_{13}$, has been found to regulate pathways involved in cellular morphogenesis and migration through their downstream effector, the small GTPase Rho. The $G\alpha_{12}$ signaling pathways have been directly linked to cancer formation and other diseases such as leukemia

and hypertension through their role in regulating cellular morphogenesis and movements²⁰.

Ric-8 regulates G α protein signaling during development

Ric-8 was originally identified in a screen for molecules resistant to inhibitors of cholinesterase (Ric) in *C. elegans*, establishing a role for Ric-8 in positively regulating the release of the neurotransmitter acetylcholine²¹; Ric-8 has since been found to modulate secretion of neurotransmitters in several different model organisms²². Shortly after Ric-8 was identified the same group published a paper showing that Ric-8 positions the centrosome during early asymmetric divisions of the *C. elegans* embryo²³. Asymmetric cell division plays an essential role in normal as well as abnormal development. Asymmetric cell division allows a dividing cell to partition its cell fate determinants, allowing daughter cells to inherit molecules, which will establish their identity, and subsequently generate cellular diversity. However, abnormal asymmetric cell division can produce aberrant numbers of cells and cell types, which can subsequently contribute to different cellular proliferative disease states, such as tumorigenesis²⁴. Further research of the role of Ric-8 in asymmetric cell division, in *C. elegans*²⁵⁻²⁸, *Drosophila*²⁹⁻³¹, and mammalian tissue culture³² has demonstrated that Ric-8 is an essential component for spindle positioning during asymmetric cell division.

Tall et al., was the first to show that Ric-8 directly interacts with G α subunits using a yeast two-hybrid assay³³. Subsequent analysis has shown that the initial biosynthesis of G α subunits relies on Ric-8 as a chaperone^{34,35}, as does localization to the appropriate site within the cell. Ric-8 is essential for targeting G α subunits in *C. elegans* and *Drosophila* to the plasma membrane^{27,29-31}, as well as in mammalian tissue culture³⁵. Finally Ric-8 has been shown to protect and stabilize G α subunits from proteasomal degradation^{36,37}. Ultimately

Ric-8 regulates the behavior of $G\alpha$ from its inception, to its (near) destruction.

Ric-8 preferentially interacts with GDP-bound $G\alpha$, and acts as a GEF (guanine nucleotide exchange factor) to disassociate GDP, forming a stabilized nucleotide-free state, until GTP binding³³. In mammals there are two genes encoding Ric-8 proteins, Ric-8A and Ric-8B. Ric-8A, has GEF activity for, and interacts with, $G\alpha_i$, $G\alpha_q$, and $G\alpha_{13}$, while Ric-8B interacts with $G\alpha_s$ and $G\alpha_q$ ^{33,38}. In invertebrates there is only one functional version of Ric-8^{21,31}, indicating a divergence in evolutionary specificity of Ric-8 for $G\alpha$ subunits between vertebrates and invertebrates. It will be interesting to see, in future studies, whether invertebrate Ric-8 is capable of interacting with any or all vertebrate $G\alpha$ family members. While Ric-8 is capable of binding monomeric $G\alpha$ -GDP subunits *in vitro*, $G\alpha$ -GDP does not exist in a monomeric form within the cell. $G\alpha$ -GDP subunits are found either complexed with guanine nucleotide dissociation inhibitors (GDIs), that lock the $G\alpha$ in an inactive, state by preventing its GDP release¹⁸ or within a heterotrimeric complex containing their $\beta\gamma$ partners. Ric-8 cannot bind to $G\alpha$ when it is part of the $G\alpha\beta\gamma$ heterotrimeric complex^{29,33}. However, it has been shown that Ric-8 can bind $G\alpha$ subunits complexed with GDIs; Ric-8 binding these complexes causes the dissociation of the GDI and release of the $G\alpha$. Examples of this process have been described during the asymmetric cell divisions of the one-cell *C. elegans* embryo^{27,28,39}, the neuroblast²⁹ in *Drosophila*, and in mammalian tissue culture models^{32,40}.

Cell divisions in the *C. elegans* early embryo produce cells of different sizes due to the increased pulling forces on, and subsequent shift of the spindle to the posterior side of the embryo. Correct spindle positioning requires the $G\alpha_i$ family members, GOA-1/GPA-16; the GDIs, GPR1/2; the GAP, RGS-7, and the non-canonical GEF, Ric-8. These components

work together in a cyclical process in which binding of Ric-8 to $G\alpha_i$ disrupts the GDP- $G\alpha_i$ -GPR1/2 complex. Ric-8 is then able to facilitate exchange of GDP for GTP on $G\alpha_i$. To return $G\alpha_i$ to its GDP-bound state RGS-7 activates hydrolysis of GTP allowing GPR1/2 to bind again. This cycling is essential for correct spindle positioning^{27,28,39}. The GDIs, Loco and Pins (Partner of Inscuteable), *Drosophila* orthologs of GPR1/2, Ric-8 and $G\alpha_i$ act analogously during asymmetric division of the *Drosophila* neuroblast; although, in this system Loco possesses an RGS domain, allowing it to act as the GAP for GTP- $G\alpha_i$ within this pathway⁴¹. In mammalian asymmetrically dividing cells, it has been proposed that a similar cyclical process involving GDIs, GEFs, and GAPs regulates spindle pulling forces through association with the microtubule spindle organizer, Numa (nuclear mitotic apparatus). Numa binds both microtubules and the GDI, LGN, but cannot bind both simultaneously. When Ric-8 binds LGN- $G\alpha$ -Numa, it causes dissociation of the complex, allowing Numa to interact with microtubules, and affect spindle positioning^{32,42}. Insight into how these pulling forces are translated into movement was found in flies, where it has been shown that the Numa homolog, Mud (mushroom body defects) forms a complex with Ctp (cut-up) the light chain of the minus-end directed motor, dynein⁴³.

The crystallographic structure of Ric-8 has not been solved; however, a model has been constructed using data from secondary sequence analysis and circular dichroism experiments with *Xenopus laevis* Ric-8. Based on this data Ric-8 is composed of 10 repeated right-twisted alpha helical domains⁴⁴. The predicted model of Ric-8 is similar in structure to molecules known to act as scaffolding proteins, such as beta-catenin and α -importin⁴⁵; although, thus far, the only proteins found to directly bind Ric-8 are $G\alpha$ subunits. It is unclear how Ric-8 and $G\alpha$ subunits physically interact. However, a truncated version

composed the N-terminal half of mammalian Ric-8 was found to be sufficient for binding $G\alpha_q$ ⁴⁶. It has also been shown that the 12 C-terminal residues of $G\alpha_{i1}$ are crucial for interacting with Ric-8A³⁴. While there is some evidence of residues important for $G\alpha$ association with Ric-8, no specific amino acids have been identified within Ric-8 that facilitate interaction with a $G\alpha$ subunit.

Dissertation Goals

To investigate the Fog signaling pathway we wanted to develop a *Drosophila* tissue culture assay in which we could apply ectopic Fog to cells to drive cellular constriction. As one of the first graduate students in Dr. Stephen Rogers's lab I helped develop many tools and techniques to examine varying aspects of cellular morphogenesis. We first made a cell line that secreted ectopic Fog into the media. By concentrating that media and applying it to different *Drosophila* tissue culture cell lines, we were able to identify one cell type that responded to Fog by altering its cytoskeleton, S2R+ cells. The development of, and detailed protocol for performing this assay is presented in Chapter II of this dissertation.

A key missing component of the Fog signaling pathway is the receptor that transmits the Fog signal to activate the pathway. One aim of this dissertation is to show that we have identified a GPCR that drives contractility downstream of Fog. While deficiency screens have been performed for zygotic genes controlling gastrulation in *Drosophila*, and identified other members within the pathway such as T48⁵, no GPCR has been revealed. Using *Drosophila* tissue culture put us at a unique advantage as we were able to quickly screen through a dsRNA library comprising all 138 known and putative GPCRs in the *Drosophila* genome^{47,48}. Doing this we found one GPCR that inhibited Fog-induced cellular constriction,

Mist. Upon identifying this receptor we further showed that Mist was capable of conferring Fog responsiveness to previously unresponsive cells, and identified specific domains important for its function. In the animal, we found that Mist drives cellular contraction in tissues known to be regulated by the Fog pathway through overexpression and targeted RNAi depletion of Mist. An in-depth analysis of the GPCR, Mist is presented in Chapter III of this dissertation.

In the initial characterization of embryos depleted of maternal and zygotic Ric-8 it was noted that phenotypes of *Ric-8*, strongly resembled *Fog* and *Cta* embryos^{29,30}. Therefore, we wanted to investigate how Ric-8 fit into the Fog signaling pathway. While clues abounded in the wealth of data linking Ric-8 to G α function, little was known about Ric-8's function within this pathway or how it interacts with G α subunits in any system. Using our tissue culture assay, I showed that Ric-8 is an essential component and acts at the level of Cta in the Fog signaling pathway. To determine how Ric-8 influences the behavior of Cta I performed pulldown assays showing that Ric-8 preferentially binds and localizes GDP-bound Cta. The ability of Ric-8 to localize Cta plays a role in sustained pathway activation, as mis-targeting of Ric-8 negatively modulates the ability of S2R+ cells to respond to Fog. To gain further insight into the functional relationship of Ric-8 and Cta I made a series of evolutionarily conserved point mutants, and assessed their ability to rescue contractility in cells depleted of endogenous Ric-8, or to bind Cta in immunoprecipitation pulldown experiments. From these experiments I identified specific residues important for establishing a functional binding interface between Cta and Ric-8. Chapter IV contains a detailed description of these experiments demonstrating an essential role for Ric-8 in the Fog signaling pathway.

Finally, this dissertation as a whole is presented to describe to you how a novel

experimental system we devised resulted in two projects, identification of the GPCR, Mist, and characterization of the cytoplasmic protein Ric-8, that have advanced our understanding of a pathway essential for cellular shape changes that drive whole-sale tissue rearrangement.

References

1. Sawyer, J. M. *et al.* Apical constriction: a cell shape change that can drive morphogenesis. *Dev. Biol.* **341**, 5–19 (2010).
2. Lecuit, T. & Lenne, P.-F. Cell surface mechanics and the control of cell shape, tissue patterns and morphogenesis. *Nat. Rev. Mol. Cell Biol.* **8**, 633–644 (2007).
3. Leptin, M. Drosophila gastrulation: from pattern formation to morphogenesis. *Annu. Rev. Cell Dev. Biol.* **11**, 189–212 (1995).
4. Simpson, P. Maternal-Zygotic Gene Interactions during Formation of the Dorsoventral Pattern in Drosophila Embryos. *Genetics* **105**, 615–632 (1983).
5. Kölsch, V., Seher, T., Fernandez-Ballester, G. J., Serrano, L. & Leptin, M. Control of Drosophila gastrulation by apical localization of adherens junctions and RhoGEF2. *Science* **315**, 384–386 (2007).
6. Leptin, M. & Grunewald, B. Cell shape changes during gastrulation in Drosophila. *Development* **110**, 73–84 (1990).
7. Costa, M., Wilson, E. T. & Wieschaus, E. A putative cell signal encoded by the folded gastrulation gene coordinates cell shape changes during Drosophila gastrulation. *Cell* **76**, 1075–1089 (1994).
8. Dawes-Hoang, R. E. *et al.* folded gastrulation, cell shape change and the control of myosin localization. *Development* **132**, 4165–4178 (2005).
9. Morize, P., Christiansen, A. E., Costa, M., Parks, S. & Wieschaus, E. Hyperactivation of the folded gastrulation pathway induces specific cell shape changes. *Development* **125**, 589–597 (1998).
10. Parks, S. & Wieschaus, E. The Drosophila gastrulation gene *concertina* encodes a G alpha-like protein. *Cell* **64**, 447–458 (1991).
11. Nikolaidou, K. K. & Barrett, K. A Rho GTPase signaling pathway is used reiteratively in epithelial folding and potentially selects the outcome of Rho activation. *Curr. Biol.* **14**, 1822–1826 (2004).
12. Häcker, U. & Perrimon, N. DRhoGEF2 encodes a member of the Dbl family of oncogenes and controls cell shape changes during gastrulation in Drosophila. *Genes Dev.* **12**, 274–284 (1998).
13. Fox, D. T. & Peifer, M. Abelson kinase (Abl) and RhoGEF2 regulate actin organization during cell constriction in Drosophila. *Development* **134**, 567–578 (2007).

14. Hopkins, A. L. & Groom, C. R. The druggable genome. *Nat Rev Drug Discov* **1**, 727–730 (2002).
15. Oldham, W. M. & Hamm, H. E. Heterotrimeric G protein activation by G-protein-coupled receptors. *Nat. Rev. Mol. Cell Biol.* **9**, 60–71 (2008).
16. Malbon, C. C. G proteins in development. *Nat. Rev. Mol. Cell Biol.* **6**, 689–701 (2005).
17. Takida, S. & Wedegaertner, P. B. Heterotrimer formation, together with isoprenylation, is required for plasma membrane targeting of Gbetagamma. *J Biol Chem* **278**, 17284–17290 (2003).
18. Siderovski, D. P. & Willard, F. S. The GAPs, GEFs, and GDIs of heterotrimeric G-protein alpha subunits. *Int. J. Biol. Sci.* **1**, 51–66 (2005).
19. Rossman, K. L., Der, C. J. & Sondek, J. GEF means go: turning on RHO GTPases with guanine nucleotide-exchange factors. *Nat. Rev. Mol. Cell Biol.* **6**, 167–180 (2005).
20. Suzuki, N., Hajicek, N. & Kozasa, T. Regulation and physiological functions of G12/13-mediated signaling pathways. *Neurosignals* **17**, 55–70 (2009).
21. Miller, K. G., Emerson, M. D., McManus, J. R. & Rand, J. B. RIC-8 (Synembryn): a novel conserved protein that is required for G(q)alpha signaling in the *C. elegans* nervous system. *Neuron* **27**, 289–299 (2000).
22. Hinrichs, M., Torrejón, M., Montecino, M. & Olate, J. Ric-8: different cellular roles for a heterotrimeric G-protein GEF. *J Cell Biochem* (2012).doi:10.1002/jcb.24162
23. Miller, K. G. & Rand, J. B. A role for RIC-8 (Synembryn) and GOA-1 (G(o)alpha) in regulating a subset of centrosome movements during early embryogenesis in *Caenorhabditis elegans*. *Genetics* **156**, 1649–1660 (2000).
24. Knoblich, J. A. Asymmetric cell division: recent developments and their implications for tumour biology. *Nat. Rev. Mol. Cell Biol.* **11**, 849–860 (2010).
25. Couwenbergs, C., Spilker, A. C. & Gotta, M. Control of embryonic spindle positioning and Galpha activity by *C. elegans* RIC-8. *Curr. Biol.* **14**, 1871–1876 (2004).
26. Afshar, K. *et al.* RIC-8 is required for GPR-1/2-dependent Galpha function during asymmetric division of *C. elegans* embryos. *Cell* **119**, 219–230 (2004).
27. Afshar, K., Willard, F. S., Colombo, K., Siderovski, D. P. & Gönczy, P. Cortical localization of the Galpha protein GPA-16 requires RIC-8 function during *C. elegans* asymmetric cell division. *Development* **132**, 4449–4459 (2005).

28. Hess, H. A., Röper, J.-C., Grill, S. W. & Koelle, M. R. RGS-7 completes a receptor-independent heterotrimeric G protein cycle to asymmetrically regulate mitotic spindle positioning in *C. elegans*. *Cell* **119**, 209–218 (2004).
29. Hampoelz, B., Hoeller, O., Bowman, S. K., Dunican, D. & Knoblich, J. A. Drosophila Ric-8 is essential for plasma-membrane localization of heterotrimeric G proteins. *Nat. Cell Biol.* **7**, 1099–1105 (2005).
30. Wang, H. *et al.* Ric-8 controls Drosophila neural progenitor asymmetric division by regulating heterotrimeric G proteins. *Nat. Cell Biol.* **7**, 1091–1098 (2005).
31. David, N. B. *et al.* Drosophila Ric-8 regulates Galphai cortical localization to promote Galphai-dependent planar orientation of the mitotic spindle during asymmetric cell division. *Nat. Cell Biol.* **7**, 1083–1090 (2005).
32. Woodard, G. E. *et al.* Ric-8A and Gi alpha recruit LGN, NuMA, and dynein to the cell cortex to help orient the mitotic spindle. *Mol. Cell. Biol.* **30**, 3519–3530 (2010).
33. Tall, G. G., Krumins, A. M. & Gilman, A. G. Mammalian Ric-8A (synembryn) is a heterotrimeric Galpha protein guanine nucleotide exchange factor. *J Biol Chem* **278**, 8356–8362 (2003).
34. Thomas, C. J. *et al.* The nucleotide exchange factor Ric-8A is a chaperone for the conformationally dynamic nucleotide-free state of G α i1. *PLoS ONE* **6**, e23197 (2011).
35. Gabay, M. *et al.* Ric-8 proteins are molecular chaperones that direct nascent G protein α subunit membrane association. *Sci Signal* **4**, ra79 (2011).
36. Nagai, Y., Nishimura, A., Tago, K., Mizuno, N. & Itoh, H. Ric-8B stabilizes the alpha subunit of stimulatory G protein by inhibiting its ubiquitination. *J Biol Chem* **285**, 11114–11120 (2010).
37. Chan, P., Gabay, M., Wright, F. A. & Tall, G. G. Ric-8B is a GTP-dependent G protein alphas guanine nucleotide exchange factor. *J Biol Chem* **286**, 19932–19942 (2011).
38. Klattenhoff, C. *et al.* Human brain synembryn interacts with G α lpha and G α qalpha and is translocated to the plasma membrane in response to isoproterenol and carbachol. *J. Cell. Physiol.* **195**, 151–157 (2003).
39. Colombo, K. *et al.* Translation of polarity cues into asymmetric spindle positioning in *Caenorhabditis elegans* embryos. *Science* **300**, 1957–1961 (2003).

40. Tall, G. G. & Gilman, A. G. Resistance to inhibitors of cholinesterase 8A catalyzes release of Galphai-GTP and nuclear mitotic apparatus protein (NuMA) from NuMA/LGN/Galphai-GDP complexes. *Proc. Natl. Acad. Sci. U.S.A.* **102**, 16584–16589 (2005).
41. Yu, F. *et al.* Locomotion defects, together with Pins, regulates heterotrimeric G-protein signaling during *Drosophila* neuroblast asymmetric divisions. *Genes Dev.* **19**, 1341–1353 (2005).
42. Du, Q. & Macara, I. G. Mammalian Pins is a conformational switch that links NuMA to heterotrimeric G proteins. *Cell* **119**, 503–516 (2004).
43. Wang, C. *et al.* An ana2/ctp/mud complex regulates spindle orientation in *Drosophila* neuroblasts. *Dev. Cell* **21**, 520–533 (2011).
44. Figueroa, M. *et al.* Biophysical studies support a predicted superhelical structure with armadillo repeats for Ric-8. *Protein Sci.* **18**, 1139–1145 (2009).
45. Coates, J. C. Armadillo repeat proteins: beyond the animal kingdom. *Trends Cell Biol.* **13**, 463–471 (2003).
46. Nishimura, A. *et al.* Ric-8A potentiates Gq-mediated signal transduction by acting downstream of G protein-coupled receptor in intact cells. *Genes Cells* **11**, 487–498 (2006).
47. Hewes, R. S. Neuropeptides and Neuropeptide Receptors in the *Drosophila melanogaster* Genome. *Genome Research* **11**, 1126–1142 (2001).
48. Brody, T. *Drosophila melanogaster* G Protein-coupled Receptors. *J. Cell Biol.* **150**, 83F–88 (2000).



Figure 1.1 Ventral furrow formation in the developing *Drosophila* embryo. Yellow cells are presumptive mesoderm, which will undergo apical constriction. Red cells represent presumptive mesoderm that are internalized, but do not apically constrict. Arrows indicate direction of cell movements. Modified from Sawyer, et al.¹

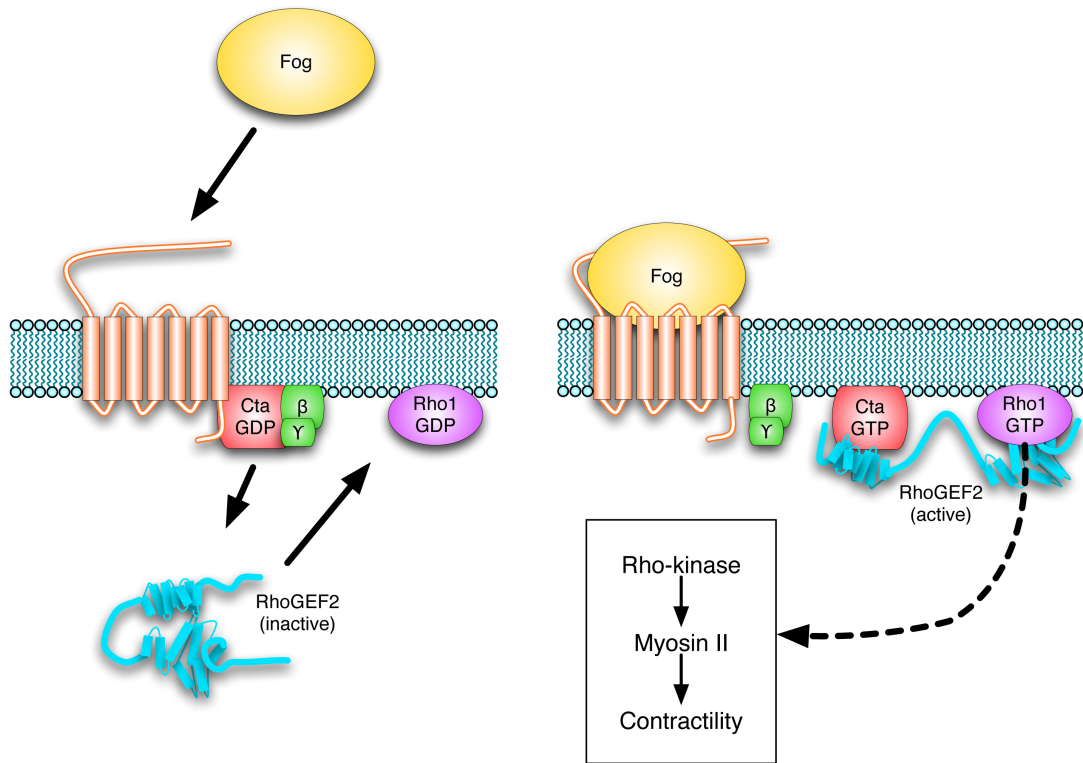


Figure 1.2 Activation of the Fog signaling pathway drives cytoskeletal changes within the cell.

Chapter II

Establishing the *Drosophila* tissue culture cell line, S2R+, as a model for studying Fog pathway signaling

Preface

This work is currently in preparation for submission for publication. All experiments were designed by my advisor, Dr. Stephen Rogers, and myself. This manuscript was written by me, and edited by Dr. Stephen Rogers. I performed all of the experiments, except Figure 2.4C, which was performed by Dr. Stephen Rogers.

Introduction

Drosophila tissue culture has been established as a powerful system to address molecular and cell biological questions. Additionally, gain- or loss- of function analyses in *Drosophila* cell based assays are quick, easy and efficient due to high transfection efficiency, and the ability of cells to take up large dsRNA molecules directly from media. A previously studied cell line, Dm-D17-C3, was established as a model for investigating basic principals of cellular migration and the regulation of the cytoskeleton^{1,2}. We wanted to develop a similar system to study a cell signaling pathway that drives cell shape changes during *Drosophila* development.

The Fog (Folded gastrulation) signaling pathway is used reiteratively during development of the *Drosophila* embryo to facilitate cell shape changes in movements of the ventral furrow and posterior midgut to establish germ layers³; to shape the epithelial imaginal

wing disc⁴; as well as to form the salivary glands^{5,6}. The Fog pathway has been most well-studied in gastrulation during ventral furrow formation. From this system a signaling cascade has been described starting with the secreted protein Fog binding to the 7-transmembrane G protein coupled receptor (GPCR), Mist, to activate a $G\alpha_{12/13}$ protein (Concertina, Cta)^{7,8}. The small GTPase Rho is activated by the Cta target RhoGEF2. Rho in turn activates Rho kinase resulting in the phosphorylation and activation of non-muscle myosin II^{4,6,8-10}; myosin-II binds F-actin resulting in cellular constriction.

We wanted to recapitulate the Fog signaling pathway, from ligand binding to pathway activation (cellular constriction), in a cultured system. To accomplish this we needed to find a cell line that responded to ectopic application of Fog. S2 cells respond to overexpression of downstream Fog pathway components (i.e. RhoGEF2, Rho, Rho Kinase) by altering their cytoskeletal morphology, changing from a flattened pancake shaped cell to a bonnet shaped cell¹¹. The cell acquires a bonnet shape due to the activation of myosin which elicits constriction in an actin dependent manner to form a tight band of activated myosin at the base of a dome, where the organelles have been displaced due to constriction (Figure 2.1). However, application of concentrated Fog has no effect on the cytoskeletal organization, or the cell morphology, of S2 cells, as these cells lack the receptor that binds Fog (Figure 2.1). We therefore began testing various immortalized cell lines, obtained from the *Drosophila* Genome Resource Center, for Fog responsiveness, and identified one cell line, S2R+ (S2 Receptors +), able to respond to Fog application. It has been shown that this cell line is responsive to the Wingless (Wg) ligand, unlike S2 cells, because these cells express the Wg receptor, Frizzled¹². Upon application of Fog, S2R+ cells undergo dramatic morphological changes. There is a re-localization of F-actin and active myosin, as visualized using an

antibody to the phosphorylated regulatory light chain of non-muscle myosin II (pRLC) (Figure 2.2). Using S2R+ cells we have established a means to investigate the Fog signaling pathway in a tissue culture based system.

Experimental data from the animal is invaluable to understanding morphological movements during embryogenesis. The transmission of inductive cues within a tissue from one cell or group of cells to another, how cells migrate and move past each another to reach their final location, and other questions involving tissue dynamics during cellular reorganization and movements to shape the embryo are well-suited to analysis in the *Drosophila* embryo. However, the system we have developed provides a streamlined approach to study the general mechanism of this signaling pathway through fast, easy, and efficient methods. The aim of this article is to describe the methodology we developed to investigate Fog-induced cellular constriction using S2R+ cells.

Experimental Design

Maintenance, transfection and RNAi of S2R+ cells.

S2R+ cells are a subclone¹² of the S2 cell line, an immortalized population of cells originally derived from late stage embryos¹³. However, unlike S2 cells, S2R+ cells do not grow well in either SF900 or Schneider's Media, and as found by Yanagawa, et al. the cells must be cultured in Shield and Sang M3 insect medium supplemented with 10% heat-inactivated FBS¹². For routine passage, S2 cells can be diluted to ~25-50% confluency and continue to propagate; however, at this density, S2R+ cells will change their morphology from a mostly homogenous lawn of rounded cells to a sparse population of long, spindly cells

that will shortly undergo cell death. We have therefore found it is best to maintain S2R+ cells at a confluency, near 50-75%, for continued propagation.

RNAi in S2R+ cells is performed identically to dsRNA treatment in S2 cells. As a positive control, we routinely use dsRNA targeted to the small GTPase Rho. Due to its role in cytokinesis, when cells are depleted of Rho they become very large and contain multiple nuclei compared to control dsRNA treated cells^{1,2}. Rho is also a member of the Fog signaling pathway, and upon its depletion cells are no longer able to respond to Fog and undergo cellular contraction⁴ (Figure 2.3). This makes Rho an ideal positive control for determining the optimal length of dsRNA treatment, as well as a useful tool to verify that dsRNA treatment has progressed long enough to prevent Fog induced cellular constriction.

To achieve high transfection efficiency in S2 cells, we utilize the Amaxa electroporation system. However, S2R+ cells do not survive electroporation under these conditions, most likely due to the inability to tolerate the high current required for introduction of plasmid DNA. Instead we have found great success using the FuGENE HD system for transfection of S2R+ cells. After performing a dilution series, based on suggested parameters outlined in the product literature, we found that the optimal transfection conditions consist of using a 2:8 ratio (2ug of plasmid DNA/8uL of transfection reagent). The procedure for transfection of S2R+ cells is outlined below.

Construction of the Fog expression vector and production of ectopic Fog

We created a construct with tagged, full-length Fog under an inducible promoter using PCR to amplify the coding sequence of the gene and introducing a 5' EcoRI site, a C-terminal Myc tag, and a 3' NotI site to allow cloning into pMT-V5/His. The pMT promoter

is inducible by addition of copper sulfate. We transfected this construct, along with a plasmid encoding the antibiotic resistance gene for Hygromycin, into S2 cells and selected for cells containing the construct by treating the cells with increased doses of the drug Hygromycin B for ~4 weeks to make a stable cell line, S2:Fog-Myc.

One can transfect two constructs simultaneously, a plasmid encoding your gene of interest and a plasmid containing a eukaryotic antibiotic resistance gene, as an efficient way to generate a stable cell line. However, it means that while most cells will contain both plasmids, there is a subpopulation that only contains the plasmid with the antibiotic resistance gene. To overcome this problem one can use the OpIE2 promoter pIZ family of vector backbones. These plasmids contain a multiple cloning site, and a eukaryotic antibiotic resistance gene all within the same backbone. Either method is suitable to make a stable cell line with high levels of construct expression. A protocol outlining the procedure for creation of stable cell lines is presented below.

Before induction, collection and concentration of Fog containing media, cells were scaled up from 25cm² (~5mLs) to 150cm² (~20mLs) flasks. We wanted to maximize the amount of Fog produced and harvested per experiment. Therefore, we tested several variables to ascertain the appropriate medium and induction time for optimal expression and collection.

To verify that Fog is being expressed and secreted into the media, we separated media concentrated from S2:Fog-Myc cells and untransfected S2 cells on SDS-PAGE gels, blotted, and probed nitrocellulose with antibodies to recognize Fog. In S2:Fog-Myc expressing cells monoclonal anti-Myc and affinity purified anti-Fog antibodies recognized a band at ~150kDa, which is absent from media collected and concentrated from untransfected S2 cells (Figure

2.4A and Figure 4.1A). S2:Fog-Myc cells are maintained in SF900 media, however we found if the media is exchanged on the day of induction with Schneider's media that we are able to collect more Fog protein per mL (Figure 2.4A). We tested various experimental conditions before finding an optimum length of induction, which we determined as ~48 hours (Figure 2.4B). Before each experiment, we tested the efficacy of the concentrated Fog. The process of concentrating Fog-containing media can yield potent Fog ligand, and we routinely determine the amount used for experiments by testing a dilution series of Fog/Schneider's media. Generally the Fog we use for experiments is diluted 1:3 with Schneider's media. S2R+ cells start to respond within minutes of Fog application. We have found that treatment of S2R+ cells for 10 minutes is sufficient for robust S2R+ cell response (Figure 2.4C).

Recapitulation of Fog Signaling events in S2R+ cells

As previously described, activation of the Fog pathway during *Drosophila* gastrulation drives the activation of the acto-myosin cytoskeleton resulting in cellular contraction. We can activate the Fog signaling pathway in S2R+ cells simply through addition of concentrated ectopic Fog (Figure 2.1 and 2.2). To verify that addition of the Fog ligand was specifically affecting the Fog signaling pathway, we depleted cells of the essential pathway components Cta, RhoGEF2, and Rho, and using phase-contrast microscopy assessed their ability to undergo cellular constriction in response to Fog. Depletion of any of these components abrogates Fog responsiveness (Figures 1.3 and 4.1B). Therefore we have developed a system wherein we can directly activate the Fog pathway in S2R+ cells, using ectopic application of concentrated Fog-containing media. The aim of this paper is to explain, in detail, the procedural methods to make a stably expressing cell line that will secrete Fog into the

medium, and how to harvest and apply concentrated Fog to cells to create a robust system to investigate dynamics of the Fog signaling pathway.

Materials and Methods

Reagents

- S2R+ cells are available from the DGRC (<http://dgrc.cgb.indiana.edu/>)
- SF900 (Gibco, cat no. 10902), Schneider's (Gibco, cat no. 11720), and Shield and Sang M3 (Sigma-Aldrich, cat no. S3652) insect medium; All medias are supplemented with 1% anti-biotic/antimycotic and Shield and Sang M3 media is additionally supplemented with 10% heat-inactivated (see-below) FBS. All preparation of media is to be performed in a sterile laminar flow hood.
- Antibiotic/antimycotic (Gibco, cat. no. 15240)
- Non-heat inactivated FBS (Gibco, cat. no. 26140); we heat-inactivate FBS at 55C, as we have found that commercially heat-inactivated FBS can inhibit sustained cell growth².
- Hygromycin B solution (CellGro, cat. no. 30-240-CR) or Zeocin antibiotic (Invitrogen, cat. no. R250)
- Concanavalin A (MP Biomedicals, cat no. 150710)

Equipment

- Sterile laminar flow hood
- Treated tissue culture flasks (25cm²; Falcon, cat. no. 353014, 75cm²; Falcon, cat. no. 353135 and 150cm²; Falcon, cat. no. 353046)

- 6-well tissue culture plates (Falcon, cat no. 353064)
- Hemocytometer (Hausser Scientific, cat. no. 02-671-54)
- Amaxa Kit V (Lonza, cat. no. VCA-1003)
- Transfection vectors for creating stable cells lines such as the pMT promoter vector family (Invitrogen, cat. no. V412020) or the OpIE2 promoter containing pIZ vector (Invitrogen, cat. no. V8000)
- Polystyrene Petri dishes (35 mm × 10 mm; Falcon, cat. no. 351008)
- Glass cover slips, (no. 1.5, 22 mm²; Corning, cat. no. 2940-225)
- Glass bottom plates (Maktek, cat. no. P35G-1.5-10)
- Microscope slides (25x75x1mm; Fisher Scientific, cat no. 12-544-2)
- FuGENE HD transfection reagent (Promega, cat. no. E2311)
- Sterile water (Fisher Scientific, cat. no. BP5611)
- Protein concentrators with a 30,000 molecular weight cutoff (MWCO) (Millipore, cat. no. UFC903008)
- Swinging bucket centrifuge
- Bright-field microscope capable of phase-contrast or DIC microscopy

Equipment Set-up

Preparation of coverslips and glass bottom plates for phase-contrast and fluorescence microscopy:

Prepare coverslips as previously described^{1,2}. To prepare glass-bottom plates for microscopy, add enough Concanavalin A (ConA) (0.5mg/mL) to cover the glass portion of the coverslip.

Immediately aspirate off and allow to air-dry. Glass bottom plates treated this way are viable for at least one month.

Procedures

Note: Handling of live cells should always be performed in a sterile laminar hood.

Creating and storing a stable S2 cell line

1. Remove 10uL from a dense flask of resuspended S2 cells. (Resuspend S2 cells by gently aspirating the media up into a pipette and running the media with some force over the attached cells). Using a bright-field microscope with either DIC or phase-contrast filters use a hemocytometer to determine the number of cells within the flask.
2. Transfect $\sim 10^6$ S2 cells with 1ug/uL of plasmid DNA as described in the instructions for Amaxa Kit V using the Amaxa nucleofector system program G-030.
3. Using a micropipette remove the transfected cells from the cuvette by adding 0.5mL of SF900 media. Add this mixture to 1mL of SF900 in a 6 well plate. Transfect 3 wells for each construct.
4. Allow the cells to recover from the transfection for 24 hours.
5. Start treating the cells with the appropriate antibiotic at low doses. For the two most commonly used antibiotics in our laboratory, Hygromycin B and Zeocin, start at 200ug/mL and 50ug/mL, respectively. Using a low dose of the drug at first is critical as many cells will undergo cell death, and if too many within the population die the paucity of cells will cause the remaining, vector-containing cells to die as well.
6. After the first treatment allow cells to recover for one week, and then resuspend all 3

wells and transfer cells to a 25cm² flask. The following day treat the cells with a low dosage of drug.

7. Over a period of a month gradually increase the amount of antibiotic, treating cells every 5-7 days, and passing cells into a new flask when necessary. A final amount of ~5X the initial drug dose should be used for the last treatment. The final doses of drug will select for cells containing high levels of transfected DNA.
8. To determine the level of protein expression for a stable cell line, plate cells out onto a ConA coated coverslip or glass bottom plate and fix and stain using an appropriate antibody. A protocol for preparing *Drosophila* tissue culture cells for microscopy has been previously described¹. Alternatively one can run cell lysate samples out on an SDS-PAGE gel to visualize and quantify protein expression levels.
9. Once you have established the desired stable cell line, it is imperative to freeze cells down as stocks for future use. Protocols for freezing cells down and thawing them out are previously described¹.

Transient transfection of S2R+ cells

1. Into 1mL of Shield and Sang M3 insect medium plate out S2R+ cells into one well of a 6-well plate to ~60-70% confluence. Allow several hours to overnight for attachment.
2. Prepare the transfection complex using FuGENE HD, per product literature guidelines, using a 2:8 ratio of DNA to transfection reagent, and sterile water as the medium.
3. After addition of the FuGENE HD transfection reagent wait at least 20 minutes before adding the mixture to cells. The media does not need to be changed before or after addition of transfection complexes.

4. If your gene of interest is under an inducible promoter wait 24 hours before induction, and a following 24 hours before experimental usage.

Harvesting secreted Fog from S2 media

1. Scale up growth of S2:Fog-Myc cells from one 25cm² (~5mLs), to one 75cm² flask (~10mLs), ultimately to (2) confluent 150cm² flasks (~20mLs).
2. Remove SF900 media from flask and discard.
3. Slowly add 10mLs of Schneider's media to flask and gently rock back and forth several times and discard. It is critical to not disrupt attachment of cells to tissue culture plastic, or allow too much time to pass in between addition and removal of media.
4. Add 20mLs of fresh Schneider's media to flask.
5. Immediately after adding Schneider's media add 100uL of 100mM CuSO₄, and wait 48 hours.
6. Remove media and transfer to a conical tube. Discard cells and flask.
7. Spin media at 4000 rpm at 4°C for 15 minutes to clear media of any cellular detritus, and transfer to a fresh conical tube, placing media on ice or at 4°C.
8. In batches, add 10mLs of pre-cleared media to protein concentrators and spin at 4000 rpm at 4°C for 30-45 minutes (or until you have decreased the amount of media to 20 percent of the original volume).
9. Remove concentrated media from the protein concentrator reservoir and transfer to a fresh tube, kept on ice or at 4°C. Concentrated Fog can be stored at 4°C for several months; however, longer periods of storage may result in bacterial contamination.

Testing the efficacy of concentrated Fog

1. Plate out S2R+ cells into 1mL of Shield and Sang M3 insect medium in a glass-bottom plate pre-coated with ConA to a density of ~50% confluence. Allow cells to attach for at least 1 hour. Cells are sufficiently attached when they become phase-dark and have wide, flattened lamellipodia.
2. Remove a small amount of Fog media from 4°C stock, and allow to warm up to room temperature.
3. Dilute concentrated Fog protein 1:1 with fresh Schneider's media.
4. Discard media from glass bottom plate and carefully add Fog media only to the glass circle containing the S2R+ cells. Usage of 150 uL is sufficient to cover the area.
5. Wait 10 minutes and using phase-contrast or DIC microscopy determine the amount of cells undergoing morphological change. Cell shape changes are clearly evident under low magnifications, such as 10X and 20X.
6. If a 1:1 ratio of Fog to Schneider's is sufficient for robust cellular constriction, continue a dilution series to determine the minimal amount of Fog necessary for robust constriction. Usually this is between a 1:3 and 1:5 ratio. If there is no or little contraction with diluted Fog, apply undiluted Fog.

Anticipated Results

Following these steps will allow the user to establish a system in which to test the morphological cell shape changes downstream of Fog application. S2R+ cells provide a tractable system for loss- and gain- of function studies due to the amenability of this tissue culture line to RNAi and transient transfection. S2R+ cells give a clear read-out of Fog

pathway activation, which can be seen using basic phase-contrast microscopy, saving time and reagents. Alternatively, commercially available antibodies are available to Fog pathway components allowing for visualization of cellular function using fluorescence microscopy. Finally, the ability to perfuse Fog into a chamber allows for live-imaging with high-resolution confocal microscopy.

References

1. Rogers, S. L. & Rogers, G. C. Culture of *Drosophila* S2 cells and their use for RNAi-mediated loss-of-function studies and immunofluorescence microscopy. *Nat Protoc* **3**, 606–611 (2008).
2. Currie, J. D. & Rogers, S. L. Using the *Drosophila melanogaster* D17-c3 cell culture system to study cell motility. *Nat Protoc* **6**, 1632–1641 (2011).
3. Leptin, M. *Drosophila* gastrulation: from pattern formation to morphogenesis. *Annu. Rev. Cell Dev. Biol.* **11**, 189–212 (1995).
4. Barrett, K., Leptin, M. & Settleman, J. The Rho GTPase and a putative RhoGEF mediate a signaling pathway for the cell shape changes in *Drosophila* gastrulation. *Cell* **91**, 905–915 (1997).
5. Myat, M. M. & Andrew, D. J. Organ shape in the *Drosophila* salivary gland is controlled by regulated, sequential internalization of the primordia. *Development* **127**, 679–691 (2000).
6. Nikolaidou, K. K. & Barrett, K. A Rho GTPase signaling pathway is used reiteratively in epithelial folding and potentially selects the outcome of Rho activation. *Curr. Biol.* **14**, 1822–1826 (2004).
7. Costa, M., Wilson, E. T. & Wieschaus, E. A putative cell signal encoded by the folded gastrulation gene coordinates cell shape changes during *Drosophila* gastrulation. *Cell* **76**, 1075–1089 (1994).
8. Dawes-Hoang, R. E. *et al.* folded gastrulation, cell shape change and the control of myosin localization. *Development* **132**, 4165–4178 (2005).
9. Häcker, U. & Perrimon, N. DRhoGEF2 encodes a member of the Dbl family of oncogenes and controls cell shape changes during gastrulation in *Drosophila*. *Genes Dev.* **12**, 274–284 (1998).
10. Martin, A. C., Kaschube, M. & Wieschaus, E. F. Pulsed contractions of an actin-myosin network drive apical constriction. *Nature* **457**, 495–499 (2009).
11. Rogers, S. L., Wiedemann, U., Häcker, U., Turck, C. & Vale, R. D. *Drosophila* RhoGEF2 associates with microtubule plus ends in an EB1-dependent manner. *Curr. Biol.* **14**, 1827–1833 (2004).
12. Yanagawa, S. I. Identification and Characterization of a Novel Line of *Drosophila* Schneider S2 Cells That Respond to Wingless Signaling. *Journal of Biological Chemistry* **273**, 32353–32359 (1998).

13. Schneider, I. Cell lines derived from late embryonic stages of *Drosophila melanogaster*. *J Embryol Exp Morphol* **27**, 353–365 (1972).

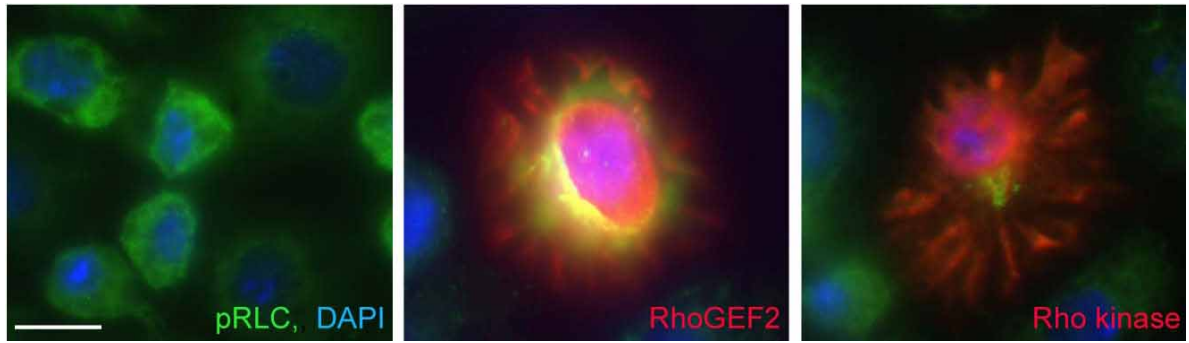


Figure 2.1 Overexpression of downstream components of the Fog signaling pathway drive cellular constriction in S2 cells. Cells were transfected with RhoGEF2-GFP or Rho Kinase-Myc, and stained for pRLC (and for Rho kinase, anti-Myc). Scale bar: 20 μ m.

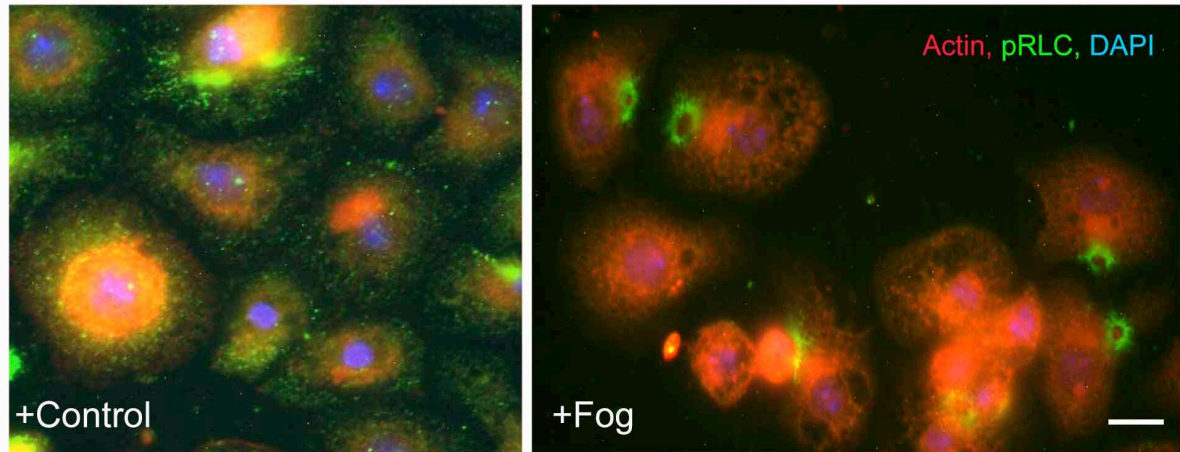


Figure 2.2 S2R+ cells treated with ectopic Fog ligand respond by reorganizing their cytoskeleton. S2R+ cells were treated with control or Fog containing media and stained for pRLC (active myosin), Phalloidin (F-Actin) and DAPI (DNA). Scale bar: 20 μm .

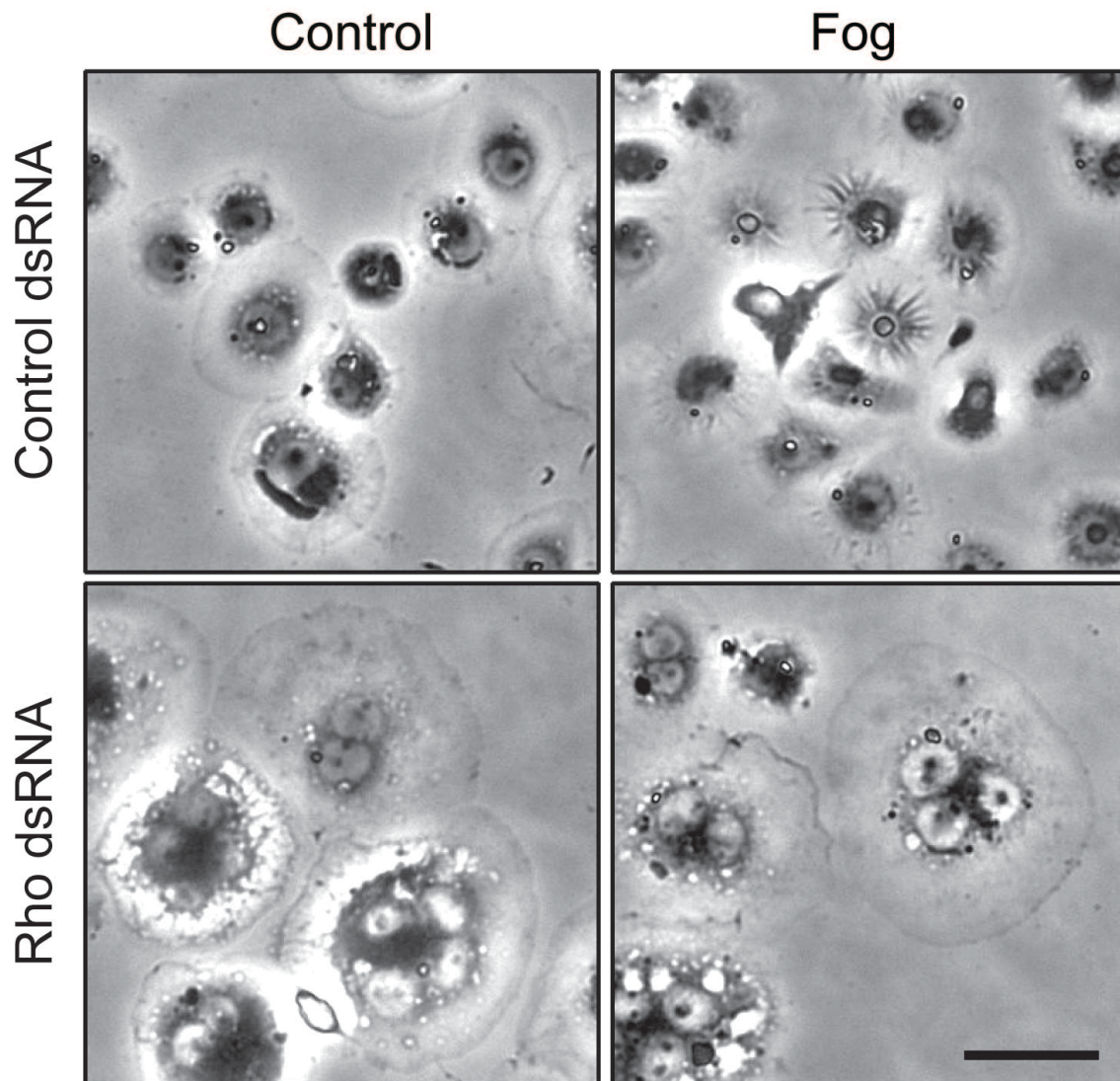


Figure 2.3 S2R+ cells treated with dsRNA targeting Rho do not respond to ectopic Fog application, unlike control dsRNA treated cells. Rho dsRNA treated cells are multi-nucleated and much larger than control dsRNA treated cells. S2R+ cells were treated for 7 days with dsRNA targeting control or Rho dsRNA, and treated with either control or Fog containing media. Scale bar: 50 μ m.

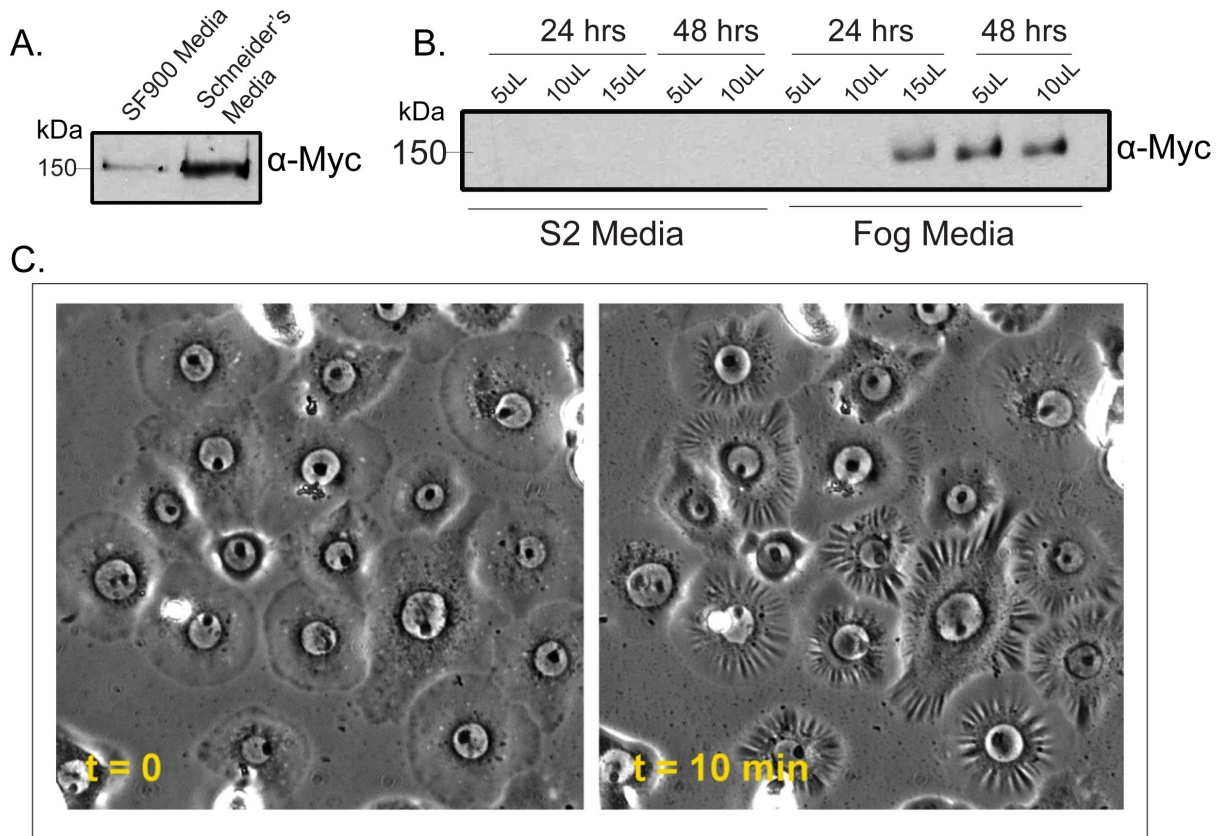


Figure 2.4 Optimization of ectopic Fog collection and application. (A) S2:Fog-Myc cells grown in Schneider's media produce more Fog than cells grown in SF900 media as visualized by anti-Myc antibodies. (B) Media concentrated from S2 and S2:Fog-Myc cells and induced for either 24 or 48 hours. Longer induction times yield more Fog ligand. Blots probed with anti-Myc to recognize Fog. (C) S2R+ cells respond robustly to Fog application. S2R+ cells treated with concentrated Fog media, before Fog application ($t=0$), and after 10 minutes ($t=10$). Phase contrast microscopy.

Chapter III

Regulation of morphogenesis by intersecting expression patterns of *Drosophila* Fog and its receptor, Mist

Preface

This chapter represents a manuscript we have submitted and are currently making revisions for resubmission.

I originally performed a first pass of this screen making dsRNA, and depleting cells of all 44 known peptide-binding GPCRs¹, assuming since Fog is a large peptide that it was probable that one of these GPCRs would bind Fog and activate the signaling pathway. This screen presented no candidates so we compiled a list of all known and putative GPCRs and we ordered plates of pre-made dsRNA from Harvard. Another graduate student in the lab, Alyssa Manning, performed the large dsRNA screen with all 138 known and candidate GPCRs^{1,2}. All experiments for this manuscript were designed by Alyssa Manning, my advisor, Dr. Stephen Rogers, Dr. Mark Peifer, and/or myself. I performed all experiments in Figure 3.1, save Figure 3.1E; Figure 3.3B, and all Figures in Figure 3.4; and Figure S3.2B. All other experiments were performed by Alyssa Manning. This manuscript was written and edited by Alyssa Manning, Dr. Stephen Rogers, Dr. Mark Peifer and myself.

Abstract

Epithelial sheet remodeling is a morphogenetic process that shapes organs and tissues

and establishes the three embryonic germ layers during gastrulation. We have used an innovative approach to identify a key molecule, connecting transcriptional patterning to the cellular machinery involved in epithelial morphogenesis. Using a novel cell-based assay and RNAi screening, we have identified a *Drosophila* G-protein coupled receptor, Mist, which triggers apical constriction to drive epithelial folding at several stages in development, including gastrulation and wing disc morphogenesis. We show that Mist acts as a receptor for the secreted morphogen Folded gastrulation, and that its zygotic expression is regulated by the transcription factor, Snail. Overlapping expression of the ligand receptor pair provides temporal and spatial regulation of tissue morphogenesis.

Introduction

During embryogenesis sheets of epithelial cells are shaped to build organs, define tissue compartments, and establish the embryonic body plan^{3,4}. The forces that drive these tissue-level rearrangements are produced by the actin cytoskeleton and its associated motor proteins and transmitted from cell-to-cell within epithelia by adherens junctions. Regulation of epithelial contractility and adhesion is governed by a complex interplay between maternally supplied proteins and patterned zygotic gene expression; understanding how these two sources of information interact to direct embryogenesis is a key question in the field of developmental biology⁵.

Studies in *Drosophila* have identified evolutionarily conserved molecules involved in apical constriction, a morphogenetic cell shape change that drives epithelial folding, and revealed key insights about the biophysical principles at work⁶. Genetic analyses identified a core-signaling pathway that triggers epithelial folding through apical constriction during

gastrulation, invagination of salivary glands, and folding of the wing imaginal disc epithelium, among others. This pathway is triggered by Folded gastrulation (Fog), a secreted protein thought to act as a ligand for an unidentified receptor on the epithelial cells that produce Fog^{7,8}. The downstream signaling cascade includes a heterotrimeric G-protein complex containing the Gα12/13 homologue Concertina (Cta)^{9,10}. Cta is thought to activate RhoGEF2, which is recruited to the apical membrane by the transmembrane protein T48¹¹. RhoGEF2 in turn activates the small GTPase Rho1^{12,13} to recruit and stimulate cytoskeletal contractile machinery, thereby inducing apical constriction^{8,11}. The Fog pathway has been best characterized during *Drosophila* gastrulation, when a transcriptional cascade triggers localized Fog expression. This initiates formation of both the ventral furrow (VF) to internalize the mesoderm and the posterior midgut (PMG) to internalize the endoderm¹⁴. Thus, *Drosophila* gastrulation provides a classical and powerful model system to study a morphogenetic pathway from the level of gene expression to cytoskeletal regulation.

Materials and Methods

Cell Culture and RNAi

S2 and S2R+ cell lines were obtained from the *Drosophila* Genome Resource Center (Bloomington, IL), and cultivated as described previously¹⁵. S2 cells were maintained in SF900 SFM (Invitrogen, Carlsbad, CA) and S2R+ cells in Sang's and Shield's medium (Invitrogen) supplemented with 5% heat-inactivated FBS (Invitrogen). Double stranded RNAs were produced using Promega (Madison, WI) Ribomax T7 kit according to instructions, or ordered from the *Drosophila* RNAi Screening Center (Boston, MA). Primers

used for dsRNA synthesis are as follows and are all preceded by the T7 sequence (5'-TAATACGACTCACTATAGG-3'). Control-fwd: 5'-TAAATTGTAAGCGTTAATATTTTG-3' and Control-rev: 5'-AATTCGATATCAAGCTTATCGAT-3' to amplify a region from the pBluescript plasmid; Cta-fwd: 5'-TGACCAAATTA ACTCAAGAACGAAT-3', Cta-rev: 5'-TTCCAGGAACTTATCAATCTCTTTG-3'; RhoGEF2-fwd: 5'-ATGGATCACCCATCAATCAAAAAACGG-3', RhoGEF2-rev: 5'-TGTCCCGATCCCTATGACCACTAAGGC-3'; Rho-fwd: 5'-GTAAAACTTGCCTTCTGATTGTCT-3', Rho-rev: 5'-ATCTGGTCTTCTTCCTCTTTTTGA-3'; Mist1-fwd: 5'-AATTGCAAATTGAGGCCAAG-3'; Mist1-rev: 5'-AGAGCATTGATCGGCTGACT-3'; Mist2-fwd: 5'-CTCCATTGCCGGTGATTG-3'; Mist2-rev: 5'-GGAACGTCCACCAGATGTT-3'. For individual RNAi treatments, cells at 50-90% confluency in 6- or 12-well plates were treated every other day for 7 days with 10 µg/ml of dsRNA. Cells were resuspended and plated on Concanavalin A (MP Biomedicals) coated coverslips, allowed to spread for 1 hour, then treated for 10min with concentrated Fog-conditioned medium or medium harvested from untransfected S2 cells (see below). For RNAi screening, 96-well plates containing dsRNAs were heated to 95°C for 3min, and then the temperature was lowered 1°C per 30sec to room temperature. 0.2-0.4 µg of a single dsRNA was added to each well of a 96-well plate; then 2.5x10⁴ cells were plated in each well and incubated at 25°C for 6 days. Cells were resuspended and 2.5x10⁴ cells were plated in each well of a ConA-coated 96-well glass bottom plate (Greiner, Frickenhausen, Germany) for 1 hour prior to Fog treatment. S2 cells were transfected using the Amaxa nucleofector system with Kit V using program G-30

(Lonza, Basel, Switzerland). For quantifying numbers of cells contracted, each condition was repeated at least in three times and ≥ 100 cells were counted per experiment. Statistical significance was determined with Student's t-test.

Production of recombinant Fog protein

We engineered a stable Fog-secreting cell line by amplifying the Fog open reading frame and ligating it into the inducible pMT-V5/His A plasmid (Invitrogen). Stable Fog-producing cells were obtained by co-transfecting S2 cells pMT-Fog-Myc with pCoHygro hygromycin selection plasmid (Invitrogen) followed by antibiotic selection as directed by the manufacturer. Fog producing cells were plated at 70-90% confluency in 150cm² flasks for 24 hours, washed two times with Schneider's SFM (Invitrogen), and induced for 48 hours in Schneider's with 100 μ M CuSO₄. Medium was collected and clarified of cells by centrifugation at 4000 x g for 10 minutes. Cleared medium was concentrated 40x in Amicon 30 k centrifugal concentration devices (Millipore, Billerica, MA). Concentrated Fog containing medium or similar control medium was diluted 1:1 with fresh Schneider's for use on cells.

Immunofluorescence microscopy

Cells

To visualize Mist, cells were plated on coverslips treated with ConA, fixed with 4% formaldehyde (EM Sciences, Gibbstown, NJ) in HL3 buffer (70 mM NaCl; 5 mM KCl; 1.5 mM CaCl₂-2H₂O; 20 mM MgCl₂-6H₂O; 10 mM NaHCO₃; 5 mM trehalose; 115 mM sucrose;

5 mM HEPES; pH to 7.2), and permeabilized with PBST (PBS+0.1% Triton X-100). Cells were blocked with 5% normal goat serum (Sigma-Aldrich, St. Louis, MO) in PBST and stained with anti-Mist antibody diluted into the same solution at 1:500. Following washing, cells were incubated with secondary antibodies (RhodamineX-conjugated goat anti-rabbit diluted 1:1000, Jackson ImmunoResearch, West Grove, PA). After washing, the cells were mounted in fluorescent mounting medium (Dakocytomation, Glostrup, Denmark). We acquired images of the cells using a CoolSnap HQ CCD camera (Roper Scientific, Ottobrunn, Germany) on a Nikon Eclipse Ti inverted microscope driven by Nikon Elements software (Tokyo, Japan).

Drosophila tissue

Embryos were collected on apple juice plates supplemented with yeast paste at 25°C, fixed in 4% formaldehyde in PBS/heptane, methanol divitilenized, and stained as above. DNA was stained with Hoescht 33342 diluted 1:10,000. Wing imaginal discs were collected by picking wandering 3rd instar larvae and dissecting them in PBS, leaving discs attached to the larval cuticles during staining. They were fixed in 4% formaldehyde in PBS with 0.1% Tween-20 and stained as above using mouse anti-actin antibody and Cy2-donkey anti-mouse secondary at 1:1000. Imaginal discs were mounted by dissecting wing discs from the larval cuticles in 70% glycerol in PBS. Images of embryos and imaginal discs were obtained using a Leica DMI 6000 microscope driven by LAS AF software (Leica Microsystems, Buffalo Grove, IL). Cross-sectioned embryos were prepared as previously described in Dawes-Hoang, et al.⁸ and imaged using a Zeiss LSM 710 and LSM software (Zeiss, Thornwood, NY), or a Vt-Hawk Swept-field confocal and Vox Cell-Scan software (Visitech, Sunderland, UK).

Immunoblotting

S2 or S2R+ extracts were produced by resuspending cell pellets in PBS + 0.1% Triton X-100. A small amount was reserved to measure protein concentration. SDS-PAGE sample buffer was then added and boiled for 5 minutes. Comparisons were made by normalizing protein loads to immunoblots performed with antibodies to α -tubulin.

Antibodies

The following antibodies were used in this study: mouse anti- α tubulin monoclonal DM1 α (Sigma), used at 1:500 dilution; mouse anti-Neurotactin (DSHB), used at 1:50; rabbit anti-Twist (gift from Maria Leptin), used at 1:1000; mouse anti-GFP JL8 (Clontech), used at 1:500; sheep anti-Digoxigenin-alkaline phosphatase (Roche, Mannheim, Germany) used at 1:2000; sheep anti-Digoxigenin-POD (Roche) used at 1:50. In addition, streptavidin-alkaline phosphatase (Jackson Immunoresearch) was used at 1:1000. Antibodies to Mist were raised in rabbit against recombinant GST fusions with the COOH-terminal 100 residues of Mist by Pocono Rabbit Farm and Laboratories (Canadensis, PA) and used at 1:500 dilution (cells) or 1:5000 (sectioned embryos).

***In Situ* Hybridization**

Probe preparation and *in situ* hybridization for embryos and imaginal discs was performed essentially as described in Kearney et al.¹⁶. dsRNA *mist* probes were made with Digoxigenin-UTP to the entire predicted coding sequence. Fog probes were made with Biotin-RNA labeling kit (Roche) to the sequence amplified with the same T7-Fog primers

used to make dsRNA for embryo injection (below). Alkaline phosphatase developing was performed in premixed BCIP/NBT (MP Biomedicals), while fluorescence developing was performed with a Cy5 TSA kit (Perkin-Elmer, Waltham, MA). Alkaline phosphatase developed tissues were mounted in 70% glycerol in PBS and imaged using a Zeiss Axiophot microscope, Sony 3XDD CCD video camera, and Zeiss Axiovision software.

Embryo Injection

Embryos were prepared as previously described in Carthew et al.¹⁷, unless noted below.

Primers used for dsRNA synthesis are as follows and are all preceded with the T7 sequence

(5'-TAATACGACTCACTATAGG-3'). Control-fwd: 5'-

TAAATTGTAAGCGTTAATATTTTG-3' and Control-rev: 5'-

AATTCGATATCAAGCTTATCGAT-3'; Fog-Fwd: 5'-

ATATTTTTGAGAAGAAATCCCCAC-3', Fog-Rev: 5'-

CTGTGGTATACTCGTCTTCCTCACT; Mist1 and Mist2: same as used in cell culture.

Embryos were injected with a final concentration of 1 µg/µl for all dsRNAs. Embryos were removed from tape using a steady stream of heptane, fixed with 37% para-formaldehyde, and hand-peeled to remove the vitelline membrane. Images were obtained using a Zeiss LSM 710 and LSM software.

Fly Stocks

The following fly lines were used in this study: UAS-*mist* RNAi , UAS-*cta* RNAi (Vienna Drosophila Resource Center), *moesin*-GFP (Edwards, et al. 1997), *yellow white*, *fog*^{S4}/FM7 *twist*-GFP, A9(wing disc specific)-GAL4, *twist*¹/CyO, *snail*¹⁸/CyO, (from Bloomington

Drosophila Stock Center, Bloomington, Indiana), UAS-*fog* (gift from Eric Wieschaus, Princeton University). UAS-*mist* flies were made by Gateway cloning (Invitrogen) the coding region of *mist* into the pPW vector (Terence Murphy, Carnegie Institution), which was sent to Best Gene (Chino Hills, CA) for injection and recovery of transformants. Wings were collected by using forceps to remove single wings from CO₂-immobilized adults. Wings were placed on white paper and imaged with Nikon SMZ1000 dissecting scope and Nikon CoolPix camera.

Results

Mist acts as a receptor for Folded gastrulation

Although traditional genetic analyses of epithelial folding have identified many of the components involved, the Fog receptor has remained elusive. We used a functional genomic approach to identify receptors for Fog by reconstituting the signaling pathway in a cell-based assay and then used RNAi screening to systematically test candidate receptors. Our previous work showed that activating Rho1 in cultured *Drosophila* S2 cells induces a characteristic contracted morphology¹⁸ and we looked for a similar response in cells upon Fog application. We engineered a stable S2 cell line that expressed and secreted Fog, and used conditioned medium from these cells to screen several immortalized *Drosophila* tissue culture cell lines for a response to Fog. S2R+ cells exhibited a robust contractile response to Fog, but S2 cells and several other epithelial-derived cell lines failed to respond (Figure 3.1A and data not shown). RNAi depletion of components known to be involved in the epithelial folding pathway, including Cta, RhoGEF2, or Rho, prevented Fog-induced S2R+ cell contraction,

indicating that we had recapitulated this morphogenetic cascade in cultured cells (Figure 3.1B).

Since Cta acts downstream of Fog, we hypothesized that Fog signals through a G-protein coupled receptor (GPCR). To identify the receptor in our cultured cell model, we performed a targeted RNAi screen in S2R+ cells, depleting the 138 known and predicted GPCRs in the *Drosophila* genome^{2,19} (Table 3.1) and tested whether the cells contracted in response to Fog. A comparison of triplicate screens revealed that a single dsRNA corresponding to the uncharacterized gene CG4521 (previously called methuselah-like 1, or *meth1*) consistently blocked Fog-induced contraction to the same extent as positive controls. This gene, designated here as Mesoderm-invagination signal transducer (Mist), encodes a predicted GPCR of the secretin receptor family. Mist is predicted to have a large 298 residue NH2-terminal extracellular domain, which is characteristic of this family, seven membrane-spanning helices, and a 93 residue cytoplasmic COOH-terminal domain (Figure 3.1C). Antibodies against Mist recognized a single protein band on immunoblots of S2R+ cells, which was depleted upon treatment with *mist* dsRNA (S3.1A). Thus, Mist is necessary for the Fog response.

We next tested whether Mist was sufficient to confer Fog responsiveness. S2 cells do not express Mist, however, ectopic expression of full-length Mist endowed this cell line with the ability to contract in response to Fog (Figure 3.1D, E, and S3.1B). To determine if Mist's extracellular domain is necessary for Fog signaling, we expressed in S2 cells a deletion construct retaining the signal sequence but lacking the predicted NH2-terminal ectodomain (Mist Δ N, Figure 3.1C). Mist Δ N failed to confer Fog responsiveness upon S2 cells, indicating that the extracellular domain of Mist is required for Fog signaling (Figure 3.1D).

In contrast, Mist Δ C, lacking the cytoplasmic domain could confer pathway activation, indicating the COOH-terminus is not essential for activating downstream effectors (Figure 3.1C, D). Together these data demonstrate that Mist is necessary for Fog signaling in cultured *Drosophila* cells, and that the receptor's large, extracellular domain is required for signaling, perhaps acting as a ligand-binding surface.

Mist regulates Fog dependent epithelial folding in the imaginal wing disc epithelium

Genetic studies revealed that loss of the Fog pathway's downstream effector, RhoGEF2, leads to aberrant folding patterns in the wing imaginal disc epithelium, resulting in malformed adult wings²⁰. Reducing Fog or Cta protein levels enhances this phenotype. To test whether Mist is involved in epithelial folding during *Drosophila* wing development we first assessed *mist* RNA expression in wild-type wing discs. Strikingly, *mist* RNA was expressed in discrete stripes precisely correlating with the folds in the wing disc tissue (Figure 3.2A). *fog* RNA showed a similar pattern of specific expression in the folds, with additional expression in the wing pouch (Figure 3.2B). The overlapping of expression patterns in the folds of the tissue suggests that Mist works with Fog in establishing the folds in the developing wing disc epithelium.

To functionally test the role of Mist we manipulated its levels in wing discs by expressing transgenic *mist* dsRNA using a wing disc specific driver. *mist* RNAi discs displayed abnormal folding patterns, although these defects were no longer apparent in adult wings; phenotypically, these were very similar to wing discs expressing *cta* dsRNA (Figure 3.2C, D). To test the effects of overexpression, we drove ectopic Mist or Fog across the entire imaginal disc. Overexpression of either gene disrupted the stereotypical epithelial

folding pattern, with Fog overexpression exhibiting a stronger effect on imaginal disc misfolding (Figure 3.2C). Fog overexpression resulted in wrinkled adult wings, whereas Mist overexpression did not (Figure 3.2D, E). The Fog overexpression phenotype allowed us to explore the epistatic relationship between Mist and Fog. If Mist is the Fog receptor, it should be essential for wing disc misfolding caused by Fog overexpression. Co-expression of ectopic Fog and *mist* dsRNA completely rescued the misfolding phenotypes induced by Fog overexpression in both imaginal and adult wing tissues, indicating that Mist functions downstream of Fog (Figure 3.2C-E). The difference in phenotypes between *mist* RNAi alone and Fog overexpression with *mist* RNAi may be due to incomplete knockdown or synthetic effects. Together these data confirm a role for Mist downstream of Fog during wing disc morphogenesis in vivo, and indicate that proper expression levels and patterning of both components are important for wing disc folding.

Mist is transcriptionally regulated by Snail in the ventral furrow

As the Fog pathway is used repeatedly in epithelial folding throughout development, we hypothesized that Mist also promotes epithelial folding during gastrulation. We first examined the embryonic localization of *mist* RNA. Low levels are present in the blastoderm, suggesting a maternal contribution corroborated by ModEncode data²¹ (Figure 3.3A). In cellularizing embryos, *mist* transcription is strongly upregulated along the ventral side and posterior end in a stripe of cells corresponding to the VF and PMG primordia, and is absent in all other cells. During VF invagination Mist protein is localized to punctae at the apical contractile surfaces of VF cells (Figure 3.3B, S3.2). *mist* RNA expression remains strong in the mesoderm and midgut after invagination (Figure S3.3A). Thus *mist* expression is

specifically upregulated in contractile cells of the VF and PMG primordia shortly after zygotic transcription begins, allowing spatial and temporal regulation of morphogenesis.

We next examined the relationship between Mist and the genetic pathway specifying mesodermal precursor cells. The embryonic dorso-ventral axis is established by maternally supplied Dorsal protein acting through the zygotic transcription factors Twist and Snail, both of which are independently required for VF invagination^{22,23}. *fog* is a known transcriptional target of Twist in the early embryo, but the Snail targets involved in VF invagination remain unclear^{7,24-26}. To test if ventral *mist* expression is downstream of Twist or Snail, we performed *in situ* hybridization to examine patterns of *mist* expression in wild-type, *twist*, and *snail* mutant embryos. Wild-type embryos exhibited robust expression of *mist* in the VF and PMG from cellularization through the beginning of germ band extension (embryonic stages 5 through 8, Figure 3.3A and insets in 3.3C). When we crossed *snail* heterozygous parents, 25% of embryos, presumably *snail* homozygous mutants, lacked *mist* expression in the VF but retained expression in the PMG (Figure 3.3C, D). In contrast, almost all embryos from *twist* heterozygous parents exhibited wild-type *mist* expression with only a few lacking VF expression (Figure 3.3D, S3.3B). As Twist enhances Snail expression in the mesoderm²⁷, the low frequency of *mist* misexpression observed in the *twist* mutants likely reflects this. Thus Snail is required for *mist* expression specifically in the VF.

Mist regulates ventral furrow formation in the developing *Drosophila* embryo

To determine whether Mist is involved in epithelial morphogenesis during VF formation we injected dsRNA into preblastoderm stage embryos. Control dsRNA injected embryos rarely exhibited morphogenetic defects, while >50% of *mist* dsRNA injected

embryos displayed disorganization of the ventral midline and/or failure of mesoderm invagination (Figure 3.4A, D-G). These defects closely resembled defects seen in *fog* dsRNA injected or *fog* hemizygous mutant embryos, though *fog* deficient embryos exhibited more severe defects than *mist* dsRNA injected embryos (Figure 3.4B, C, G). This discrepancy may be caused by incomplete knockdown of *mist* due to maternal contribution. The similarities in phenotypes between *mist* and *fog* depleted embryos is further evidence that the two act in conjunction during epithelial folding many times during development.

Discussion

The Fog pathway is a premier example of how transcriptional programming is translated into cell behavior, but a key component was missing from our knowledge. Our data strongly support that the *Drosophila* GPCR Mist is a receptor for the secreted factor Fog. We revealed the identity of a long-sought part of a morphogenetic pathway leading from the transcription factors Twist and Snail to the cellular machinery involved in triggering epithelial folding (Figure 3.4H). Mist also represents the first downstream transcriptional target activated by Snail to induce gastrulation movements. These data help explain how the branches of the Twist and Snail regulatory pathway are ultimately integrated, by driving independently patterned, yet overlapping expression of the ligand receptor pair (Figure 3.4I). We favor a model in which apical constriction is regulated during multiple points throughout *Drosophila* development by patterned expression of both Fog and Mist. In the ventral furrow, Twist activates production of Fog and T48 and reinforces Snail expression in the ventral presumptive mesoderm cells. Snail, in turn, promotes Mist expression. Fog is secreted and activates Mist via autocrine signaling, leading to activation of Cta, recruitment of RhoGEF2 to the apical membrane via T48, and localized contractility through the Rho pathway. The

patterned expression of receptor-ligand pairs is likely to reflect a general principle of embryonic morphogenesis in *Drosophila*, as well as in other organisms.

Acknowledgments

We thank S. Crews, B. Goldstein, and K. Slep for feedback on the manuscript. We thank M. Leptin and E. Wieschaus for reagents. This work was supported by grants from the NIH (RO1-GM081645 to SLR and RO1-GM47857 to MP) and the Arnold and Mabel Beckman Foundation (Beckman Young Investigator Award to SLR). KAP was supported by funding from the Lineberger Comprehensive Cancer Center.

References

1. Hewes, R. S. Neuropeptides and Neuropeptide Receptors in the *Drosophila melanogaster* Genome. *Genome Research* **11**, 1126–1142 (2001).
2. Brody, T. *Drosophila melanogaster* G Protein-coupled Receptors. *J. Cell Biol.* **150**, 83F–88 (2000).
3. Lecuit, T. & Lenne, P.-F. Cell surface mechanics and the control of cell shape, tissue patterns and morphogenesis. *Nat. Rev. Mol. Cell Biol.* **8**, 633–644 (2007).
4. Kasza, K. E. & Zallen, J. A. Dynamics and regulation of contractile actin-myosin networks in morphogenesis. *Curr. Opin. Cell Biol.* **23**, 30–38 (2011).
5. Leptin, M. *Drosophila* gastrulation: from pattern formation to morphogenesis. *Annu. Rev. Cell Dev. Biol.* **11**, 189–212 (1995).
6. Sawyer, J. M. *et al.* Apical constriction: a cell shape change that can drive morphogenesis. *Dev. Biol.* **341**, 5–19 (2010).
7. Costa, M., Wilson, E. T. & Wieschaus, E. A putative cell signal encoded by the folded gastrulation gene coordinates cell shape changes during *Drosophila* gastrulation. *Cell* **76**, 1075–1089 (1994).
8. Dawes-Hoang, R. E. *et al.* folded gastrulation, cell shape change and the control of myosin localization. *Development* **132**, 4165–4178 (2005).
9. Parks, S. & Wieschaus, E. The *Drosophila* gastrulation gene *concertina* encodes a G alpha-like protein. *Cell* **64**, 447–458 (1991).
10. Izumi, Y., Ohta, N., Itoh-Furuya, A., Fuse, N. & Matsuzaki, F. Differential functions of G protein and Baz-aPKC signaling pathways in *Drosophila* neuroblast asymmetric division. *J. Cell Biol.* **164**, 729–738 (2004).
11. Kolsch, V., Seher, T., Fernandez-Ballester, G. J., Serrano, L. & Leptin, M. Control of *Drosophila* Gastrulation by Apical Localization of Adherens Junctions and RhoGEF2. *Science* **315**, 384–386 (2007).
12. Barrett, K., Leptin, M. & Settleman, J. The Rho GTPase and a putative RhoGEF mediate a signaling pathway for the cell shape changes in *Drosophila* gastrulation. *Cell* **91**, 905–915 (1997).
13. Häcker, U. & Perrimon, N. DRhoGEF2 encodes a member of the Dbl family of oncogenes and controls cell shape changes during gastrulation in *Drosophila*. *Genes Dev.* **12**, 274–284 (1998).

14. Sweeton, D., Parks, S., Costa, M. & Wieschaus, E. Gastrulation in *Drosophila*: the formation of the ventral furrow and posterior midgut invaginations. *Development* **112**, 775–789 (1991).
15. Rogers, S. L. & Rogers, G. C. Culture of *Drosophila* S2 cells and their use for RNAi-mediated loss-of-function studies and immunofluorescence microscopy. *Nat Protoc* **3**, 606–611 (2008).
16. Kearney, J. B., Wheeler, S. R., Estes, P., Parente, B. & Crews, S. T. Gene expression profiling of the developing *Drosophila* CNS midline cells. *Dev. Biol.* **275**, 473–492 (2004).
17. Carthew, R. W. Microinjection of dsRNA into *Drosophila* Embryos. *Cold Spring Harbor Protocols* **2006**, pdb.prot4516–pdb.prot4516 (2006).
18. Rogers, S. L., Wiedemann, U., Häcker, U., Turck, C. & Vale, R. D. *Drosophila* RhoGEF2 associates with microtubule plus ends in an EB1-dependent manner. *Curr. Biol.* **14**, 1827–1833 (2004).
19. Broeck, J. V. Insect G protein-coupled receptors and signal transduction. *Arch. Insect Biochem. Physiol.* **48**, 1–12 (2001).
20. Nikolaidou, K. K. & Barrett, K. A Rho GTPase signaling pathway is used reiteratively in epithelial folding and potentially selects the outcome of Rho activation. *Curr. Biol.* **14**, 1822–1826 (2004).
21. Gerstein, M. B. *et al.* Integrative analysis of the *Caenorhabditis elegans* genome by the modENCODE project. *Science* **330**, 1775–1787 (2010).
22. Leptin, M. & Grunewald, B. Cell shape changes during gastrulation in *Drosophila*. *Development* **110**, 73–84 (1990).
23. Zusman, S. B. & Wieschaus, E. F. Requirements for zygotic gene activity during gastrulation in *Drosophila melanogaster*. *Dev. Biol.* **111**, 359–371 (1985).
24. Simpson, P. Maternal-Zygotic Gene Interactions during Formation of the Dorsoventral Pattern in *Drosophila* Embryos. *Genetics* **105**, 615–632 (1983).
25. Alberga, A., Boulay, J. L., Kempe, E., Dennefeld, C. & Haenlin, M. The snail gene required for mesoderm formation in *Drosophila* is expressed dynamically in derivatives of all three germ layers. *Development* **111**, 983–992 (1991).
26. Seher, T. C., Narasimha, M., Vogelsang, E. & Leptin, M. Analysis and reconstitution of the genetic cascade controlling early mesoderm morphogenesis in the *Drosophila* embryo. *Mech. Dev.* **124**, 167–179 (2007).

27. Leptin, M. twist and snail as positive and negative regulators during *Drosophila* mesoderm development. *Genes Dev.* **5**, 1568–1576 (1991).

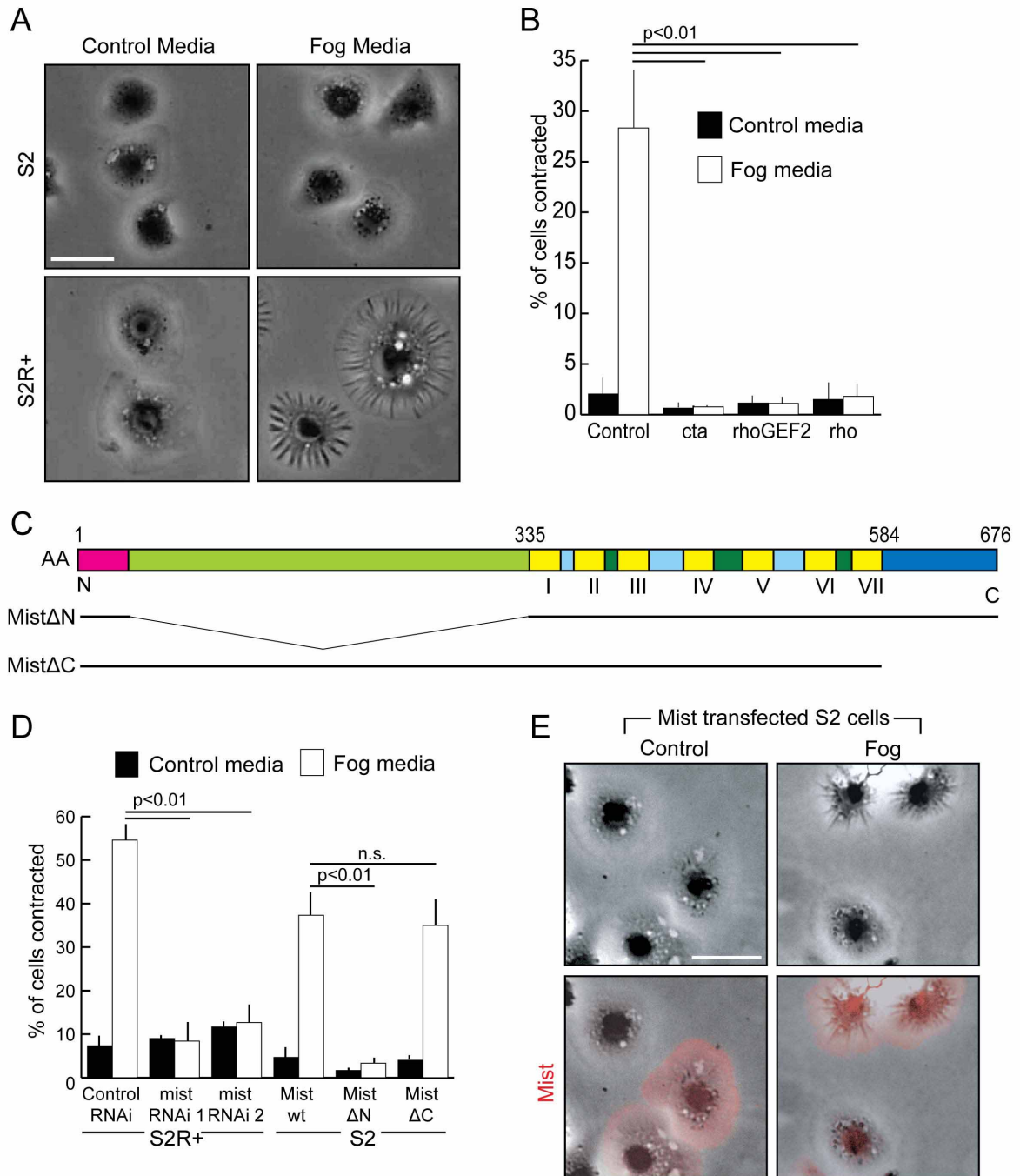


Figure 3.1 Mist acts as a Fog receptor. (A) S2R+ and S2 cells treated with control- or Fog-conditioned media. (B) Percentage of S2R+ cells contracted in response to 10-minute treatment with control- or Fog-conditioned media after RNAi knockdown of known Fog pathway components Cta, RhoGEF2, and Rho. (C) Mist predicted structure. Top: 37aa signal sequence (pink), 298aa extracellular domain (light green), 7 predicted transmembrane domains (yellow, numbered with Roman numerals), and a 93aa intracellular domain (dark

blue). Extracellular loops are dark green and intracellular loops light blue. Bottom: Mist truncations used in D. (D) Percentage of cells contracted in response to 10-minute control or Fog treatment after *mist* knockdown (in S2R+ cells) or overexpression on Mist constructs (in S2 cells). n.s.: not significant. (E) S2 cells transfected with untagged Mist treated with control or Fog media and stained for Mist (red). Scale bar A, E: 20 μ m.

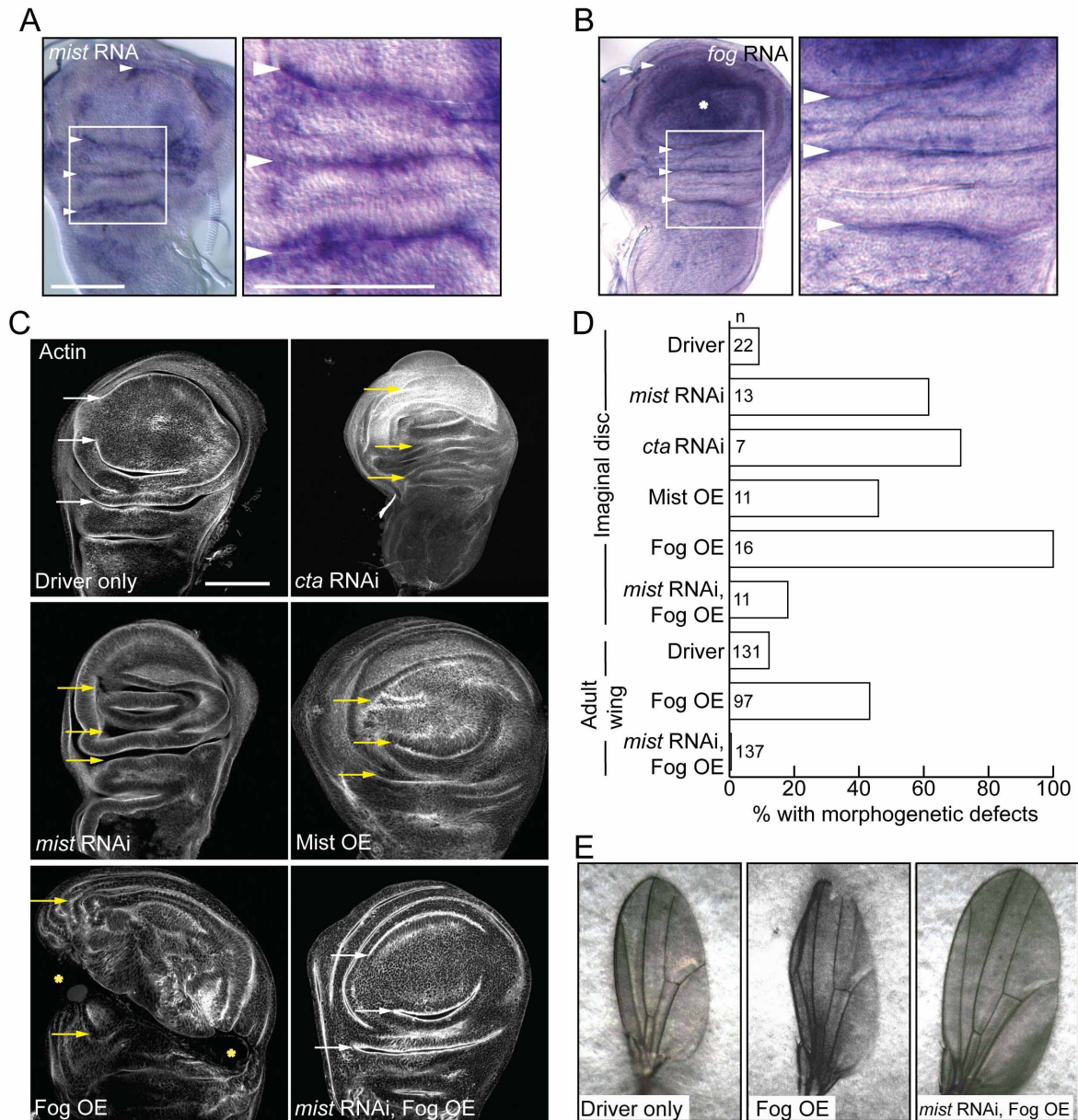


Figure 3.2 Proper Mist and Fog expression is required for wing imaginal disc morphogenesis. (A-B). Left: *In situ* hybridization for *mist* (A) or *fog* (B) RNA in wildtype wing imaginal discs. Right: Higher magnification of boxed areas in left-hand panels. Arrowheads indicate furrows with RNA expression. *: RNA in wing pouch. (C). Actin staining of wing imaginal discs. The driver line alone exhibits the stereotypical wild-type folding pattern of the disc. *cta* RNAi or *mist* RNAi results in misfolding of the tissue. Overexpressing Mist or Fog leads to minor or major disruptions in tissue folding, respectively. The Fog OE disc has a gap between the two asterisks. Reducing *mist* levels in discs with overexpressed Fog greatly reduces the level of disc misfolding. White arrows: proper folds; yellow arrows: misfolding. (D). Percentages of wing imaginal discs and adult wings with morphogenetic defects. n= number of imaginal discs or adult wings scored for

each condition. (E). Individual wings from Driver only, Fog OE, and mist RNAi Fog OE adults. Scale bar A-C: 100 μ m.

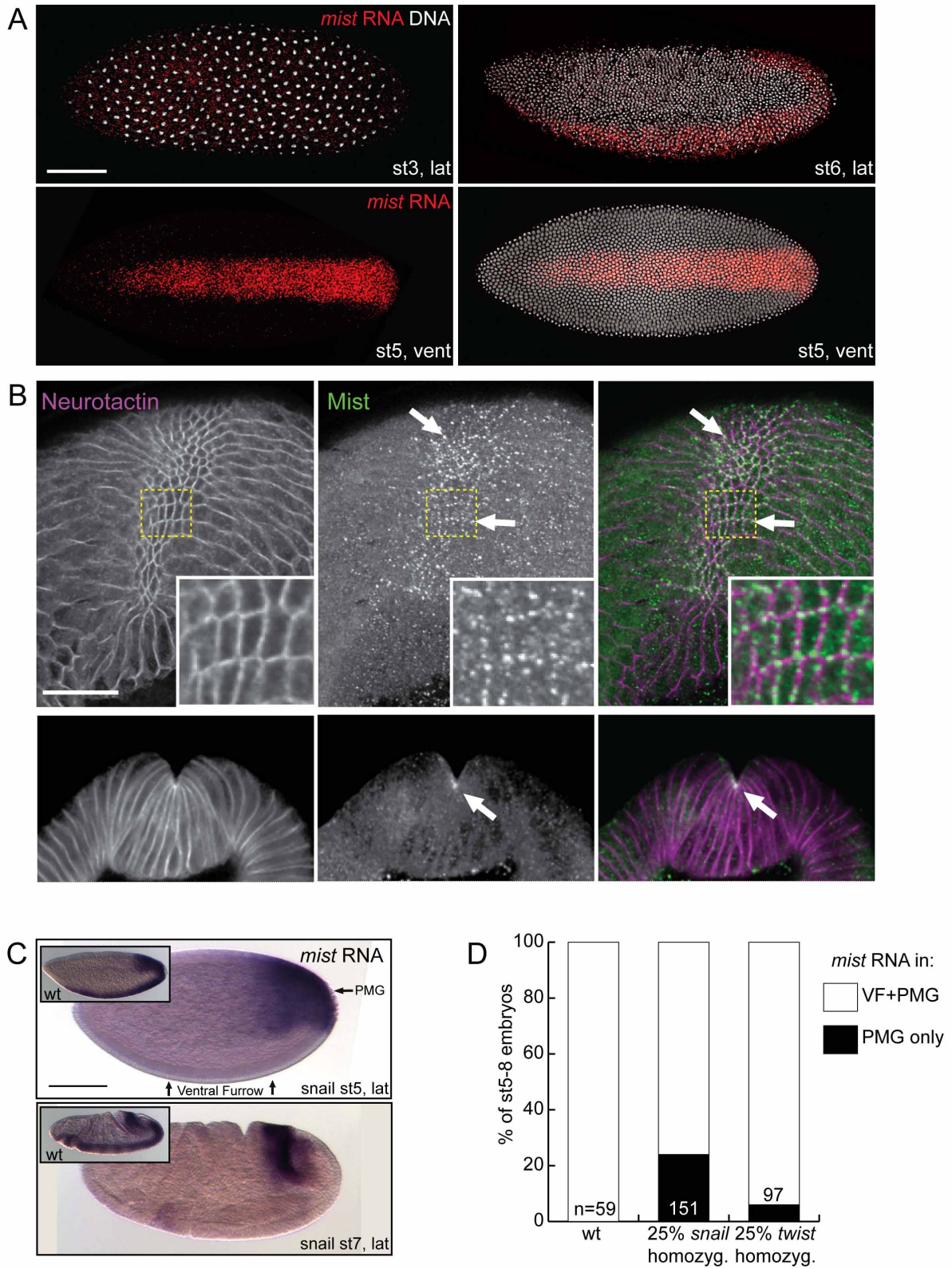


Figure 3.3 *mist* expression is upregulated in the ventral furrow downstream of Snail.
 (A). Fluorescent *in situ* hybridization for *mist* RNA (red) in wild-type embryos

counterstained for DNA (white). There is a low ubiquitous maternal contribution of *mist* RNA. At cellularization and into VF formation, *mist* RNA is restricted to a ventral stripe of cells. Bottom left is *mist* channel alone from bottom right image. Anterior is to the left. lat: lateral view; vent: ventral view. (B). *Mist* immunofluorescence in VF. During apical constriction *Mist* protein is localized apically and is enriched in the presumptive mesodermal cells. Top: Grazing apical section, insets show enlarged image of boxed area; bottom: cross section. Membranes are marked with Neurotactin (magenta) and *Mist* is in green. Arrows point to areas of *Mist* enrichment. (C). *In situ* hybridization to *mist* RNA in snail mutant embryos. Corresponding stages of wild-type embryos are shown in insets. (D). Percentages of stage 5-8 embryos with PMG only or PMG and VF localization of *mist* RNA. n=number of embryos scored for each condition. Scale bar A, C: 100 μ m; B: 25 μ m.

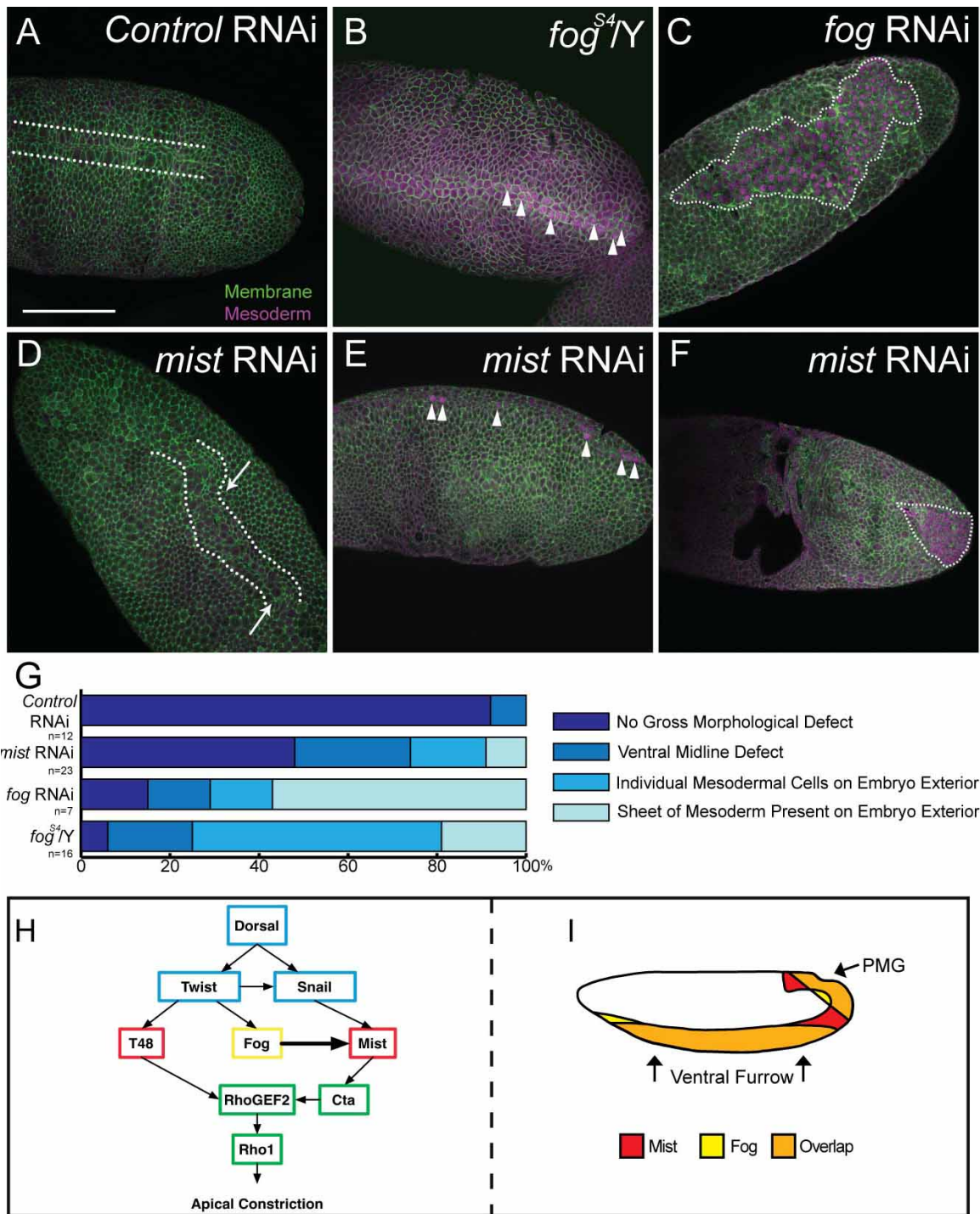


Figure 3.4 Mist depletion causes defects during VF invagination. (A). Moesin-GFP expressing embryo injected with control dsRNA has a normal, straight ventral midline (flanked by dotted lines). (B). *fog* hemizygous mutant exhibiting improperly internalized mesoderm. (Arrowheads indicate mesoderm on embryo surface). (C). *fog* dsRNA injected embryo displays a wide swath of mesoderm on the exterior surface (outlined with dotted line). (D). *mist* dsRNA injected embryo with minor morphological defects in the ventral midline

(arrows). (E). *mist*-injected embryo with improper invagination of individual mesodermal cells, or (F). with a large area of mesoderm present on the exterior of the embryo. Cell membranes (green) are outlined with either Moesin-GFP (A, C-F), or Neurotactin (B). Mesoderm (magenta) is stained for Twist (A-F). (G). Quantification of morphological defects in dsRNA injected embryos and *fog* hemizygous mutants. n=number of embryos scored for each condition. (H). Model for Mist regulation and function within Fog signaling pathway. Colored boxes denote classification of Fog pathway components. Blue: Transcription factor, Yellow: Secreted protein, Red: Transmembrane protein, Green: Cytoplasmic protein. I. Schematic of *mist* and *fog* RNA expression in cellularizing embryos. Areas of overlapping expression are where the VF and PMG invaginate. Scale bar A: 100 μ m.

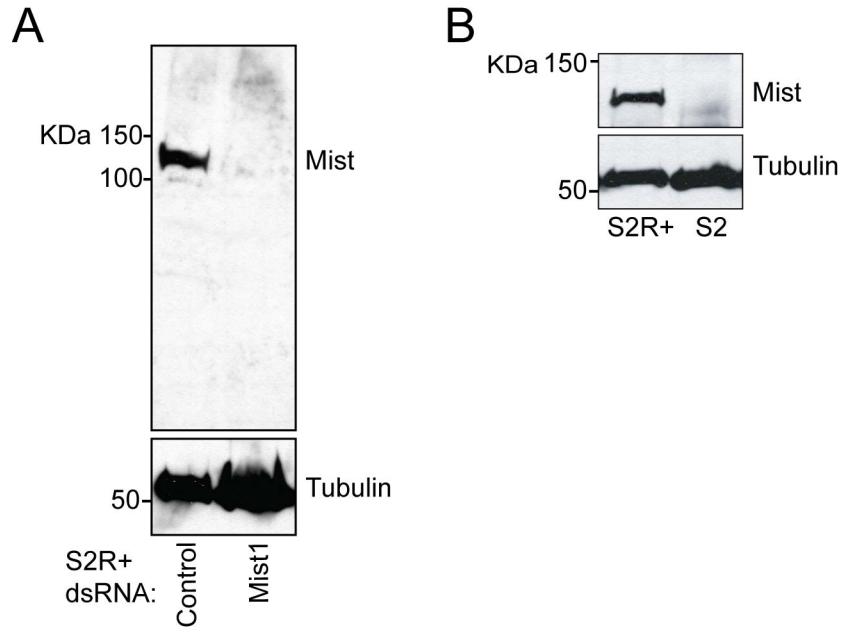


Figure S3.1 Mist is expressed in S2R+, but not S2 cells. (A). Western blot of S2R+ cell lysates for Mist, after control or *mist* dsRNA treatment. (B). Mist is expressed in S2R+ cultured cells, but absent from S2 cultured cells. α -tubulin used as loading control.

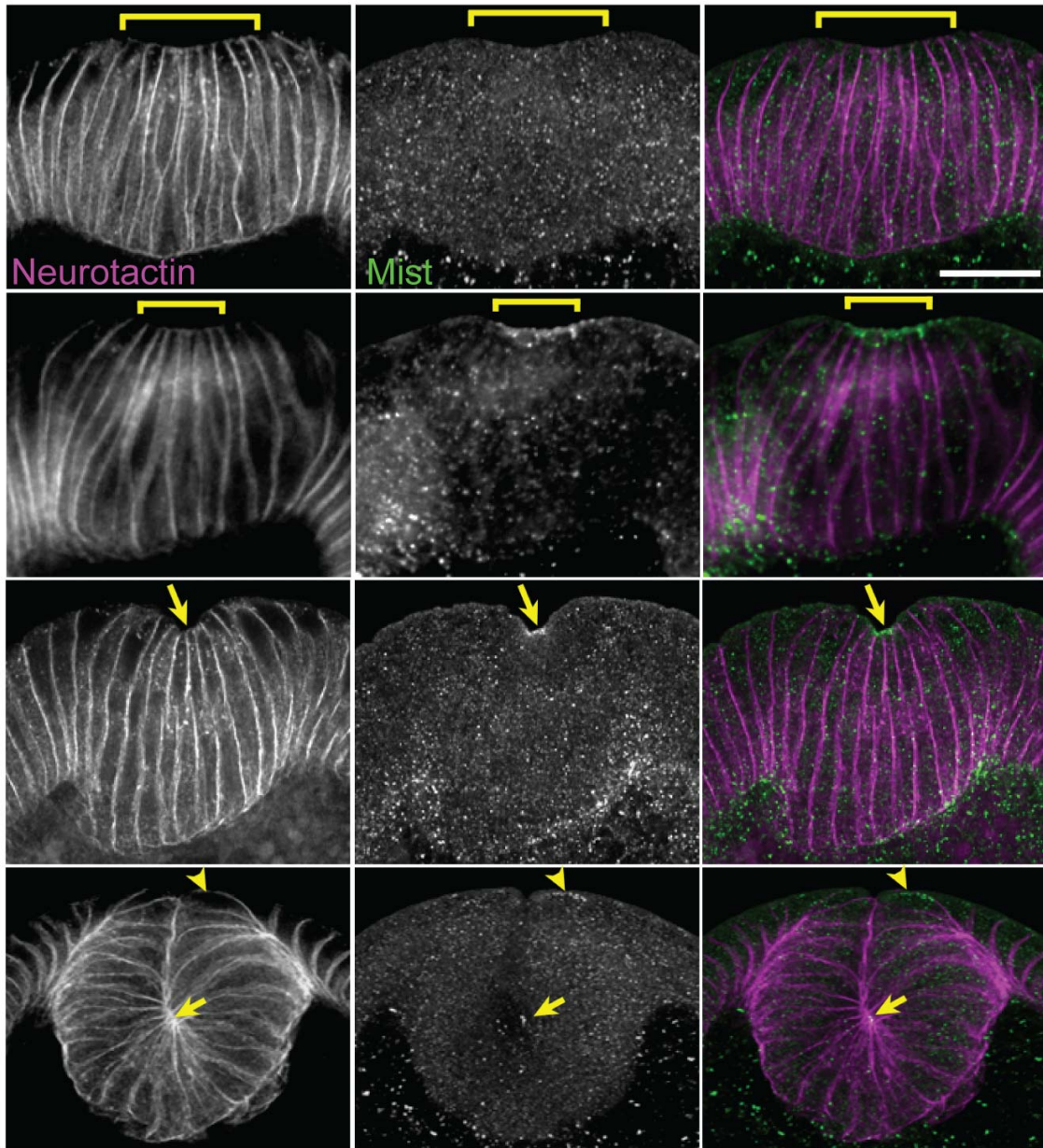


Figure S3.2 Mist is temporally and spatially localized during VF formation. Series of cross-sectioned embryos over time show that Mist is specifically enriched at the apical ends of cells that are actively undergoing apical constriction during VF formation. Brackets designate ventral furrow. Arrows and arrowheads indicate areas of Mist enrichment. Scale bar: 20 μ m.

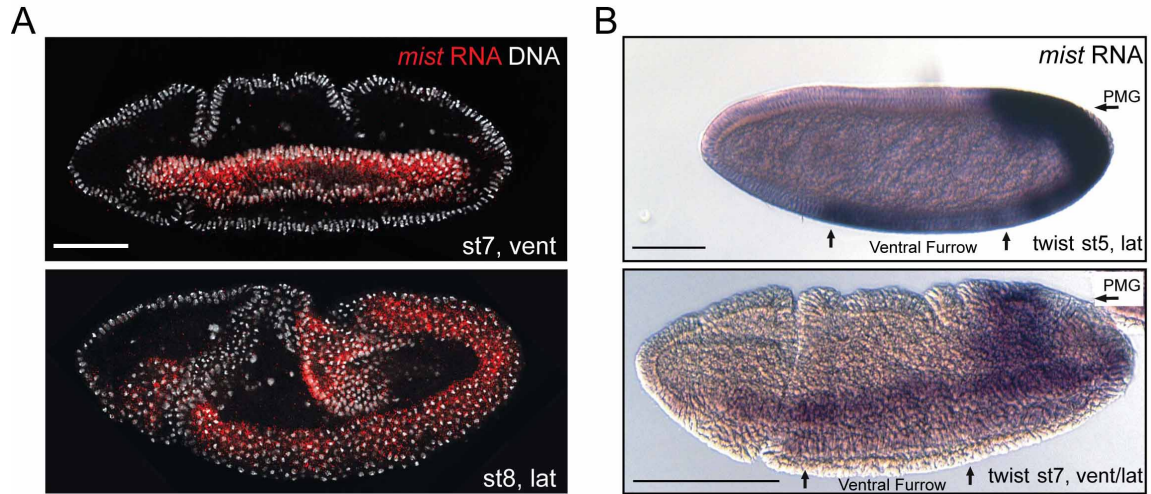


Figure S3.3 *mist* is expressed in embryos depleted of *twist*. (A). *mist in situ* hybridization in wild-type embryos shows mesodermal *mist* expression after VF and PMG invagination. (B). *mist in situ* hybridization in embryos from *twist* heterozygous parents shows both VF and PMG expression. vent: ventral view; lat: lateral view. Scale bars: 100 μ m.

5-HT1A	CG13802	CG4313	ETHR	mthl13	Rh4
5-HT1B	CG13995	CG4395	FR	mthl14	Rh5
5-HT2	CG14593	CG4875	Fsh	mthl2	Rh6
5-HT7	CG15556	CG7431	fz	mthl3	Rh7
AdoR	CG15614	CG7497	fz2	mthl4	rho
AlcR2	CG18208	CG7536	fz3	mthl5	rho-4
AlstR	CG2061	CG7918	fz4	mthl6	rho-5
AR-2	CG2901	CG7994	GABAB-R1	mthl7	rho-6
boss	CG30106	CG8007	GABAB-R2	mthl8	rho-7
capaR	CG30340	CG8784	GABAB-R3	mthl9	rk
CcapR	CG31660	CG8795	GRHR	mXr	ru
CCKLR17D1	CG31720	CG9643	GRHR11	NepYr	SIFR
CCKLR17D3	CG31760	CG9918	kek3	ninaE	smo
CG10481	CG32447	Cirl	Lgr3	NPFR1	SPR
CG10483	CG32547	cry	Lkr	NPFR76F	stan
CG11318	CG32843	Cyp1	mAcR-60C	oa2	star1
CG11910	CG33310	D2R	mGluRA	Oamb	stet
CG12290	CG33639	Dh44-R1	moody	Octbeta2R	Takr86C
CG12370	CG33696	DmsR1	mth	Octbeta3R	Takr99D
CG12796	CG34372	DmsR2	mthl1 (Mist)	pdfr	Tre
CG13229	CG34381	DopEcR	mthl10	Proc-R	Tre1
CG13575	CG34411	DopR	mthl11	Rh2	TyrR
CG13579	CG4168	DopR2	mthl12	Rh3	TyrR11

Table 3.1 List of genes targeted with dsRNAs in cell culture screen. Each was targeted by at least one dsRNA. Mist is highlighted in red.

Chapter IV

***Drosophila* Ric8 interacts with the G α 12/13 subunit, Concertina, during activation of the Folded gastrulation pathway**

Preface

This work has been submitted for review for publication. All of the experiments were designed by my advisor Dr. Stephen Rogers, and myself. All experiments were performed by me. The manuscript was edited by Dr. Stephen Rogers and myself.

Abstract

Heterotrimeric G proteins are composed of α , β , and γ subunits and are activated by exchange of GDP for GTP on the G α subunit, a reaction that leads to the separation of G α and G $\beta\gamma$ to allow targeting of downstream effectors. Canonically, G α is stimulated by the guanine-nucleotide exchange factor (GEF) activity of ligand-bound G protein coupled receptors (GPCRs). However, G α subunits may also be activated in a non-canonical manner by members of the Ric-8 family, cytoplasmic proteins that also act as GEFs for G α subunits. We have used a signaling pathway active during *Drosophila* gastrulation as a model system to study Ric-8/G α interactions. A component of this pathway, the *Drosophila* G α 12/13 subunit, Concertina (Cta), is necessary to trigger acto-myosin contractility during gastrulation events. *Ric-8* mutants exhibit similar defects to *Cta* mutants in this process. Here we describe a novel tissue culture system to study a signaling pathway that controls cytoskeletal rearrangements necessary for cellular morphogenesis. We show that Ric-8 regulates this

pathway through a physical interaction with Cta, and that Ric-8 preferentially interacts with inactive Cta and directs its localization within the cell. We also used this system to conduct a structure-function analysis of Ric-8 and identified key residues required for interaction with Cta and cellular contractility. Our data demonstrate that evolutionarily conserved residues facilitate Ric-8/Cta interaction downstream of receptor activation to localize inactive Cta.

Introduction

G protein coupled receptors (GPCRs) are a highly conserved family of transmembrane receptors that have evolved to detect a wide range of signals including neurotransmitters, hormones, odorants, and light. These receptors have a characteristic topology that spans the membrane via 7 α -helices and are oriented with their N-termini towards the extracellular space, their C-termini inside the cell, and three inter-helical loops on each side. Ligand binding allows the cytoplasmic domains of the GPCR to activate heterotrimeric G proteins, downstream signaling molecules that consist of a GTP-binding α subunit that exists in a 1:1:1 stoichiometry with a β and γ subunit. These three proteins form a tightly-bound inactive heterotrimer when $G\alpha$ is in its GDP-bound state. Activation of the GPCR induces a conformational change that triggers its guanine nucleotide exchange factor (GEF) activity for $G\alpha$ causing $G\alpha$ to exchange bound-GDP for GTP. Active $G\alpha$ -GTP dissociates from the $G\beta\gamma$ heterodimer and both species are able to regulate downstream effector molecules, such as ion channels and enzymes that produce second messengers. $G\alpha$ subunits have an intrinsic GTPase activity that hydrolyzes GTP to GDP causing the complex to reform into its inactive state. This cycle of activation and inactivation may be modulated by accessory factors, such as RGS (regulator of G protein signaling) proteins that accelerate the rate of GTP hydrolysis

by G α subunits (for review see¹⁻³). Thus, although the core regulatory component in heterotrimeric G protein signaling is the nucleotide-bound state of the G α subunit, the activities of these molecules are affected by accessory factors that may reflect various signaling inputs into the pathways.

At the biochemical level Ric-8 has been found to act as a non-canonical GEF for multiple families of G α subunits^{4,5} by associating with G α -GDP, often complexed with a GDI (guanine-nucleotide dissociation inhibitor), such as the Go-Loco repeat containing family of proteins (for example GPR1/2 in *C. elegans* and Pins in *Drosophila melanogaster*). Ric-8 binding inactive G α facilitates GDP release and promotes the formation of a transient nucleotide-free state, which allows G α -GTP exchange by cytosolic excess of GTP⁴. Additionally, Ric-8 has been shown to bind to and drive dissociation of G α -GDP complexed with a GDI, subsequently freeing G α to engage other effectors⁶⁻⁸. Recently, Ric-8 was identified as a chaperone involved in the biosynthesis of mammalian G α subunits and their subsequent localization to the plasma membrane⁹. Thus, it is evident that Ric-8 regulates multiple aspects of G α function.

A growing body of evidence has implicated the Ric-8 family of proteins as important accessory molecules involved in heterotrimeric G protein signaling in a variety of developmental processes (for review see¹⁰). Ric-8 is a highly conserved cytosolic protein that was originally identified in a screen for proteins required for G α_q signaling in the *C. elegans* nervous system¹¹. Since then, Ric-8 has been implicated as a regulator of signaling in events as diverse as fungal pathogenesis and development^{12,13} to modulation of mammalian vision, taste, olfaction and bone formation¹⁴⁻²³. Ric-8 plays a well-defined role in spindle orientation during mitosis of asymmetrically dividing cells. During early divisions

of the *C. elegans* embryo Ric-8 acts through $G\alpha_i$ family members to establish the position of the mitotic spindle through modulation of pulling forces along the anterior-posterior axis²⁴⁻²⁷. Similarly, in *Drosophila*, Ric-8 functions through $G\alpha_i$ to align the mitotic spindle in both neuroblast and sensory organ precursor cells^{7,28,29}. Recent findings also show that Ric-8 is important for spindle alignment in asymmetric cell division in mammalian tissue culture³⁰. In addition to spindle positioning, Ric-8 regulates cytoskeletal rearrangements during dorsal ruffle formation via $G\alpha_{13}$ in mammalian tissue culture³¹. These data demonstrate that Ric-8, through its interaction with $G\alpha$ subunits, functions to regulate diverse processes during G protein signaling events, including cytoskeletal behavior.

Drosophila gastrulation has proven to be a powerful model system to study heterotrimeric G protein signaling within a developmental context. During this process, the *Drosophila* blastoderm undergoes a series of highly orchestrated cell movements to drive subsets of cells into the interior of the embryo to establish the germ layers. One of the hallmarks of gastrulation is the invagination of a subset of epithelial cells along the ventral midline to form a structure called the ventral furrow³². Furrow formation is driven by concerted cellular shape changes in which apical constriction of the actin network by myosin II has the net effect of driving the internalization of the mesodermal precursor cells^{33,34}. Genetic analysis of this pathway has identified several components that are thought to act sequentially to trigger apical constriction. First, the midline epithelial cells destined to invaginate secrete an extracellular protein, Folded gastrulation (Fog), from their apical domains. Fog acts as an autocrine signal and binds to an unidentified transmembrane receptor that then signals through a heterotrimeric G protein complex containing the *Drosophila* $G\alpha_{12/13}$ subunit, Concertina (Cta)^{35,36}. Mutations in the $G\beta_{13F}$ and $G\gamma_1$

subunits exhibit gastrulation defects and, presumably, comprise the $\beta\gamma$ subunits of the heterotrimer along with Cta²⁸. Cta activates a guanine nucleotide exchange factor, RhoGEF2, relocalizing RhoGEF2 from the plus end tips of growing microtubules to the cortex, where it is docked by its interaction with a transmembrane protein, T48³⁷⁻³⁹. RhoGEF2 then activates the small G protein Rho1 which activates myosin II at the apical domain via Rho kinase (Rok), thus producing contraction^{33,38,40}. Mutations in any Fog pathway component interfere with the timing or execution of normal gastrulation. This pathway has been implicated in epithelial remodeling during later stages of development, as well³⁸. *Drosophila* gastrulation events are highly analogous to epithelial remodeling in other multi-cellular organisms, most notably neural tube formation in the developing vertebrate embryo, and downstream signaling components are conserved between invertebrates and vertebrates⁴¹. Thus, we are using the *Drosophila* Fog signaling pathway as a model system to investigate general mechanisms of signaling during tissue remodeling.

Given the central importance of Cta to *Drosophila* gastrulation, it is a useful model to study potential interactions between Ric-8 and G α 12/13-class subunits. Two previous studies showed that Ric-8 mutants exhibited gastrulation defects that resembled Cta loss-of-function^{7,28}, however, the mechanistic details through which Ric-8 functions in this process remain to be determined. Here, we examined the role of Ric-8 signaling in the Fog pathway using a novel cell-based assay for Fog-induced cellular contractility. We used RNAi to show that Ric-8 is necessary for Fog signaling and that it functions within the pathway at the level of Cta. Ric-8 directly interacted with Cta and exhibited higher affinity for inactive Cta mutants (GTP-free). We present biochemical data that shows Ric-8 preferentially binds and specifically acts, to localize inactive Cta downstream of Fog/GPCR signaling. Finally, by

mutating electrostatic amino acids conserved across species we identified specific residues within Ric-8 required for Cta function and/or establishing a binding interface between the two molecules. Based on our results we propose a model wherein Ric-8 acts downstream of Fog pathway activation to localize/scaffold inactive Cta, potentiating Fog signaling to drive persistent cellular constriction.

Materials and Methods

Tissue Culture, Transfection, and RNAi

S2 and S2R+ cell lines were obtained from the *Drosophila* Genome Resource Center (Bloomington, IL), and propagated as previously described⁴². S2 cells were maintained in SF900 SFM (Invitrogen, Carlsbad, CA) and S2R+ cells in Sang's and Shield's medium (Invitrogen) supplemented with 5% heat-inactivated FBS (Invitrogen). S2 and S2R+ cells were transfected with 2µg/µL of DNA using the Amaxa nucleofector system with Kit V using program G-30 (Lonza, Basel, Switzerland), or with Fugene HD (Promega) (except the Mito-tag constructs where 1µg/µL concentration of DNA was used). For individual RNAi treatments, cells at 75-90% confluency in 6- or 12-well plates were treated every other day for at least 10 days with 15µg/ml of dsRNA. dsRNAs were produced using Promega (Madison, WI) Ribomax T7 kit according to instructions. Primers used for dsRNA synthesis are as follows and are all preceded by the T7 sequence (5'-TAATACGACTCACTATAGG-3'). Control-fwd: 5'-TAAATTGTAAGCGTTAATATTTTG-3' and Control-rev: 5'-AATTCGATATCAAGCTTATCGAT-3' to amplify a region from the pBluescript

plasmid; Cta-fwd: 5'-TGACCAAATTA ACTCAAGAACGAAT-3', Cta-rev: 5'-
TTCCAGGAACTTATCAATCTCTTTG-3'; Cta 5'UTR-fwd: 5'-
ATATACAGGCAAAAATTATTATCACCGCTGTTGTTTGC-3', Cta 5'UTR-Rev: 5'-
CGCTGGCAAGCCAACGCCTGATGCTCGCACTTTCTATA-3'; RhoGEF2-fwd: 5'-
ATGGATCACCCATCAATCAAAAACGG-3', RhoGEF2-rev: 5'-
TGTCCTCGATCCCTATGACCACTAAGGC-3'; Rho-fwd: 5'-
GTAAACTTGCCTTCTGATTGTCT-3', Rho-rev: 3'-
ATCTGGTCTTCTTCCTCTTTTTGA-3' Ric-8-fwd: 5'-
GCAGGCGCCAGTGCCTGCGGC-3', Ric-8-rev: 5'-CCGGAGATGTTTGTTCAGCA-3';
Ric-8 5'UTR-fwd: 5'-GCAAAGGTGCGGTCAC-3', Ric-8 5'UTR-rev: 5'-
GTCGCCAACGGTGGC-3'; Ric-8 3'UTR-fwd: 5'-GTATTGCGGGATCTG-3', Ric-8
3'UTR-rev: 5'-GGGCGTGTATTTAA-3'.

Contractility Assay

S2R+ cells were resuspended and plated on Concanavalin A (MP Biomedicals) coated coverslips, allowed to spread for 1-3 hours, then treated for 10 minutes with concentrated Fog-conditioned medium or medium harvested from S2 cells. To produce Fog conditioned medium, we created a stable S2 cell line carrying a Fog-Myc expression construct driven by an inducible metallothionein promoter. Fog-stable S2 cells were grown to 75-90% confluency in T150 flasks before SF-900 media was exchanged for Schneider's media (Invitrogen) and induced with 1mM CuSO₄ for 48 hours. Cells were then pelleted, and the supernatant was concentrated using protein concentrators (Millipore, Billerica, MA,) to approximately 2.5-5% of the original volume. For control media, the same process was

applied to non-Fog expressing S2 cells. Control (S2) and Fog concentrated media was diluted 1:1 with Schneider's media before application. For each experiment, we scored the number of cells within a population that contracted in response to Fog treatment, repeating each condition at least three times and counted ≥ 500 cells. Error bars were calculated using standard error.

Molecular Biology

The Fog-Myc expression construct was generated using PCR to amplify the coding sequence of the gene and introduce a 5' EcoRI site, a C-terminal Myc tag, and a 3' NotI site to allow cloning into pMT-V5/His (Invitrogen). Construction of N-terminally Myc-tagged Cta, and C-terminally GFP-tagged RhoGEF2 constructs was described previously³⁷. The dual expression constructs were created by sub-cloning Myc-Cta constructs into pMT-V5/His containing a second transcriptional unit for membrane-mCherry marker containing the *sqh* promoter and 3' untranslated region⁴³. To generate the expression construct for constitutively active Rho kinase, we used PCR to amplify the catalytic domain (amino acids 1–506) from a cDNA (EST clone LD15203) and introduced a 5' EcoRI site, a 3' NotI site and incorporated the Myc epitope tag at the 5' end of the coding sequence. This insert was then subcloned into pMT-A for inducible expression. Full-length Ric-8a cDNA was subcloned using the Gateway TopoD pEntr system (Invitrogen) into a final zeocin-selectable pIZ backbone that has a metallothionein promoter, Gateway (Invitrogen) LR recombination sites in the multiple cloning site, and a C-terminal eGFP tag. All mutagenesis was performed on this construct using KOD Xtreme Hot Start Polymerase (Novagen, Gibbstown, NJ). Mitochondrial localization of Ric-8 was achieved by N-terminally attaching *Listeria*

monocytogenes ActA residues 310-338⁴⁴.

Immunoprecipitation and Immunoblotting

We bacterially expressed a His and Fc tagged GFP binding protein (Fc-GFP-BP). The Fc-GFP-BP was first purified on a Ni column and the eluted Fc-GFP-BP fractions incubated with Protein A beads. GFP-binding protein was covalently linked to the beads using 20mM dimethylpimelimidate (DMP) (Sigma-Aldrich, St. Louis, MO). Before use in IP experiments beads were washed with IP lysis buffer (50 mM Tris, 150 mM NaCl, 0.5 mM EDTA, 1mM Dithiothreitol, 0.5% Triton X-100, 2.5 mM Phenylmethylsulfonyl fluoride, and Complete EDTA-Free Protease Inhibitor Cocktail [Roche, Indianapolis, IN]).

S2 cells used for IPs were transfected (see above) and induced 24 hours later with 1mM CuSO₄. The following day cells were resuspended, pelleted, and washed before lysing with IP lysis buffer. Samples were removed for input controls, and the rest of the sample was incubated with GFP-binding protein beads. Samples were resuspended in SDS-PAGE sample buffer and boiled for 10 minutes. SDS-PAGE sample buffer was also added to input samples, and boiled for 10 minutes. Samples were run on SDS-PAGE gels, and transferred to nitrocellulose membranes for western blotting using anti-Myc9e10 (DSHB, Iowa City, IA), and anti-GFPJL8 (Clontech). For immunoblot quantitation the pulldown:input ratios were determined using densitometry using ImageJ software (National Institutes of Health, Bethesda, MD) on scanned film images. All immunoblot quantitation was performed at least 3 times on 3 distinct blots. Error bars represent SEM.

Microscopy

Cells were plated onto ConA coated coverslips and prepared for imaging as previously described⁴². Antibodies used for immunofluorescence were, anti-phospho-myosin light chain 2 (Ser19) (Cell Signaling Technology, Inc., Danvers, MA), anti-Ric-8 (gift from William Chia), anti-Fog (gift from Eric Wieschaus), anti-dsRed (Clontech), anti-GFPJL8 (Clontech), anti-Myc9e10 (DSHB), anti-DM1 α and Alexa Fluor 564 Phalloidin (Invitrogen). All cells were imaged using a CoolSnap HQ CCD camera (Roper Scientific) mounted on an Eclipse Ti-E and driven by Nikon Elements software (Nikon, Melville, NY) except cells in Figure 4.4 which were imaged using a TIRF system (Nikon) mounted on an inverted Ti-E microscope using an Andor-Clara Interline camera (Andor Technology, Belfast, UK) and driven by Nikon Elements software.

Results

Reconstitution of Fog-stimulated cellular contractility in a cultured cell model

In order to study the effect of Fog signaling on cell morphology, we developed a cell culture system to allow us to replicate *in vivo* signaling events. We began by engineering a stable S2 cell line that expresses full-length Fog tagged at its C-terminus with the Myc epitope under an inducible metallothionein promoter (S2:Fog-Myc). Costa et al. originally hypothesized that Fog is a secreted protein based on hydropathy analysis of the protein's primary sequence which revealed the presence of an N-terminal 12 amino acid hydrophobic region predicted to function as a signal sequence³⁵. Later analysis of Fog localization in cells of the embryonic ventral furrow and posterior midgut showed that the protein localized to membrane-bound organelles targeted for the apical surface of the blastoderm epithelia³³. To

test whether Fog is secreted from S2:Fog-Myc cells we induced its expression with copper sulfate for 48 hours, collected the conditioned medium, and concentrated it ~20-fold. An affinity-purified antibody against the N-terminus of Fog recognized a single protein with a molecular weight of ~150 kD on immunoblots of conditioned medium from induced S2:Fog-Myc cells and the same sized band was also recognized by a monoclonal anti-Myc antibody. Neither antibody recognized the protein in conditioned medium collected from untransfected S2 cells (Figure 4.1A). Thus, as found in tissues in the *Drosophila* blastoderm preceding cellular shape change, ectopic Fog-Myc is expressed in S2 cells as a secreted protein.

We next screened an assortment of immortalized *Drosophila* cell lines for their ability to respond to Fog-conditioned medium. Previously we showed that activation of the Rho1 pathway in S2 cells caused the cells to adopt a contracted morphology³⁷. We, therefore, used this read-out to test the ability of S2 cells, S2R+ cells, and several immortalized lines derived from imaginal discs, to respond to Fog. S2R+ cells are a sub-line derived from S2 cells that express receptors not found in S2 cells⁴⁵. Neither S2 cells nor the other epithelial lines we tested changed their shape in response to Fog perfusion (data not shown). However, S2R+ cells exhibited a robust morphological response upon perfusion with Fog. S2R+ cells adopt a flattened, discoid morphology when plated on concanavalin A-treated coverslips. Within 10 minutes of Fog treatment the cells adopted a “puckered” shape and pushed their nuclei and organelles up and away from the coverslip. At the same time, radial, phase-dark furrows appeared at the cell periphery and moved centripetally to the center of the cell (Figure 4.1B). One of the downstream effects of Rho pathway signaling is activation of non-muscle myosin II by phosphorylation of the motor’s regulatory light chain (RLC). Therefore, we treated S2R+ cells with concentrated Fog or control cell medium and examined the RLC

phosphorylation state using phospho-specific antibodies. Immunofluorescence with P-RLC (phosphorylated-regulatory light chain) antibodies revealed an overall increase in phosphorylation, along with a dramatic incorporation of myosin II into acto-myosin purse string structures (Figure 4.1C). To verify that Fog was acting via the canonical pathway involved in gastrulation, we used RNAi to deplete Cta, RhoGEF2, or Rho from S2R+ cells prior to Fog treatment. RNAi targeting Cta, RhoGEF2, or Rho prevented cellular constriction following Fog treatment (Figure 4.1B, D) as did pretreatment of S2R+ cells with the Rho-kinase small molecule inhibitor Y-27632 (data not shown). Previous work revealed that embryos mutant for the beta subunit, β 13F, and the gamma subunit, γ 1, exhibited gastrulation phenotypes similar to Cta mutants²⁸. We introduced RNAi targeted to these subunits, predicting they comprise the heterodimer that associates with Cta, and found these treatments blocked Fog mediated contractility (Figure 4.1D). Thus, we conclude that treatment of S2R+ cells with Fog activates the identical signaling pathway utilized in cellular contraction during *Drosophila* gastrulation.

Ric-8 is necessary for Fog pathway activation in *Drosophila* S2R+ cells

Next, we tested the hypothesis that Ric-8 acts in the Fog pathway. We designed dsRNAs to target the coding region or the 5' and 3' untranslated regions of the Ric-8 mRNA and found that each effectively depleted Ric-8 from S2R+ cells (Figure S4.1). When tested in the contractility assay, Ric-8-depleted cells were unable to contract following treatment with Fog (Figure 4.1B, D). The effect of our RNAi was specific as we were able to rescue the ability of S2R+ cells to respond to Fog by expressing Ric-8-GFP in cells depleted of endogenous Ric-8 (Figure 4.2 A, B). Ectopic overexpression of Ric-8-GFP was not

sufficient to induce contractility in the absence of Fog, however (data not shown). From these data, we conclude that Ric-8 is a necessary component of the Fog signaling cascade.

To identify where Ric-8 is functioning within the Fog signaling pathway we performed a series of epistasis experiments using RNAi. Overexpression of Myc-Cta-Q303L (Cta_{QL}), a mutation predicted to lock Cta in its GTP-bound conformation⁴⁶, in S2R+ cells is sufficient to trigger contractility in the absence of Fog (Figure 4.4A). However, expression of Myc-Cta_{QL} in S2R+ cells depleted of endogenous Ric-8 does not drive cellular constriction (Figure 4.2C, D). To verify the inability of Myc-Cta_{QL} to trigger constriction in Ric-8 depleted cells was not due to the absence of overall Cta protein we created expression constructs with two distinct metallothionein promoters within the same vector: 1) preceding full-length Myc-Cta and 2) preceding the coding sequence for mCherry. We then transfected these constructs into S2 cells treated with either control or Ric-8 dsRNA and compared levels of wild-type Myc-Cta, constitutively active Myc-Cta_{QL}, and constitutively inactive Myc-Cta-G302A (Cta_{GA}). Mutation of glycine 302 to alanine is predicted to trap Cta in either its GDP bound conformation or in a nucleotide-free state, based on homology with similar mutations in other Gα12/13 family members (⁴⁷ and personal communication with Ted Meigs). Using these constructs we show that levels of ectopic Myc-Cta are not affected by Ric-8 depletion (Figure 4.2E). In the converse experiment, S2R+ cells depleted of endogenous Cta and over-expressing Ric-8-GFP do not constrict upon Fog treatment. However, over-expression of RhoGEF2, which is directly downstream of Cta, in either Cta- or Ric-8-depleted cells is sufficient for cellular constriction (Figure 4.2 C, D). Therefore, Ric-8 functions upstream of RhoGEF2 implicating a role for Ric-8 at the level of either the putative GPCR, Cta, or the β subunits. It has been well documented, in *Drosophila* and other systems, that Ric-8 does not

interact with $G\alpha$ when it is complexed with its $\beta\gamma$ subunits^{4,7,28}. To date there is no evidence that Ric-8 interacts with a receptor in receptor dependent activation of Ric-8, however this possibility has not been directly tested.

Ric-8 directly binds Cta and exhibits higher affinity for the inactive form of Cta

It is probable that in our system Ric-8 interacts with the $G\alpha$. Using immunoprecipitation we tested the hypothesis that Ric-8 and Cta directly interact. A disadvantage of this strategy is that antibodies against Cta have not been published and our own attempts to develop them were unsuccessful. However, we found that Myc-Cta is functional and able to restore Fog sensitivity to S2R+ cells depleted of endogenous Cta by RNAi (Figure S4.2 A, B), thus, we used this construct as a proxy for endogenous protein. We transfected Myc-Cta into S2 cells, immunoprecipitated with an anti-Myc monoclonal antibody, and found that endogenous Ric-8 co-precipitated (Figure 4.3A). As expected from our rescue experiments, Ric-8-GFP also co-immunoprecipitated with Myc-Cta (Figure 4.3B). Thus, Ric-8 and Cta are able to interact in *Drosophila* tissue culture cells.

Given that Ric-8 functions as a GEF for $G\alpha$ subunits in other systems, we wanted to test the hypothesis that Ric-8 exhibits a preferred interaction with GTP-free Cta; to do this we used an inactive version of Cta, Cta_{GA}. Overexpression of Myc-Cta_{GA} in S2R+ cells depleted of endogenous Cta inhibited Fog-mediated contractility (Figure S4.2B). To determine whether nucleotide association affected Ric-8 interaction we co-transfected Ric-8-GFP together with wild-type Myc-Cta, Myc-Cta_{QL}, or Myc-Cta_{GA} into S2 cells. We prepared lysates from transfected cultures, immunoprecipitated GFP, and compared the amount of Myc-Cta in each sample by quantitative immunoblot. We found that Ric-8 binding to Cta is

dependent on the nucleotide state of Cta, as pulldowns performed with constitutively inactive Myc-Cta_{GA} and constitutively active Myc-Cta_{QL} showed greater and lesser binding affinity to Ric-8 respectively, as compared to wild-type Myc-Cta (Figure 4.3B, C). These data indicate that Ric-8 discriminates between Cta nucleotide states and preferentially binds to inactive Cta.

Ric-8 acts to selectively localize nucleotide-free Cta within the cell

Ric-8 plays a role in localizing Gα_i to the cortex in *Drosophila* neuroblasts and sensory organ precursor cells^{7,28,29}; therefore, we wanted to test the hypothesis that Ric-8 also functions to localize Cta and determine whether its nucleotide state plays a role in this interaction. Our strategy was to co-express Myc-Cta along with a version of Ric-8-GFP that was mis-targeted to mitochondria by tagging it with residues 310-338 of *Listeria* ActA (Mito-Ric-8-GFP). When wild-type Myc-Cta or Myc-Cta_{QL} was co-expressed with Mito-Ric-8-GFP, neither Cta construct exhibited discrete localization (Figure 4.4A). However, co-expression of Myc-Cta_{GA} and Mito-Ric-8-GFP resulted in robust accumulation of Cta to the mitochondria (Figure 4.4A). These data indicate that Ric-8 acts to selectively localize inactive Cta within the cell.

Our results suggest a mechanism in which Ric-8 localizes Cta to the cell cortex to mediate Fog signaling. To test this model, we transfected S2R+ cells depleted of endogenous Ric-8 with either Ric-8-GFP or Mito-Ric-8-GFP, and scored for the ability of each construct to rescue contractility. Ric-8-GFP restored the normal constriction of Ric-8 depleted cells, however cells expressing Mito-Ric-8-GFP exhibited a significantly diminished response to Fog (Figure 4.4B). Together, these findings clearly demonstrate that Ric-8 binds to, and can localize, Cta based on its nucleotide state. They further suggest that

Ric-8 is required for Cta cycling through its nucleotide state downstream of Fog pathway activation.

Ric-8 binds to Cta through an interface of conserved residues

While previous work has provided insight into the structure of Ric-8, a rigorous investigation of specific residues important for interactions with G α has not been performed. Ric-8 is predicted to be composed of 10 Armadillo repeats⁴⁸. Armadillo repeats adhere to a canonical fold and global elongated structure⁴⁹. The Olate group recently used molecular modeling to construct an *in silico* model of the Ric-8 structure⁴⁸. Based on sequence conservation of Ric-8 across species (Figure S4.3), we made fourteen cluster mutations in Ric-8-GFP, targeting conserved electrostatic residues likely to be surface exposed and that were exposed in the Ric-8 model (Table 4.1, Figure 4.5A). These mutations consisted of charge reversals, with the intent to not only diminish, but repel an interaction with Cta. We co-expressed the Ric-8-GFP mutants with the three Cta variants (Myc-Cta, Myc-Cta_{QL}, Myc-Cta_{GA}) in S2 cells, and assessed their ability to interact. Several of our Ric-8-GFP mutant constructs exhibited altered affinities for Cta and are described below. The mutants span the length of the protein and are ordered in succession from N-terminus to C-terminus. While Ric-8-GFP robustly bound Myc-Cta_{GA}, it exhibited lower affinity interactions with Myc-Cta and Myc-Cta_{QL} (Figure 4.2B, C) and the Ric-8-GFP pulldown data displayed a high degree of variance with those two mutants making it difficult to determine the binding activity of Ric-8-GFP with Myc-Cta and Myc-Cta_{QL}. Therefore, we focused our analyses on pulldowns performed with Myc-Cta_{GA}.

We identified four Ric-8-GFP mutants (1, 9, 10, and 13) that had significantly reduced

binding to Myc-Cta_{GA} by testing the ability of the cluster mutants to interact with Cta (Figure 4.5B, C and Table 4.1). To further parse out the individual residues responsible for this interaction we made single point mutants for each cluster of more than one mutated amino acid (Figure S4.4 and Table 4.1). Mutant 10 is a singular mutation, so it was not tested again. We identified specific residues within mutants 1, 9, and 13 that attenuated the ability of Cta to bind Ric-8 (Figure 4.6A, B and Table 4.1). The remaining mutations had moderate to no effect on binding when co-expressed with Myc-Cta_{GA} (Table 4.1). Although not statistically significant, both Myc-Cta and Myc-Cta_{QL} variants exhibited decreased binding to mutant 1, and moderate-high binding to mutants 9, 10 and 13. These latter three mutants exhibited decreased interaction with Myc-Cta_{GA}, however, they displayed increased affinity for Myc-Cta and Myc-Cta_{QL} (Figure 4.5B, C and S5A-D). The fact that these mutations severely inhibited binding to Myc-Cta_{GA} but did not strongly affect Myc-Cta and Myc-Cta_{QL} binding suggests a model in which the C-terminal region of Ric-8 may be important for the high affinity binding seen specifically in the Ric-8/GTP-free Cta interaction, while the N-terminal residues are important for global Ric-8 association and function.

We next tested the hypothesis that the residues mediating Ric-8/Cta interactions are required for Fog signaling. We depleted endogenous Ric-8 from S2R+ cells and transfected the cells with the clustered and individual point mutant variants of Ric-8-GFP. We then treated the cells with Fog and assessed the ability of the transfected cells to rescue constriction. Of the fourteen clustered point mutants tested in the binding assay, six mutants: 1, 6, 7, 8, 9, and 13, failed to rescue Fog-induced constriction (Figure 4.5C and Table 4.1). Testing the individual point mutants within the cellular constriction assay revealed a similar pattern in the residues that prevented pathway activation to the individual residues deficient

in binding Cta in the pulldown assay (Figure 4.6A, B and Table 4.1). This suggests that residues R71, R75, R414, D484, T485, and E487 within Ric-8 are important for establishing a binding interface, as well as for successful G protein signaling.

Finally to determine if Cta localization was affected by binding mutants with low binding affinity we made Mito-tagged versions of cluster mutants 1, 9, 10 and 13. We transfected S2 cells with the Mito-Ric-8-GFP cluster mutants and Myc-Cta_{GA} and screened for co-localization of the two proteins. Myc-Cta_{GA} did not co-localize with Mito-Ric-8-GFP mutant 1, while, surprisingly, co-localization of Myc-Cta_{GA} was seen with Mito-Ric-8-GFP mutants 9, 10 and 13 (Figure 4.4C). Hypothetically, mutants 9, 10, and 13 could be affecting the binding kinetics of Myc-Cta_{GA}, which may account for the co-localization of the two in our mis-targeting assays, as well as the absence of interaction within the pull-down assay.

Mutants 1, 9, and 13 had low binding affinity to Cta_{GA} as well as dramatically decreased contractility in Fog-treated S2R⁺ cells; however, mutant 10 rescues contractility to wild-type levels (Figure 4.5B, C and Table 4.1). It is probable that mutant 10, while impeding the binding interface between Ric-8 and Cta, is sufficient in its interaction to function in pathway activation. Intriguingly, mutants 6-8 are capable of binding Cta, as shown in pull-down assays, (Figure 4.5B, C and Table 4.1) but have diminished ability in activating the pathway (Figure 4.5C and Table 4.1), suggesting that these residues may have an important functional role outside of binding. The majority of the residues that affected both binding and functional pathway rescue map to a conserved face of the Arm repeats, and show a potential clamp-like binding of Ric-8 to Cta (Figure S4.4). Our findings suggest that residues within the inner face of the N-terminus (R71 and R75) of Ric-8 facilitate global interaction with Cta, while residues found in the C-terminus (R414, D484, T485, and E487)

modulate binding based on nucleotide specificity. While previous work has found residues important in G α subunits for facilitating interaction with Ric-8⁵⁰ here we identify some of the first residues found to be important for Ric-8 binding to a G α .

Discussion

In this study we conducted an in-depth analysis of the interaction between Ric-8 and Cta downstream of the Fog-activated morphogenetic pathway. We established a novel assay for testing potential Fog pathway components and found that in *Drosophila* tissue culture Ric-8 is required for pathway activation and that Ric-8 not only binds the G α 12/13, Cta, but also preferentially binds the inactive, GTP-free version of Cta. We defined a role for Ric-8 as an escort/scaffold for inactive Cta by using artificially induced localization of Ric-8 to the mitochondria. Upon Ric-8 translocation we found that inactive Cta co-localized with ectopically localized Ric-8, while the cellular localization of wild-type and constitutively active Cta were unaffected. Additionally, when Ric-8 was mis-targeted to the mitochondria, cells were impaired in their ability to constrict in response to Fog application. We identified evolutionarily conserved residues within Ric-8 important for 1) establishing a binding interface between Ric-8 and Cta, 2) recognition of nucleotide specific variants of Cta, and 3) successful G protein signaling downstream of Fog pathway activation. These data establish a role for Ric-8 in Cta localization and attenuation of pathway signaling through Cta.

Our novel cell-based assay is ideal for examining Fog-induced activation of the Rho pathway, due to the ease in which we are able to deplete cells of specific proteins using RNAi, the rapidity of screening multiple genes simultaneously, and the ability to visualize pathway activation using a simple microscope-based examination. This assay opens

numerous possibilities for the identification of other pathway components, including the unidentified GPCR involved in transduction of the Fog signal, as well as investigation of general cellular functions such as mechanochemical force production and regulation of the acto-myosin cytoskeleton. Additionally, although not highlighted in this study, we are able to view Fog-induced cell morphological changes in real-time. This allows for further investigation of pathway components that specifically affect the kinetics with which cells are able to respond to Fog, and/or the longevity and persistence of pathway activation.

The fundamental importance of Ric-8 for productive G α signaling has been well documented. Ric-8 plays a key role in modulating the behavior of G α subunits in receptor-independent and dependent signaling events during asymmetric cell division, neurotransmitter release and maturation, both vertebrate and invertebrate gastrulation, and numerous other developmental processes across species¹⁰. Due to its role in establishing asymmetry in dividing cells and subsequently controlling cell proliferation rates, Ric-8 has become of interest to the field of cancer biology^{51,52}. Our model cell culture system provides a streamlined approach for further investigation into parsing out the complicated signaling networks involved in establishing these disease states.

The role of Ric-8 as a non-canonical GEF has been established in a variety of biological systems¹⁰. Our efforts to directly determine if Ric-8 was acting as a GEF for Cta were thwarted as our efforts to purify both Cta and Ric-8 resulted in insoluble, or aggregated protein fractions. If Ric-8 is acting as a GEF one might predict that overexpression of Ric-8 in our cellular assay would drive constriction, however, overexpression of Ric-8 in S2 or S2R+ cells does not elicit Fog pathway activation. The reason for this may be explained by data showing that Ric-8 is unable to interact with an intact heterotrimeric complex consisting

of $G\alpha\beta\gamma$ ⁴, and that Ric-8 and GPCRs potentially compete for the same binding sites on $G\alpha$ ⁵⁰. Therefore, it is possible that, in the absence of Fog-mediated receptor activation, Ric-8 is unable to bind $G\alpha$ to stimulate (potentially as a GEF) downstream pathway components.

Previous work has implicated Ric-8 as a chaperone during $G\alpha$ biosynthesis to stabilize nascent protein production, and in turn as an essential factor in $G\alpha$ membrane targeting. This function of Ric-8 has been shown to affect the stability of all classes of mammalian $G\alpha$ subunits^{9,50}. Given the necessity of Ric-8 in mammalian systems for $G\alpha$ stabilization and membrane localization it is likely that Ric-8 acts similarly in *Drosophila*, as evidenced by the mis-targeting of $G\alpha_i$ and Cta, in the absence of Ric-8, to the cortex of the epithelium of *Drosophila* embryos^{7,28,29,53}. However, unlike $G\alpha_i$ ⁷, levels of Cta are not decreased in whole cell lysate in the absence of Ric-8 (Figure 4.2E); additionally, we see some rescue in cells depleted of endogenous Ric-8, overexpressing constitutively active Cta (Figure 4.2C), indicating that at least a small amount of Cta is localized correctly and functional. Therefore, while initial localization⁵³ of Cta to the plasma membrane and later localization of Cta is dependent on Ric-8, stabilization of Cta is independent of Ric-8 function (this study).

Many molecules are involved in the complex signaling networks downstream of receptor activation, and all of these components must be precisely regulated to interact and communicate in a specific way for effective signal transmission. Though signaling nodes involving GPCRs, $G\alpha$ subunits, GDIs and Ric-8 have been extensively studied there is little known about the structure of Ric-8 and how it interacts with $G\alpha$ subunits during these events. We used a predicted model⁴⁸ of Ric-8 as a conceptual basis to visualize mutants and identify key conserved residues important for Cta binding, nucleotide specificity and execution of productive G protein pathway activation. Based on these data our structure/function assay of

Ric-8 provided information into the structural components important for comprising the Cta/Ric-8 binding interface, as well as the minimal mutations necessary to abrogate Fog-induced pathway activation.

We identified four cluster mutations, mutants 1, 9, 10 and 13 (Figure S4.4), that inhibited Myc-Cta_{GA} binding, of which three: 1, 9, and 13, also failed to rescue constriction to wild-type levels. Of these four mutants we found that only mutant 1 (located in the N-terminus of Ric-8) had an inhibitory effect on binding to wild-type, constitutively active and constitutively inactive versions of Cta, while mutants 9, 10 and 13 (located in the C-terminus of Ric-8) were only deficient in binding inactive Cta. The Itoh lab found that a truncated version consisting of the N-terminal half (residues 1-301) of Ric-8 was sufficient to bind G α_q ⁵⁴. In accordance with these data, we suggest that the residues in mutant 1 are important for non-nucleotide specific Cta interaction, while the residues in mutants 9, 10 and 13 confer nucleotide specific recognition of Cta.

Several mutants had effects in only the binding or contractile assay. Mutant 10 inhibited binding, while mutants 6-8 prevented Fog-induced constriction. Mutant 10 was able to rescue cellular constriction but exhibited decreased binding to Cta, implying this mutant is still functional but perhaps folded in a manner unproductive for robust binding to Cta; this may be due to its proximity to mutant 13 (Figure 4.5A). Mutants 6-8 are capable of binding Cta, but not rescuing Ric-8 function downstream of pathway activation. While the function of mutant clusters 6-8 is unclear, it is tempting to hypothesize that the region encompassing mutants 6-8 is a potential site for Ric-8 GEF activity. Our data is the first evidence of specific residues within Ric-8 facilitating interaction with a G α .

In the early dividing *C.elegans* embryo²⁶, *Drosophila melanogaster* neuroblasts and

epithelium^{7,28,29} and several mammalian tissue culture cell lines^{9,30,31} Ric-8 has been found to localize G α subunits to the plasma membrane. Our data suggest there is an additional level of regulation of G α localization that is dependent on the nucleotide-bound state of G α . We have identified a cluster of residues that may facilitate this interaction with Cta. Clustered Ric-8 mutants, deficient in binding Cta_{GA} in immunoprecipitation assays, when tagged with a sequence directing them to the mitochondria had varying effects in their ability to ectopically localize Cta_{GA}. Mito-Ric-8 mutant 1 did not recruit Cta_{GA} to its ectopic location at the mitochondria, while Mito-Ric-8 mutants 9, 10, and 13 triggered mis-localization of Cta_{GA} to the mitochondria (Figure 4.4C). Interestingly, mutants 9, 10 and 13 exhibited preferential binding to constitutively inactive Cta, Cta_{GA}, but not wild-type nor constitutively active Cta, Cta_{QL} (Figure 4.5B, C and S5). This implies that these residues of Ric-8 may be important in conferring temporally regulated nucleotide specific recognition sites for Cta.

Based on our characterization of Ric-8, we propose the following model (Figure 4.4F). Ric-8 acts to initially chaperone the folding of Cta, allowing Cta, G β 13F, and G γ 1 to form a complex which is then transported to the plasma membrane. Upon Fog/GPCR interaction, GTP-bound Cta is released from the G $\beta\gamma$ heterodimer, and interacts with RhoGEF2 (via its RGS domain), causing hydrolysis of GTP to GDP. Specific, evolutionarily conserved residues regulate the binding of GDP-bound Cta to Ric-8, or alternatively Ric-8 facilitates stabilization of a nucleotide-free version of Cta. This allows Cta to bypass destruction and be re-inserted into the Fog pathway to activate downstream targets.

Acknowledgements

We thank T. Meigs, M. Peifer, K. Slep, and J. Sondek for thoughtful discussion and feedback

on the manuscript. We thank D. Bosch and D. Siderovski for collaborative efforts to purify *Drosophila* Ric-8 and Cta. We thank J. Olate for the xRic-8 PDB file. We thank G. Rogers, W. Chia and E. Wieschaus for reagents. This work was supported by grants from the NIH (RO1-GM081645 to SLR) and the Arnold and Mabel Beckman Foundation (Beckman Young Investigator Award to SLR). KAP was supported by funding from the Lineberger Comprehensive Cancer Center.

References

1. Siderovski, D. P. & Willard, F. S. The GAPs, GEFs, and GDIs of heterotrimeric G-protein alpha subunits. *Int. J. Biol. Sci.* **1**, 51–66 (2005).
2. Oldham, W. M. & Hamm, H. E. Heterotrimeric G protein activation by G-protein-coupled receptors. *Nat. Rev. Mol. Cell Biol.* **9**, 60–71 (2008).
3. Rossman, K. L., Der, C. J. & Sondek, J. GEF means go: turning on RHO GTPases with guanine nucleotide-exchange factors. *Nat. Rev. Mol. Cell Biol.* **6**, 167–180 (2005).
4. Tall, G. G., Krumins, A. M. & Gilman, A. G. Mammalian Ric-8A (synembryn) is a heterotrimeric Galpha protein guanine nucleotide exchange factor. *J Biol Chem* **278**, 8356–8362 (2003).
5. Chan, P., Gabay, M., Wright, F. A. & Tall, G. G. Ric-8B is a GTP-dependent G protein alphas guanine nucleotide exchange factor. *J Biol Chem* **286**, 19932–19942 (2011).
6. Tall, G. G. & Gilman, A. G. Resistance to inhibitors of cholinesterase 8A catalyzes release of Galpha1-GTP and nuclear mitotic apparatus protein (NuMA) from NuMA/LGN/Galpha1-GDP complexes. *Proc. Natl. Acad. Sci. U.S.A.* **102**, 16584–16589 (2005).
7. Hampoelz, B., Hoeller, O., Bowman, S. K., Dunican, D. & Knoblich, J. A. Drosophila Ric-8 is essential for plasma-membrane localization of heterotrimeric G proteins. *Nat. Cell Biol.* **7**, 1099–1105 (2005).
8. Thomas, C. J., Tall, G. G., Adhikari, A. & Sprang, S. R. Ric-8A catalyzes guanine nucleotide exchange on G alpha1 bound to the GPR/GoLoco exchange inhibitor AGS3. *J Biol Chem* **283**, 23150–23160 (2008).
9. Gabay, M. *et al.* Ric-8 proteins are molecular chaperones that direct nascent G protein α subunit membrane association. *Sci Signal* **4**, ra79 (2011).
10. Hinrichs, M., Torrejón, M., Montecino, M. & Olate, J. Ric-8: different cellular roles for a heterotrimeric G-protein GEF. *J Cell Biochem* (2012).doi:10.1002/jcb.24162
11. Miller, K. G., Emerson, M. D., McManus, J. R. & Rand, J. B. RIC-8 (Synembryn): a novel conserved protein that is required for G(q)alpha signaling in the *C. elegans* nervous system. *Neuron* **27**, 289–299 (2000).
12. Li, Y. *et al.* MoRic8 Is a novel component of G-protein signaling during plant infection by the rice blast fungus *Magnaporthe oryzae*. *Mol. Plant Microbe Interact.* **23**,

317–331 (2010).

13. Wright, S. J., Inchausti, R., Eaton, C. J., Krystofova, S. & Borkovich, K. A. RIC8 is a guanine-nucleotide exchange factor for Galpha subunits that regulates growth and development in *Neurospora crassa*. *Genetics* **189**, 165–176 (2011).
14. Dhingra, A. *et al.* Probing neurochemical structure and function of retinal ON bipolar cells with a transgenic mouse. *J. Comp. Neurol.* **510**, 484–496 (2008).
15. Tõnissoo, T., Meier, R., Talts, K., Plaas, M. & Karis, A. Expression of ric-8 (synembryn) gene in the nervous system of developing and adult mouse. *Gene Expr. Patterns* **3**, 591–594 (2003).
16. Tõnissoo, T. *et al.* Nucleotide exchange factor RIC-8 is indispensable in mammalian early development. *Dev. Dyn.* **239**, 3404–3415 (2010).
17. Maldonado-Agurto, R. *et al.* Cloning and spatiotemporal expression of RIC-8 in *Xenopus* embryogenesis. *Gene Expr. Patterns* **11**, 401–408 (2011).
18. Fenech, C. *et al.* Ric-8A, a Galpha protein guanine nucleotide exchange factor potentiates taste receptor signaling. *Front Cell Neurosci* **3**, 11 (2009).
19. Dannecker, Von, L. E. C., Mercadante, A. F. & Malnic, B. Ric-8B, an olfactory putative GTP exchange factor, amplifies signal transduction through the olfactory-specific G-protein Galphaolf. *J. Neurosci.* **25**, 3793–3800 (2005).
20. Dannecker, Von, L. E. C., Mercadante, A. F. & Malnic, B. Ric-8B promotes functional expression of odorant receptors. *Proc. Natl. Acad. Sci. U.S.A.* **103**, 9310–9314 (2006).
21. Kerr, D. S., Dannecker, Von, L. E. C., Davalos, M., Michaloski, J. S. & Malnic, B. Ric-8B interacts with G alpha olf and G gamma 13 and co-localizes with G alpha olf, G beta 1 and G gamma 13 in the cilia of olfactory sensory neurons. *Mol. Cell. Neurosci.* **38**, 341–348 (2008).
22. Yoshikawa, K. & Touhara, K. Myr-Ric-8A enhances G(alpha15)-mediated Ca²⁺ response of vertebrate olfactory receptors. *Chem. Senses* **34**, 15–23 (2009).
23. Grandy, R. *et al.* The Ric-8B gene is highly expressed in proliferating preosteoblastic cells and downregulated during osteoblast differentiation in a SWI/SNF- and C/EBPbeta-mediated manner. *Mol. Cell. Biol.* **31**, 2997–3008 (2011).
24. Miller, K. G. & Rand, J. B. A role for RIC-8 (Synembryn) and GOA-1 (G(o)alpha) in regulating a subset of centrosome movements during early embryogenesis in *Caenorhabditis elegans*. *Genetics* **156**, 1649–1660 (2000).

25. Afshar, K. *et al.* RIC-8 is required for GPR-1/2-dependent Galpha function during asymmetric division of *C. elegans* embryos. *Cell* **119**, 219–230 (2004).
26. Afshar, K., Willard, F. S., Colombo, K., Siderovski, D. P. & Gönczy, P. Cortical localization of the Galpha protein GPA-16 requires RIC-8 function during *C. elegans* asymmetric cell division. *Development* **132**, 4449–4459 (2005).
27. Couwenbergs, C., Spilker, A. C. & Gotta, M. Control of embryonic spindle positioning and Galpha activity by *C. elegans* RIC-8. *Curr. Biol.* **14**, 1871–1876 (2004).
28. Wang, H. *et al.* Ric-8 controls *Drosophila* neural progenitor asymmetric division by regulating heterotrimeric G proteins. *Nat. Cell Biol.* **7**, 1091–1098 (2005).
29. David, N. B. *et al.* *Drosophila* Ric-8 regulates Galphai cortical localization to promote Galphai-dependent planar orientation of the mitotic spindle during asymmetric cell division. *Nat. Cell Biol.* **7**, 1083–1090 (2005).
30. Woodard, G. E. *et al.* Ric-8A and Gi alpha recruit LGN, NuMA, and dynein to the cell cortex to help orient the mitotic spindle. *Mol. Cell. Biol.* **30**, 3519–3530 (2010).
31. Wang, L. *et al.* Resistance to inhibitors of cholinesterase-8A (Ric-8A) is critical for growth factor receptor-induced actin cytoskeletal reorganization. *J Biol Chem* **286**, 31055–31061 (2011).
32. Leptin, M. *Drosophila* gastrulation: from pattern formation to morphogenesis. *Annu. Rev. Cell Dev. Biol.* **11**, 189–212 (1995).
33. Dawes-Hoang, R. E. *et al.* folded gastrulation, cell shape change and the control of myosin localization. *Development* **132**, 4165–4178 (2005).
34. Martin, A. C., Kaschube, M. & Wieschaus, E. F. Pulsed contractions of an actin-myosin network drive apical constriction. *Nature* **457**, 495–499 (2009).
35. Costa, M., Wilson, E. T. & Wieschaus, E. A putative cell signal encoded by the folded gastrulation gene coordinates cell shape changes during *Drosophila* gastrulation. *Cell* **76**, 1075–1089 (1994).
36. Morize, P., Christiansen, A. E., Costa, M., Parks, S. & Wieschaus, E. Hyperactivation of the folded gastrulation pathway induces specific cell shape changes. *Development* **125**, 589–597 (1998).
37. Rogers, S. L., Wiedemann, U., Häcker, U., Turck, C. & Vale, R. D. *Drosophila* RhoGEF2 associates with microtubule plus ends in an EB1-dependent manner. *Curr. Biol.* **14**, 1827–1833 (2004).

38. Nikolaidou, K. K. & Barrett, K. A Rho GTPase signaling pathway is used reiteratively in epithelial folding and potentially selects the outcome of Rho activation. *Curr. Biol.* **14**, 1822–1826 (2004).
39. Kölsch, V., Seher, T., Fernandez-Ballester, G. J., Serrano, L. & Leptin, M. Control of *Drosophila* gastrulation by apical localization of adherens junctions and RhoGEF2. *Science* **315**, 384–386 (2007).
40. Barrett, K., Leptin, M. & Settleman, J. The Rho GTPase and a putative RhoGEF mediate a signaling pathway for the cell shape changes in *Drosophila* gastrulation. *Cell* **91**, 905–915 (1997).
41. Lecuit, T. & Lenne, P.-F. Cell surface mechanics and the control of cell shape, tissue patterns and morphogenesis. *Nat. Rev. Mol. Cell Biol.* **8**, 633–644 (2007).
42. Rogers, S. L. & Rogers, G. C. Culture of *Drosophila* S2 cells and their use for RNAi-mediated loss-of-function studies and immunofluorescence microscopy. *Nat Protoc* **3**, 606–611 (2008).
43. Martin, A. C., Gelbart, M., Fernandez-Gonzalez, R., Kaschube, M. & Wieschaus, E. F. Integration of contractile forces during tissue invagination. *J. Cell Biol.* **188**, 735–749 (2010).
44. Pistor, S., Chakraborty, T., Niebuhr, K., Domann, E. & Wehland, J. The ActA protein of *Listeria monocytogenes* acts as a nucleator inducing reorganization of the actin cytoskeleton. *EMBO J.* **13**, 758–763 (1994).
45. Yanagawa, S. I. Identification and Characterization of a Novel Line of *Drosophila* Schneider S2 Cells That Respond to Wingless Signaling. *Journal of Biological Chemistry* **273**, 32353–32359 (1998).
46. Xu, N., Bradley, L., Ambdukhar, I. & Gutkind, J. S. A mutant alpha subunit of G12 potentiates the eicosanoid pathway and is highly oncogenic in NIH 3T3 cells. *Proc. Natl. Acad. Sci. U.S.A.* **90**, 6741–6745 (1993).
47. Gohla, A., Offermanns, S., Wilkie, T. M. & Schultz, G. Differential involvement of Galpha12 and Galpha13 in receptor-mediated stress fiber formation. *J Biol Chem* **274**, 17901–17907 (1999).
48. Figueroa, M. *et al.* Biophysical studies support a predicted superhelical structure with armadillo repeats for Ric-8. *Protein Sci.* **18**, 1139–1145 (2009).
49. Coates, J. C. Armadillo repeat proteins: beyond the animal kingdom. *Trends Cell Biol.* **13**, 463–471 (2003).

50. Thomas, C. J. *et al.* The nucleotide exchange factor Ric-8A is a chaperone for the conformationally dynamic nucleotide-free state of Gai1. *PLoS ONE* **6**, e23197 (2011).
51. Luo, X. *et al.* Characterization of gene expression regulated by American ginseng and ginsenoside Rg3 in human colorectal cancer cells. *Int. J. Oncol.* **32**, 975–983 (2008).
52. Muggerud, A. A. *et al.* Data integration from two microarray platforms identifies bi-allelic genetic inactivation of RIC8A in a breast cancer cell line. *BMC Med Genomics* **2**, 26 (2009).
53. Kanesaki, T., Hirose, S., Grosshans, J. & Fuse, N. Heterotrimeric G protein signaling governs the cortical stability during apical constriction in *Drosophila* gastrulation. *Mech. Dev.* (2012).doi:10.1016/j.mod.2012.10.001
54. Nishimura, A. *et al.* Ric-8A potentiates Gq-mediated signal transduction by acting downstream of G protein-coupled receptor in intact cells. *Genes Cells* **11**, 487–498 (2006).

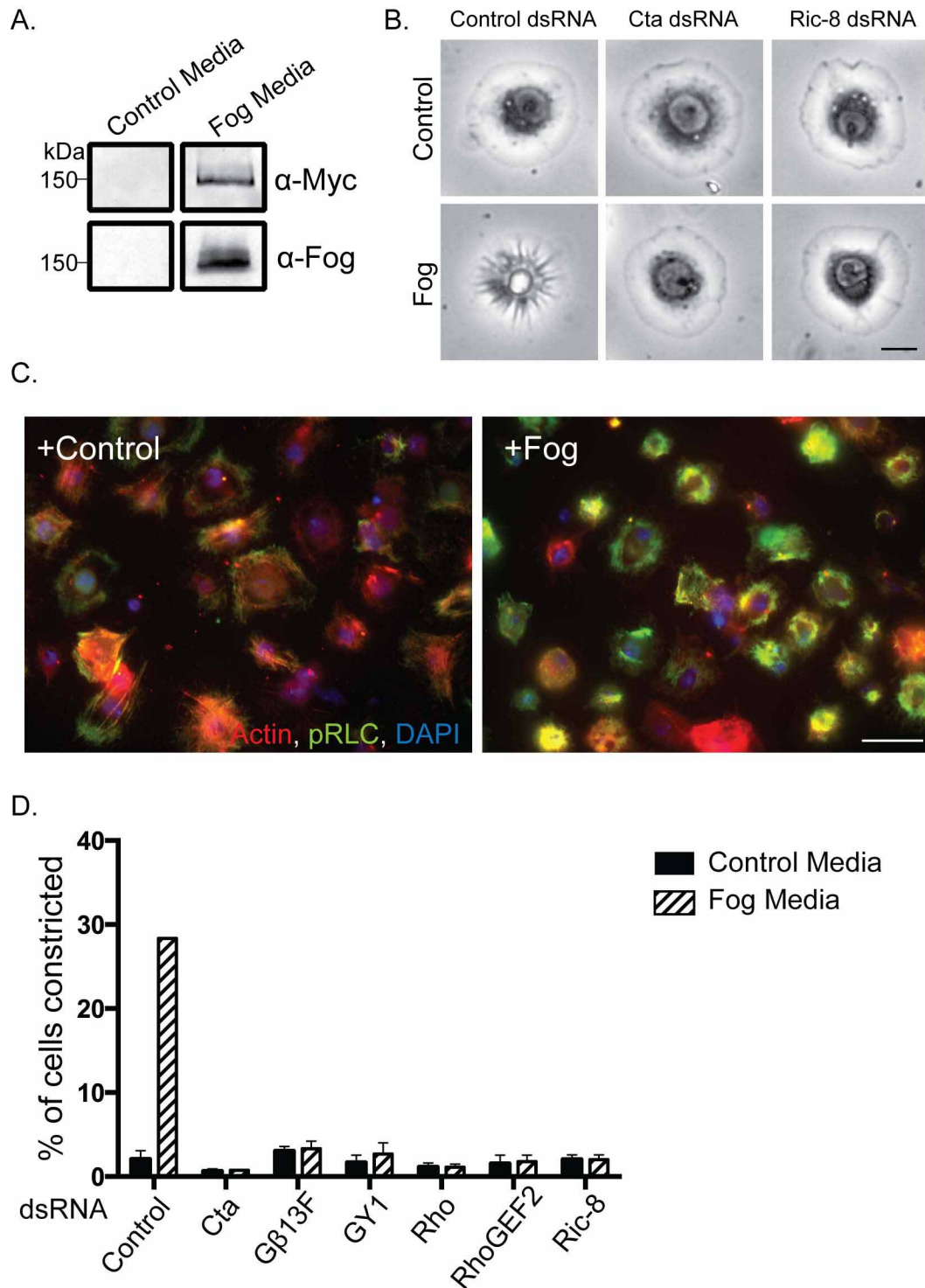


Figure 4.1 Recapitulation of Fog signaling in S2R+ cells. (A) Fog-Myc is secreted into the medium of a stable cell line expressing the construct, but not by un-transfected control S2 cells. Fog-Myc is recognized by anti-Myc and anti-Fog by immunoblot. (B) S2R+ cells undergo cellular shape changes in response to ectopic Fog application. RNAi-mediated depletion of Cta or Ric-8 prevents Fog-induced cellular constriction. Scale = 10 μ m. (C)

Fog-induced S2R⁺ contraction is accompanied by an increase in active phosphorylated non-muscle Myosin II (pRLC). S2R⁺ cells were treated with either control or Fog containing media and stained for actin (red), pRLC (green), and DNA (blue). Scale: 100 μm . (D) S2R⁺ cells lose their responsiveness to Fog following RNAi against known pathway components, as well as Ric-8. Percentage of cells constricting in response to Fog was measured within a population of cells ($\pm\text{SEM}$).

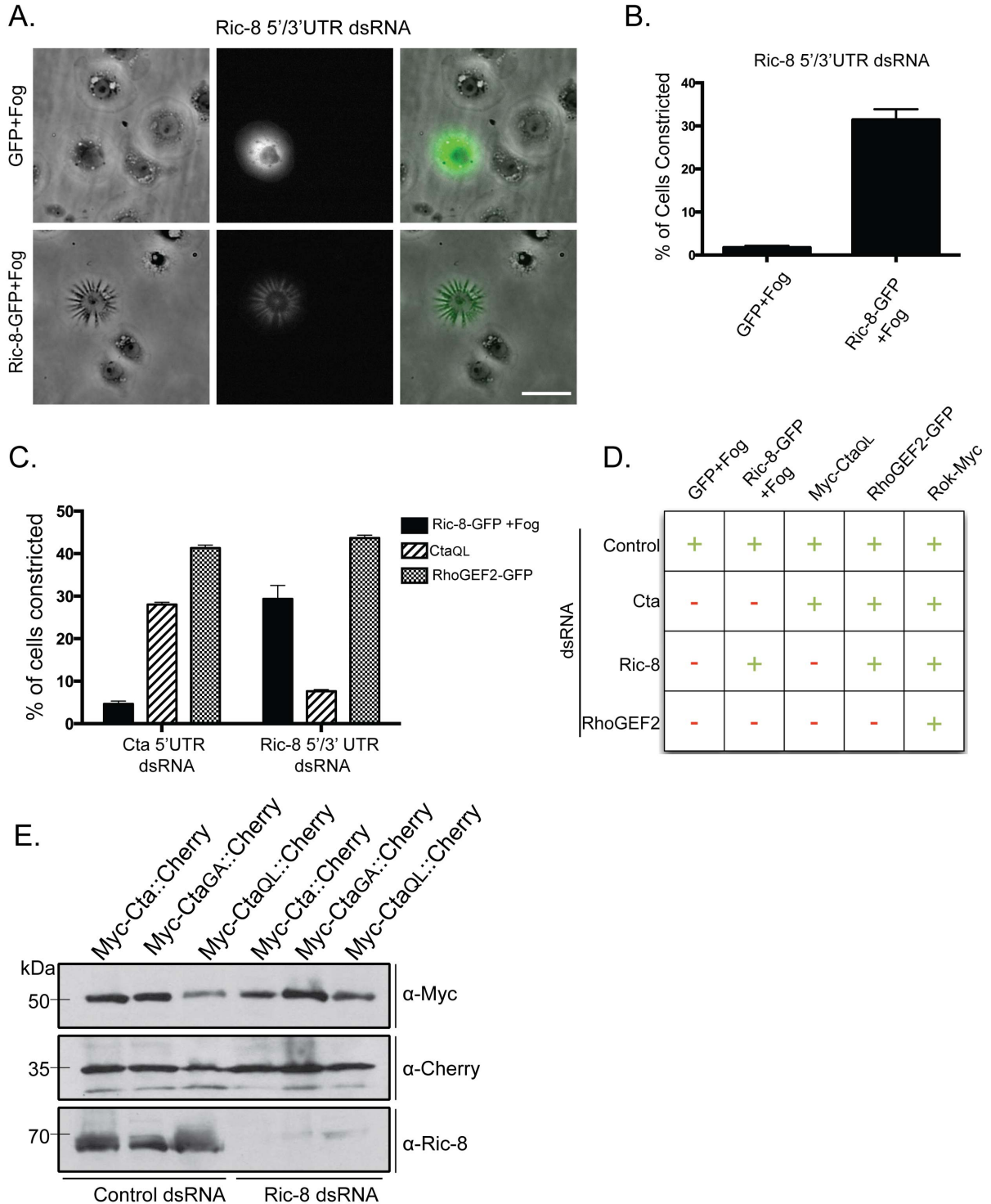


Figure 4.2 Ric-8 regulates the function of Cta within the Fog signaling pathway. (A) Expression of Ric-8-GFP, but not GFP alone, rescues the ability of cells depleted of endogenous Ric-8 to respond to Fog. Scale = 20 μ m. (B) The number of GFP or Ric-8-GFP transfected cells within a population depleted of endogenous Ric-8 were scored for their ability to contract in response to Fog (\pm SEM). (C) Cells depleted of endogenous Ric-8 or Cta

were transfected with constitutively active Cta (Cta_{QL}), RhoGEF2-GFP or Ric-8-GFP+Fog treatment. Their ability to drive constriction was quantified as a percentage of the number of cells contracting within the population (\pm SEM). (D) Summary chart illustrating the epistatic relationship of Ric-8 in the Fog pathway. Transfected DNA and targeted dsRNA are indicated. (+) represents that $\geq 15\%$ of transfected cells within a population constricted, (-) represents that $\leq 15\%$ of transfected cells within a population constricted. (E) Cells were treated with control or Ric-8 dsRNA and transfected with a dual expression construct for both Cta (WT, constitutively inactive:GA, or constitutively active:QL) and mCherry under separate promoters. Immunoblotting revealed equal amounts of Cta in control and Ric-8 dsRNA treated cells, while anti-dsRed was used as a protein loading control and anti-Ric-8 to verify protein depletion.

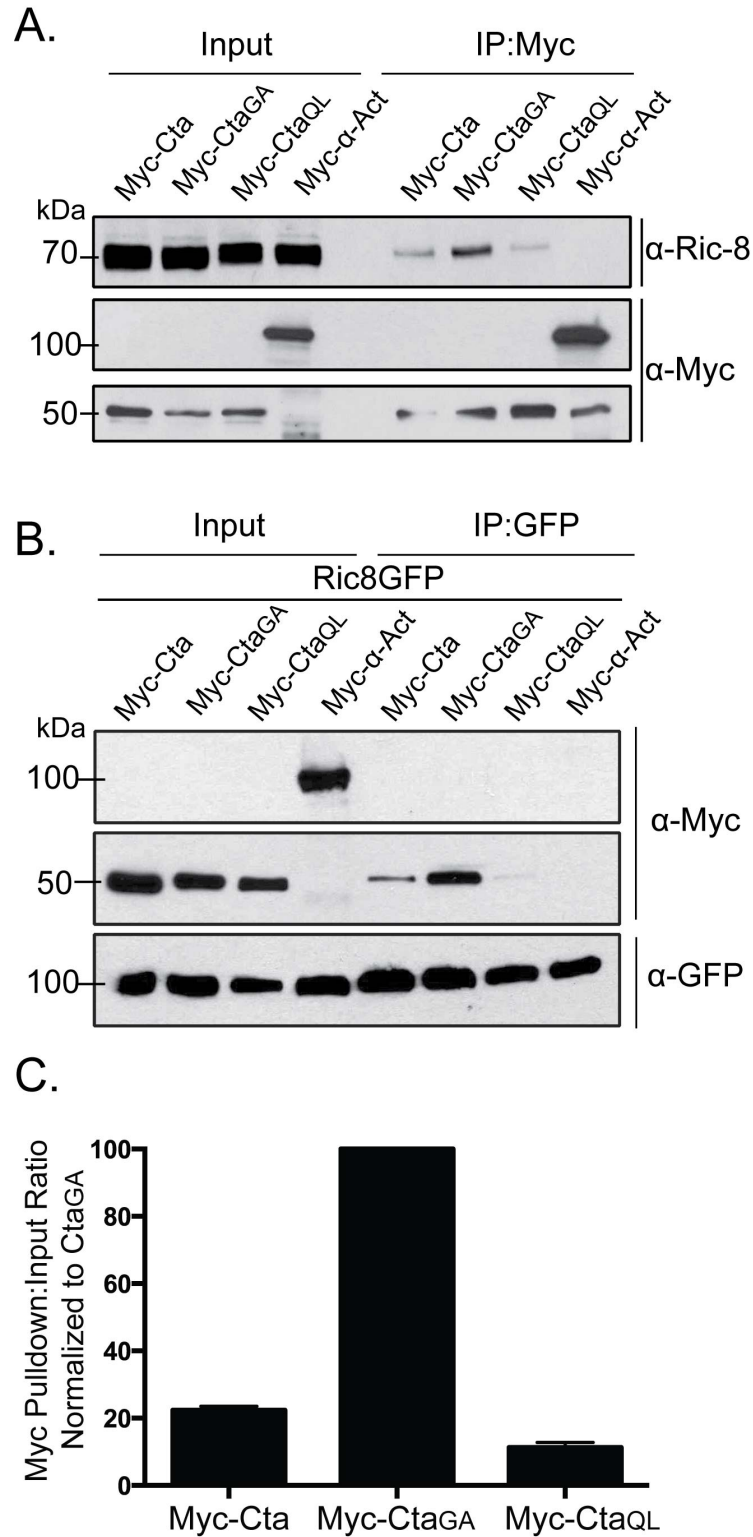


Figure 4.3 Ric-8 and Cta physically interact, and Ric-8 preferentially binds the constitutively inactive Cta_{GA}. Ric-8 binds to a lesser extent to the other two variants of Cta,

but not the control, α -actinin. (A) Cells were transfected with the three variants of Cta or α -actinin. IPs were carried out using anti-myc antibodies and probed with anti-Ric-8 and anti-Myc. (B) All cells were transfected with Ric-8-GFP and the three variants of Cta or α -actinin. IPs were performed with GFP-binding protein and probed with anti-GFP and anti-Myc. (C) Ric-8 preferentially binds to constitutively GDP-bound Cta. Quantification of IPs performed as outlined in (3B). Input:pulldown ratios were determined using quantitative densitometry, and normalized against Cta_{GA}.

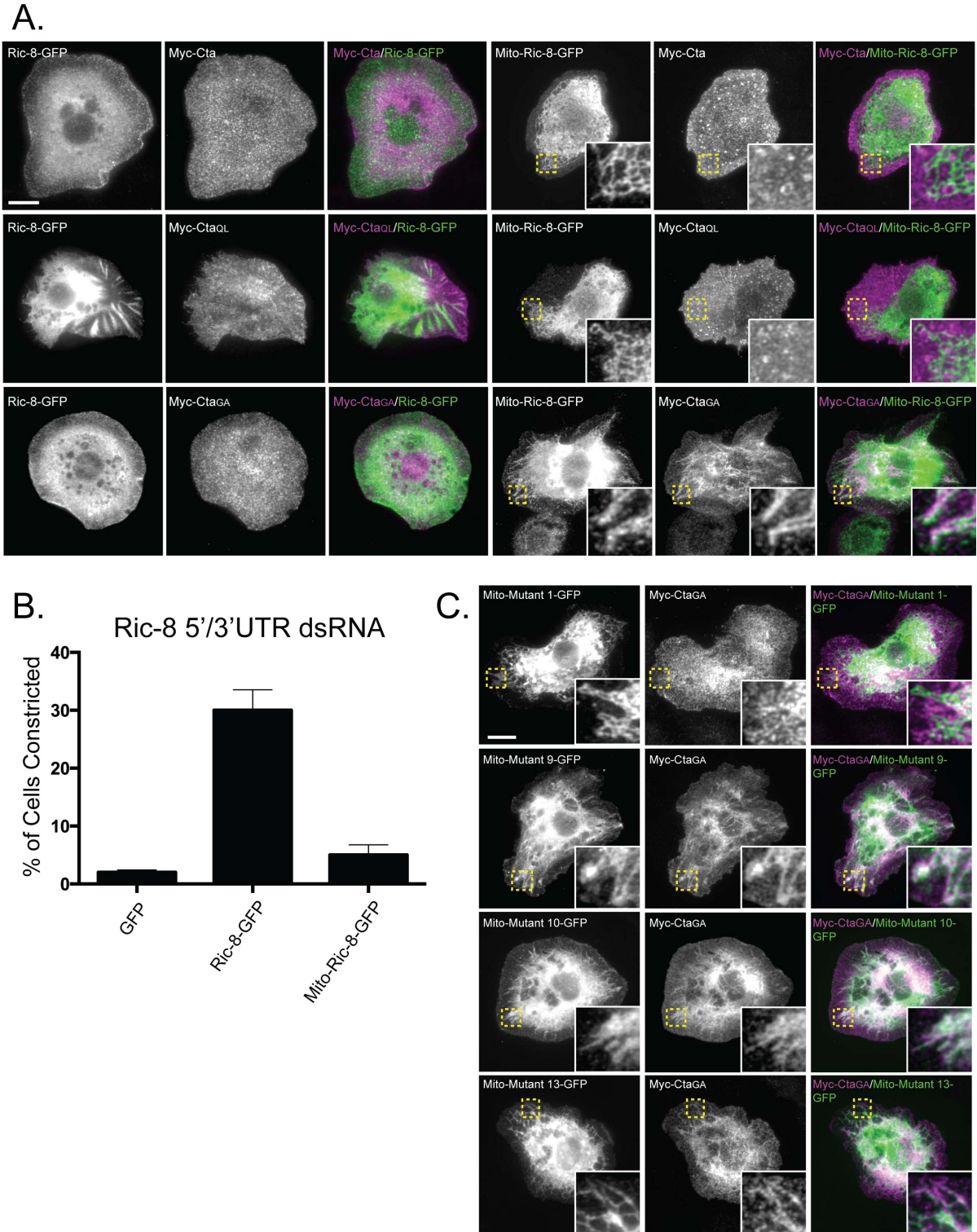


Figure 4.4 Ectopic localization of Ric-8 drives mis-localization of constitutively inactive Cta, and attenuates the efficacy of Fog signaling. (A) Targeting Ric-8 to the mitochondria causes Cta_{GA}, but not Myc-Cta nor Myc-Cta_{QL} to localize to the mitochondria. S2 cells were transfected with Ric-8-GFP, or Mito-Ric-8-GFP, and Myc-Cta, Myc-Cta_{GA}, or Myc-Cta_{QL}

and stained for anti-Myc, and anti-GFP. Enlarged views of boxed images in Mito-Ric-8-GFP and Cta variants are shown in insets. Scale bar = 20 μm . (B) Mis-localized Ric-8 fails to compensate to drive Fog induced cellular constriction. S2R+ cells depleted of endogenous Ric-8 transfected with GFP, Ric-8-GFP, and Mito-Ric-8-GFP were treated with Fog and scored for their ability to constrict (\pm SEM). (C) Evolutionarily conserved residues contribute to localization of Cta_{GA}. Mito-tagged versions of Ric-8-GFP mutants that exhibit decreased Myc-Cta_{GA} binding (see Figure 5B, C) were co-expressed with Myc-Cta_{GA}. While mutants 9, 10 and 13 co-localized with Myc-Cta_{GA}, mutant 1 did not. Enlarged images of boxed areas are shown in insets. Scale bar: 20 μm .

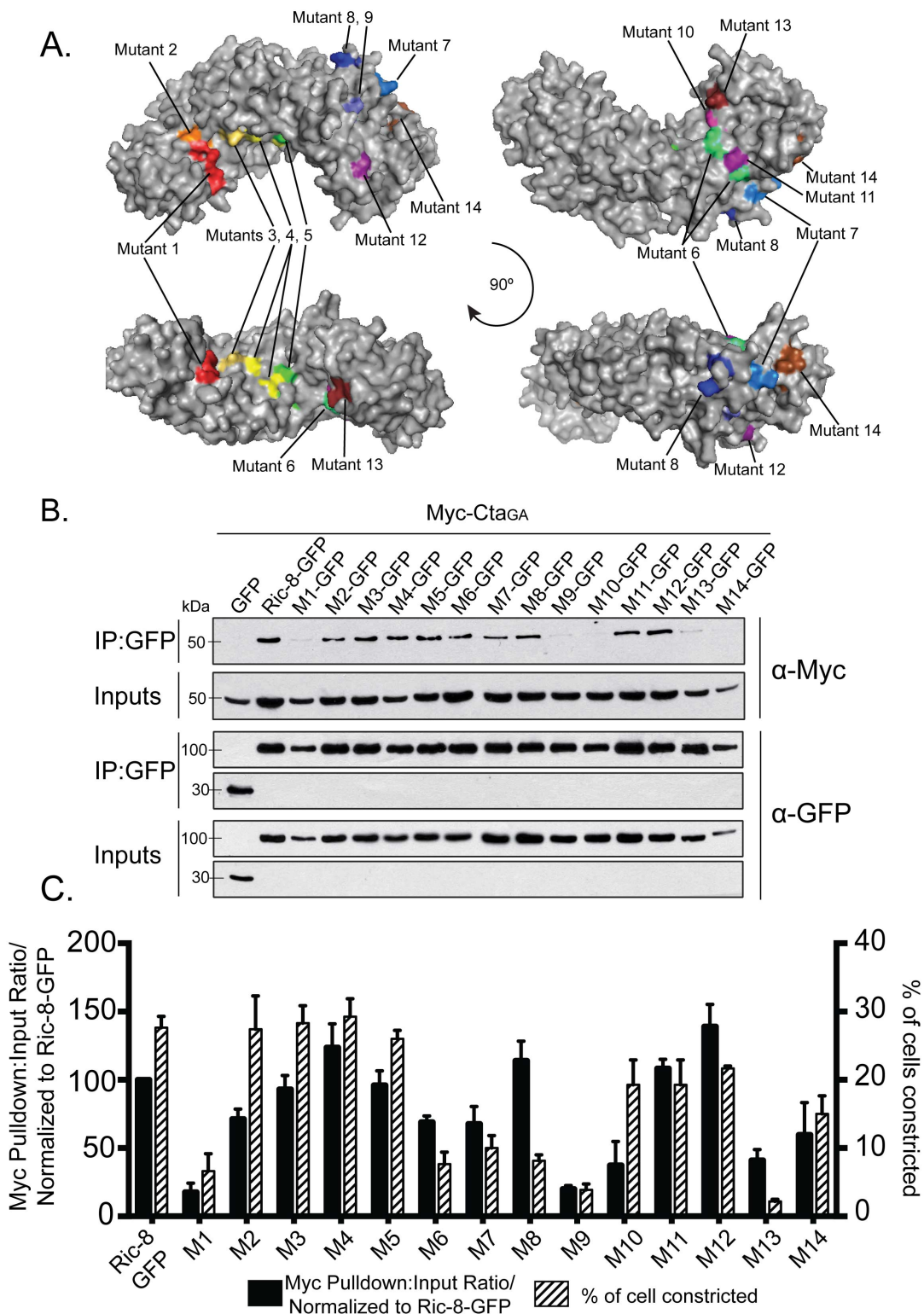


Figure 4.5 Evolutionarily conserved electrostatic residues are required for binding between Ric-8 and Cta_{GA}. (A) Clusters of point mutants used in our screen are represented

by different colors on a model of Ric-8. (B-C) Mutant clusters within Ric-8 disrupt binding to Cta_{GA}, and inhibit pathway activation downstream of Fog. (B) S2 cells were transfected with GFP, Ric-8-GFP or cluster Ric-8-GFP mutants and Cta_{GA}. IPs were performed with GFP-binding protein and probed with anti-GFP and anti-Myc. (C) The pulldown:input ratios for Ric-8-GFP and Myc-Cta_{GA} were quantified using densitometry, and normalized to Ric-8-GFP (\pm SEM) (black bars). S2R+ cells were depleted of endogenous Ric-8 and transfected with Ric-8-GFP and cluster Ric-8-GFP mutants, and then scored for the percentage of transfected cells constricting within the population (\pm SEM) (hatched bars).

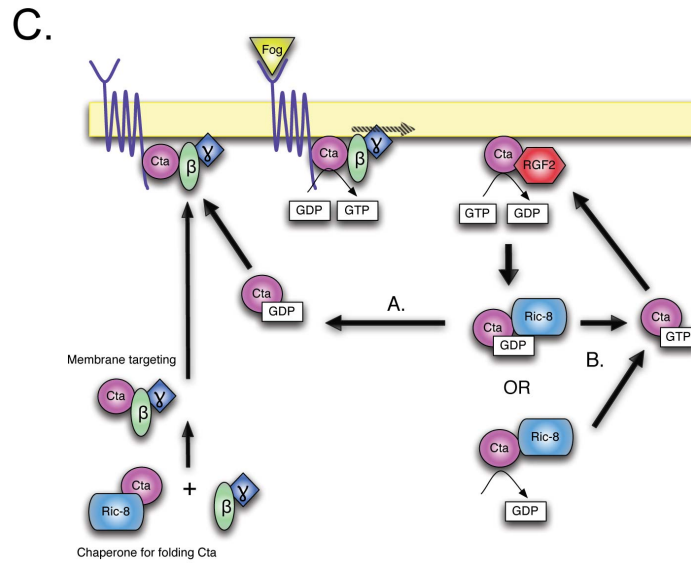
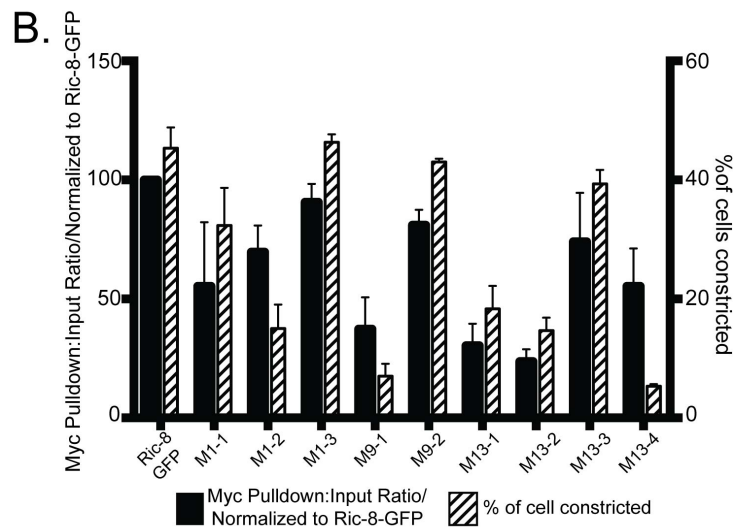
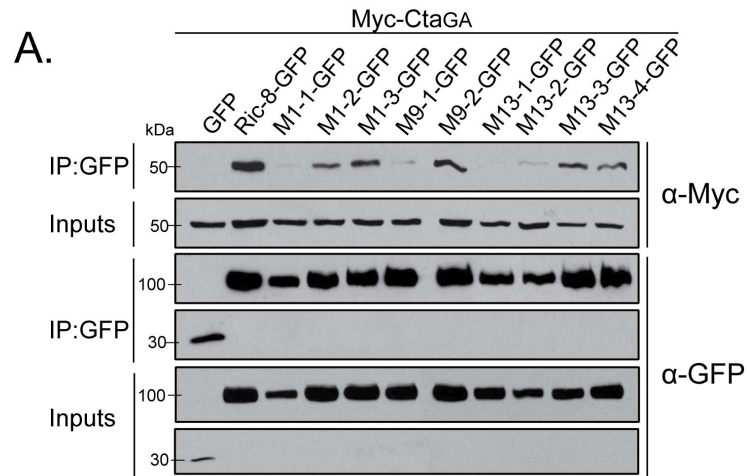


Figure 4.6 Individual residues derived from Ric-8 cluster mutants comprise key interaction sites for Cta binding and function. (A) Individual Ric-8 point mutants from

cluster mutants (1, 9, and 13) negatively regulate binding to Myc-Cta_{GA}. Cells were transfected with GFP, Ric-8-GFP or individual Ric-8-GFP point mutants and Cta_{GA}. IPs were performed with GFP-binding protein and probed with anti-GFP and anti-Myc. (B) Quantification of the IP experiments in 6A are presented (black bars). The pulldown:input ratios were determined using quantitative densitometry, and normalized to Ric-8-GFP (\pm SEM). S2R+ cells were depleted of endogenous Ric-8, transfected with Ric-8-GFP or individual Ric-8-GFP point mutants, and scored for the percentage of transfected cells constricting within the population (\pm SEM) (hatched bars). (C) Proposed model for Ric-8 function within the Fog signaling pathway. Ric-8 initially acts to chaperone the folding of Cta, and is released prior to Cta association with β 13F and γ 1. The heterotrimer is targeted to the plasma membrane where it interacts with a GPCR for Fog. Fog binding activates Cta through exchange of GDP for GTP. Cta-GTP activates RhoGEF2, and RhoGEF2's GAP activity catalyzes hydrolysis of GTP to GDP. Ric-8 may then bind either Cta-GDP or stabilize a nucleotide-free version of Cta. Ric-8 then localizes the inactive Cta for reactivation and reinsertion into the Fog signaling pathway, either by returning it to the heterotrimer to be re-activated by the GPCR (A) or through disassociation of GDP, which facilitates GTP binding, and subsequent pathway re-insertion directly upstream of RhoGEF2 (B).

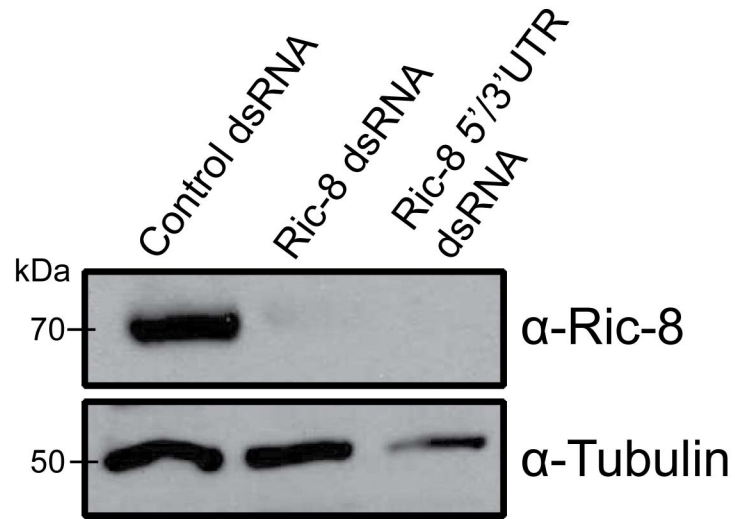


Figure S4.1 Ric-8 is depleted by dsRNAs directed against the 5'/3' UTR of the gene. Protein levels were determined by immunoblot with anti-Ric-8 and an antibody to α -tubulin was used as a loading control.

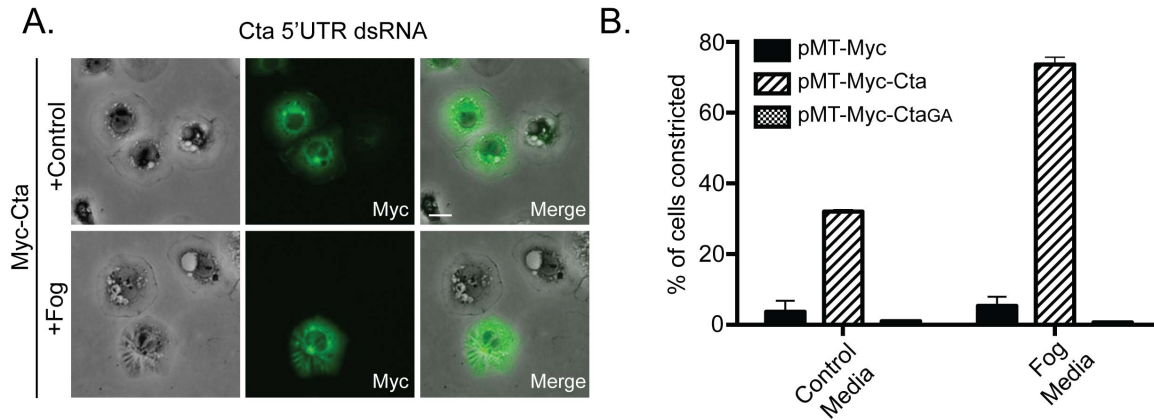


Figure S4.2 Myc-tagged Cta functions as a proxy for wild-type and constitutively inactive Cta. (A) Expression of Myc-Cta rescues the ability of cells depleted of endogenous Cta to respond to Fog. Transfected cells were identified using an anti-Myc antibody. Scale bar: 20 μ m. (B) Myc-Cta can rescue constriction in response to Fog in the absence of endogenous Cta, while constitutively inactive Myc-Cta_{GA} cannot. Quantification shows percentage of S2R+ cells within a population transfected with Myc-Cta or Myc-Cta_{GA} depleted of endogenous Cta able to contract in response to Fog application (\pm SEM).

Xenopus MPAMDLGALLDELESGDQELVQKSLAEYNQENSQCFFFNAEQRE-ERKKLGELVISFNLN 59
 Zebrafish ---MDLNAIIEKMETGDQDAALTALQTYNKEKSCQCFSTSGEEE-DRERLGELVLSFLER 56
 Mouse ---MEPRAVADALETGEEDAVTEALRSFNREHSQSFTFDDAQQE-DRKRLAKLLVSVLEQ 56
 Chicken ---MELRTVAVTVESGEQDAVLKVLQIYNQEKSCQCFSTFDDERE-ERKKMAQLLIKFLER 56
 Human -----RDYSDKHRATFKFESTDED-KRKKLCEGIFKVLIK 34
 Drosophila ----METEHLKRLEAKEADHIPAILDEFNTKNADLLVFDSPRTDNLWHELWLAIFGILDD 56
 :. :: : * : ..: :. .*

Xenopus DLQPSQIACLETIRILSRDKYALSPFTGRSAIQTLAQYAGLDYS----- 104
 Zebrafish DLQPSQCLACLETIRILSRDKKSLSPFATRHAMQILIRHAGLGQ----- 100
 Mouse GLSPKHRVTWLQTIIRILSRDRSCLDSFASRQSLHALACYADITV----- 100
 Chicken ELQPSQVTCLESIRILSRDKYCLEPFTTEEGLKTLRSHAGIDY----- 100
 Human DIPTTCQVSCLEVLRIILSRDKKVLVPVTTKENMQILLRLAKLNE----- 78
 Drosophila QRLSHLHTQCLNTRILTRDEFSLQNTYIEQVNTLLKLARIEAGSLKLPATPDELKQEE 116
 . : * :***:**. * . . :: * * :
 Mutant 1

Xenopus --EEMEMPCIPDGESAVEALMGLCNIIYNSVEAQEVAKDLRLVCGLARRLKLYNETRSSH 162
 Zebrafish --GEGVTPPEIPDLEVIVEALMGLCNIVFNSAAQEEAADLQLMVGLAERLKQCREPQWNH 158
 Mouse --SEEPQPSPDMVLLSESLKCLCNLVLSPTAQMLAAEARLVVRLAERVGLYRKRSPH 158
 Chicken --SEELIREVPDLEVILESLKCLCNIVFSSPRAQELTAEARLVVGLTKRIKLYNERSLPH 158
 Human --LDDSLEKVSFPPVIVSESLKCLCNIVFNSQMAQQLSLELNLAAKLCNLRKCKDRKFIN 136
 Drosophila REEPQLEPSQAQSEVIAEALMGLCNLVYQSSDCRRQCLRQHCLDAILKRVA--MRHPC 174
 . : * :** **:: . * . : . : :
 Mutant 2

Xenopus ESKFFDLRLFLLTALSVDMRQQLAQELRGVSLTDALESTLALKWSDIYEVVTDHLA-- 220
 Zebrafish DVRFDDLRLTFLITALRVDVRAQLAHELRLGVSLSEALDATFGLCWPDMYEVARAGFDGC 218
 Mouse EVQFFDLRLFLLTALRVDVRRQQLFQELHGVRLTDALELTGL-----VAPKENP-- 208
 Chicken EVKFFDLRLFLLTALRVDIRQQLAQELRGISLMTDTLELTGLVKWMDPYEVATEEGL-- 216
 Human DIKCFDLRLFLLSLLHTDIRSQLRYELQGLPLLTQILESFAFTIKWTDYESAIDHNG-- 194
 Drosophila ALEYDDMLLFLLTALPEAARSRLQIDLNGLTYMTKWLDKGLGE----- 218
 . :*** * **:: * * : * : * : : . : * : :
 Mutant 3

Xenopus ---PPLGKEETERVMEILKALFNITFDISRREVDEEEAALYRHAAILRHCLLRQSDGED 277
 Zebrafish SELPPLGRQETERVMEILKILFNVTFDNRRHVDEEEAATYRHLGAILRHCMSSAEGEE 278
 Mouse --PVMLPAQETERAMEILKVLFNITFDSVKREVDEEDAALYRYLGTLLRHCVMEVAAAG-D 265
 Chicken --LPPLRQETERAMEILKVLFNITFDSSKREVDEEDAALYRHGALLRHCLMISADGED 274
 Human ---PPLSPQETDCAIEALKALFNVTVDSWKVKH-ESDSHQFRVMAAVLRHCLLIVGPTED 250
 Drosophila ---DSVGEEQLNIICELLVFMFNVTAP-DKSPNEYEIQSLHLTGVLRELLLRFGDLATE 274
 : :: : * ** :***: * : : : . : . : :
 Mutant 4

Xenopus RTEEFHGHTVNLVNLPLMCLDVLLTPKVEQG----- 309
 Zebrafish RTEEMHSHTVNLGNLPLCLDVLLMPKVQGG----- 310
 Mouse RTEEFHGHTVNLGNLPLKCLDVLLALELHEG----- 297
 Chicken RTEEFHSHTVNLGNLPLKCLDVLLTPKVRPG----- 306
 Human KTEELHSNAVNLLSNVPVSCLDVLI CPLTHEETAQEATLDELPSNKTAEK---ETVLKN 307
 Drosophila KDRAVVTHAINLLTNISGSCLTELTLRCSNAELESKEREQDNEKEKDTTEAGAGAKPREC 334
 : . . :*** ** . * * .
 Mutant 5

Xenopus -SVEYMGVMDTVEVLLQFLHRRLLDR---GHKLEMLTPVLNLLTESSRVHRET RKFLRA 365
 Zebrafish -SIEYMGVMDAVKVLVEFMKRLDR---GNLKEITLLPSLNLLETESARIHRET RKFLRN 366
 Mouse -SLEFMGVMDVISALLAFLEKRLHQ---THRLKECVAPVNLVTECARMHHPARKFLKA 353
 Chicken -SLEYMGVMDAVNILLDFLERRLLDR---GHKLESLETPVLNLLTESARVHRET RKFLKA 362
 Human NTMVYNGMNEAIVLLNFMKRIK---GSSYREGLTPVLSLLTECSRAHFNIRKFLKD 364
 Drosophila CSQCFEKRNVRLDVLLRYLRQSLAQQEAEEASSHELLSPVLTVLVKCARSDRVMRHYLRQ 394
 : : * : : * : : : : : : * : * * . : . : * * : * : :
 Mutant 6

```

Xenopus      KVLPPRLDVKNRPEVGNLTKLVLRLMTHVDTDVKHCAAEFLFVLCKENVSRFVKYTYGYG 425
Zebrafish    KVLPPRLDVKNRPEVGNLTKLVLRLMTHIDTDVKHCAAEFLFVLCKESVSRFIKYTYGYG 426
Mouse        QVLPPLRDVTRRPEVGDLLRNLVLRLMTHLDTDVKRVAAEFLFVLCSESVPRFIKYTYGYG 413
Chicken      KVLPPRLDVKNRPEVGNLTKLVLRLMTHIDTDVKHCAAEFLFVLCKESVSRFVKYTYGYG 422
Human        QVLPPLRDVTNRPEVGSTVTKLVLRLMTHVDLGVKQIAAEFLFVLCKERVDSLLKYTYGYG 424
Drosophila   EILPPLRDVSQRPEVGQELRNHLCRFLTLPAMILRDLSELLFVLCKENVGRMIKYTYGYG 454
::*****  *****  :*: *  *::*  :  :*:*****  *  *  :*****
Mutant 7,    8,    9,    10,    11

Xenopus      NAAGLLAAGLLAGGRGEG--CYSEDDTDTEEYREAKANINPVTGRVEEKQPNPMDGMT 483
Zebrafish    NAAGLLAAGLMRGGRDPG--HYSEDESDTEEYREAKPHINPVTGRVEEQPNPMEGMT 484
Mouse        NAAGLLAAGLMAGGRPEG--QYSEDEDTDTEEYREAKASINPVTGRVEEKPPNMEGMT 471
Chicken      NAAGLLAAGLMAGGREEG--EYSEDEDTDTEEYKEAKPNINPVTGRVEEKLPNMEGMT 480
Human        NAAGLLAAGLLAGGRGDN--WYSEDEDTDTEEYKNAKPNINLITGHLEEPMPNPIDEMT 482
Drosophila   NAAGLFAKIGILDCCRVEGTDYSSDSESDTEEYKQQQQGINPVLGCVEPRSKSHLDDIS 514
*****: *  *::  *  .  *::*:*****::  :  *  *  :  *  *  .  :  :
Mutant 12    Mutant 13

Xenopus      EEQKEYEAMKLVNMFDKLSREQIIQPMGVTS DGR LGPLDEAAQKMLQRQ---ESSDLDSD 540
Zebrafish    DEQKEYEAMKLVNMFDKLSREQVIQPMKIGADGKMTSMEPHELHHLASQQFGESNNSDSD 544
Mouse        EEQKEHEAMKLVNMFDKLSRHVVIQPMGMSPRGHLSLQDAMCETMEGQ---LSSDPDSD 528
Chicken      EEQKEYEAMKLVNMFDKLSREQVIQPMGITPSGNLAPMENAIRDMADER---SSSDSLG 537
Human        EEQKEYEAMKLVNMLDKLSRYCIPIHFLLG F----- 513
Drosophila   EEQKEYEAMQLVNLIEQLRQGGIVKPAIDKDRPQPLEHILQLQEELPQQQLDQKRKT- 573
:****:***:***:***:***:***:***:***:***:***:***:***:***:***:***:***:
Mutant 14

Xenopus      SD-- 542
Zebrafish    SDTN 548
Mouse        PD-- 530
Chicken      LD-- 539
Human        ----
Drosophila   ----

```

Figure S4.3 Sequence alignment of Ric-8 across taxa reveals evolutionarily conserved residues. Residue clusters used for Ric-8 mutational analysis are highlighted in yellow. The number of the mutant cluster is indicated below its residues.

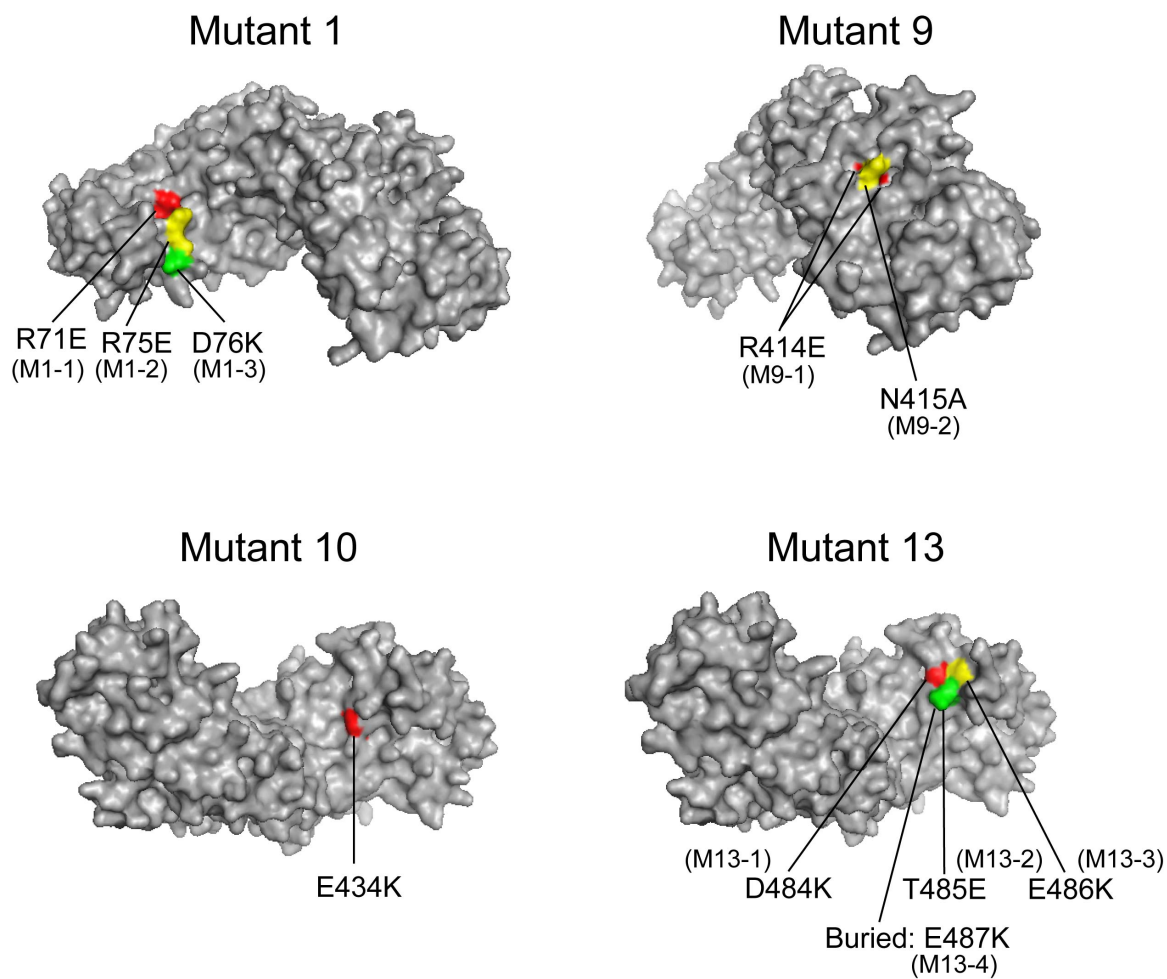


Figure S4.4 Location of individual point mutants comprising mutant clusters that strongly inhibit Cta_{GA} binding are mapped onto a structural model of Ric-8. Note that glutamic acid-487 is buried within the predicted molecule.

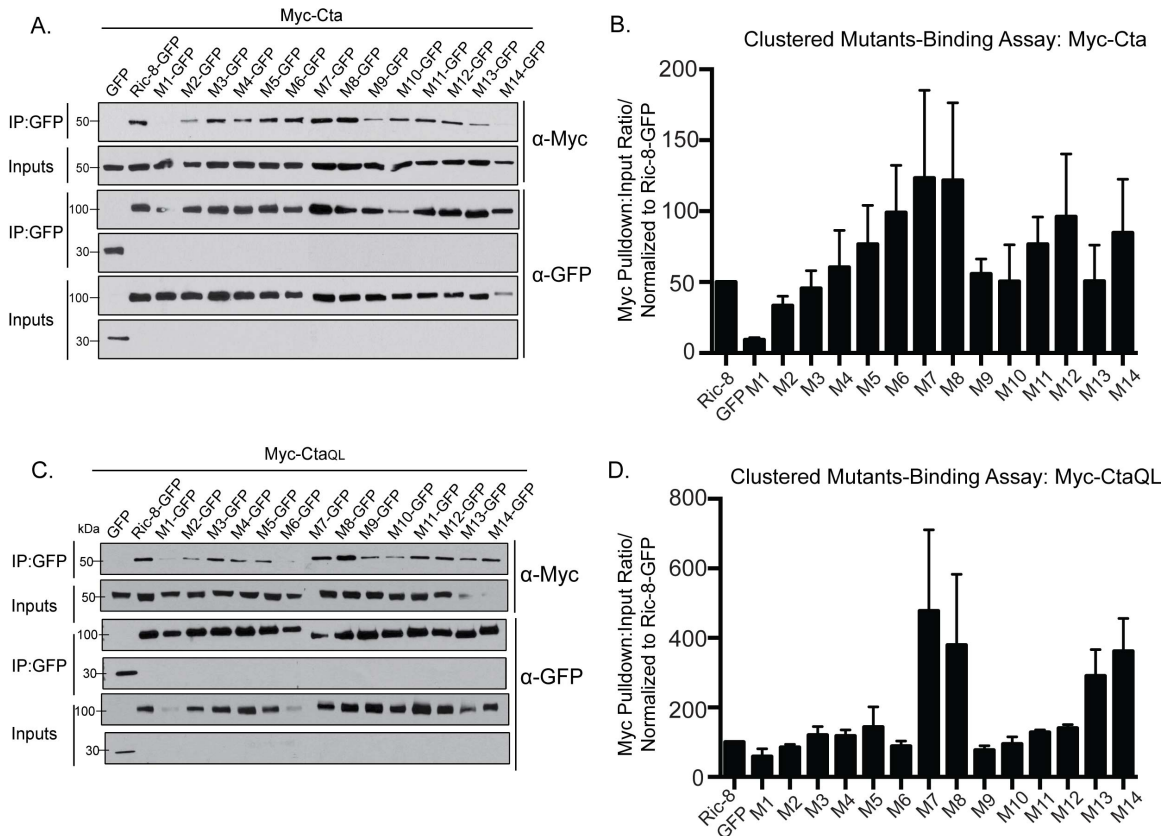


Figure S4.5 Wild-type and constitutively active Cta exhibit differential binding to Ric-8 cluster mutants as compared to inactive Cta. (A-D) Similarly to Myc-CtaGA, both Myc-Cta and Myc-CtaQL are deficient in binding Ric-8-GFP cluster mutant 1. However, unlike Myc-CtaGA, Myc-Cta and Myc-CtaQL are capable of binding mutants 9, 10 and 13. (A) S2 Cells were transfected with GFP, Ric-8-GFP or cluster Ric-8-GFP mutants and wild-type Myc-Cta. IPs were performed with GFP-binding protein and probed with anti-GFP and anti-Myc. (B) Quantification of IPs presented in S5A. The pulldown:input ratios were determined using quantitative densitometry, and normalized to Ric-8-GFP (\pm SEM). (C) S2 Cells were transfected with GFP, Ric-8-GFP or cluster Ric-8-GFP mutants and Myc-CtaQL. IPs were performed with GFP-binding protein and probed with anti-GFP and anti-Myc. (D) Quantification of IPs presented in S5C. The pulldown:input ratios were determined using quantitative densitometry, and normalized to Ric-8-GFP (\pm SEM).

Ric-8 Mutations	Binding Assay (with Cta _{GA})	Cellular Constriction Assay
Mutant 1:	++++	+++
R71E	++	++
R75E	++	+++
D76E	-	-
Mutant 2:	++	-
E134K	N/A	N/A
K137E	N/A	N/A
Mutant 3:	-	-
D180K	N/A	N/A
K182E	N/A	N/A
Mutant 4:	-	-
E231K	N/A	N/A
K234E	N/A	N/A
Mutant 5:	-	-
N285A	N/A	N/A
N289A	N/A	N/A
Mutant 6:	-	+++
R383E	N/A	N/A
R386E	N/A	N/A
R389E	N/A	N/A
Mutant 7:	-	+++
R401E	N/A	N/A
D402K	N/A	N/A
Mutant 8:	-	+++
R406E	N/A	N/A
E408K	N/A	N/A
Mutant 9:	++++	++++
R414E	++++	++++
N415A	+	-
Mutant 10: E434K	+++	+
Mutant 11: E442K	-	-
Mutant 12: R462E	-	-
Mutant 13:	+++	++++
D484K	+++	+++
T485A	++++	+++
E486K	+	+
E487K	+	+
Mutant 14:	+	++
E516K	N/A	N/A
Q517E	N/A	N/A
K518E	N/A	N/A
E519K	N/A	N/A

Table 4.1 Summary of data collected from Ric-8/Cta_{GA} binding and contractile assays.

The individual point mutants comprising each cluster are denoted below the clustered point mutants. Individual point mutants tested experimentally have binding and contractility scores, the remainder were untested (N/A). The effect of each mutant in the pathway is measured in strength from (-) no effect in assay, (+) weak effect (++) moderate effect (+++), to very strong effect (++++). For the binding assay a mutant with a very strong effect (++++) showed little to no binding in pulldown experiments, while mutants with no effect (-) were capable of robustly binding Cta_{GA}. In the contractility assay mutants with no effect (-) rescued contractility to wild-type levels, while mutants with a strong effect (++++) dramatically affected the ability of cells to constrict in response to Fog. Mutants that had both strong affects in binding and contractility assays are high-lighted in yellow.

Chapter V

Discussion and Future Directions

Summary of presented work

The goal of this dissertation was to provide insight into the regulation and dynamics of the Folded gastrulation signaling pathway, specifically addressing the modulation of the $G_{\alpha 12/13}$ family member, Concertina. To achieve these goals we established a novel assay in *Drosophila* tissue culture, utilizing the S2R+ cell line, to recapitulate Fog signaling events, as presented in Chapter II. The S2R+ system was invaluable to the research presented in Chapters III and IV of this dissertation. It allowed us to identify essential novel pathway components, establish epistatic relationships, determine localization patterns of proteins downstream of Fog pathway activation, and much more. The scope of this assay is not limited to these two projects. One could utilize this cell line to investigate several outstanding questions in the field, as well as address the general mechanisms of mechano-chemical signaling and subsequent contractile-based force production. This assay will be an essential tool for future research within our laboratory.

Using the tissue culture system we developed we were able to identify a singular GPCR, Mist, that binds to the Fog ligand, and confers Fog responsiveness to non-responsive cell lines. Additionally, we were able to transfect in modified, truncated versions of the receptor to investigate structural aspects of the protein and determine specific domains important for its function. Localization studies within the embryo revealed that Mist is transcriptionally

localized in a ventral/posterior stripe corresponding to the presumptive mesodermal and endodermal cells comprising the ventral furrow and posterior midgut, respectively. Protein localization of Mist is tightly regulated and expression is highest in cells undergoing contraction within the ventral furrow. Specific localization of Mist protein is first observed very early during ventral furrow formation, when cells start to move their nuclei basally and begin to constrict their apices, and reaches maximum expression when cells are at the peak of apical constriction and have formed a deep furrow. By the time the presumptive mesodermal cells have invaginated as a tube Mist protein is no longer present, indicating that Mist expression is very tightly spatially and temporally regulated during this gastrulation event. Mist RNAi and overexpression experiments in the *Drosophila* embryo showed that Mist is necessary for regulating epithelial folding in several different tissue types, including the Fog signaling pathways active during ventral furrow and posterior midgut (PMG) invagination, as well as in the wing imaginal disc. We found that Mist is transcriptionally regulated in the ventral furrow by the mesodermal zygotic transcription factor Snail. To our knowledge Mist is the first identified transcriptional target of Snail. However, while Snail itself is expressed in the tissue of the ventral furrow it is not expressed in the posterior midgut. This distinct patterning in Snail/Mist expression indicates that Mist expression is regulated by one or more, as yet to be determined, differing transcription factors during gastrulation. Thus, within this project, combinatorial studies using *Drosophila* tissue culture and the *Drosophila* embryo have yielded identification of a GPCR capable of binding Fog and facilitating Fog pathway activation.

The highly conserved cytosolic protein Ric-8 is a modulator of G α dynamics and the work presented in Chapter IV establishes Ric-8 as an essential pathway component in the

Fog signaling pathway. In the absence of Ric-8 S2R+ cells are no longer able to respond to ectopic Fog application, which can be rescued with the expression of Ric-8-GFP. Ric-8 is essential in the Fog signaling pathway as Cta function is dependent on expression of Ric-8. Ric-8 preferentially binds to GTP-free Cta, and data from Ric-8 mis-targeting studies revealed that Ric-8 can localize the constitutively inactive version of Cta, Cta_{GA}, but not the wild-type nor the constitutively active version of Cta, Cta_{QL}. Further, we show that Ric-8 acts to localize inactive Cta downstream of Fog signaling, and is necessary for robust pathway activation. We made a series of fourteen point mutations in the *Drosophila* Ric-8 protein, based on evolutionarily conserved residues found throughout species. We tested all of these mutants for 1) their ability to physically interact with Ric-8, and 2) their ability to drive Fog-induced cellular constriction in the absence of endogenous Ric-8.

Of the fourteen mutants we tested we found four that strongly inhibited binding between Ric-8 and Cta_{GA} and six that inhibited the ability to rescue constriction in Fog-induced contractile experiments. Three mutants were found that strongly inhibited Cta binding as well as Fog induced cellular contraction. Two of these mutants (mutants 9 and 13 found in the C-terminal half of the protein) exhibited nucleotide specific recognition of Cta, while one mutant (mutant 1 found in the N-terminal half of the protein) showed non-nucleotide specific recognition of Cta. We made individual Ric-8 point mutants for each of these three clustered mutants and tested their ability to bind Ric-8 and rescue contraction. From these individual point mutants we found singular residues that negatively affected both binding and contractile assays. To connect the localization, binding, and contractility assay data we mis-targeted the Ric-8 mutants deficient in Cta binding to the mitochondria and examined their ability to co-localize with constitutively inactive Cta. Only one mutant

(mutant 1), of the three that had a strong affect in both pulldown and contractile assays, did not co-localize with ectopically localized Ric-8. We therefore propose that the N-terminal cluster mutant, mutant 1, facilitates non-nucleotide specific binding and localization of Cta; while residues found in mutants 9 and 13, found in the C-terminal half of the protein confer temporal, nucleotide specific binding and localization. Using *Drosophila* tissue culture we have demonstrated a role for Ric-8 in the Fog signaling pathway, further defined the mechanism of Ric-8/G α function, and identified nucleotide specific residues important for Cta function as well as its interaction with Ric-8.

Discussion and Future Directions

Chapter III

While we have made major strides in examining modulators of the G α , Cta, there are several aspects of the pathway that require further investigation. The identification of a GPCR, Mist, that transduces the Fog signal is a major boon to the field. Previously performed screens for zygotic genes essential for gastrulation used deficiencies that covered both the Rok and Mist genes^{1,2}. Rok is an essential Fog pathway component and upon its depletion completely prevents invagination of the ventral furrow³. Our S2R+/Fog signaling assay was ideal for identification of Mist due to the ability to easily, and individually deplete cells of all known GPCRs, and test for abrogation of contraction in response to Fog.

Knowing the identity of Mist allows us to investigate how the receptor is regulated. Our lab is interested in addressing how GPCR signaling is regulated on a temporal level, as well as identifying the molecules necessary for receptor internalization and recycling. S2R+

cells are highly amenable to phase-contrast microscopy and time-lapse imaging. The ability to capture cells responding to Fog in real-time will address questions involving the temporal dynamics of normal Fog signaling pathway activation, and allow for investigation into molecules involved in receptor deactivation.

Although this dissertation has focused on how the Fog signaling pathway is activated, it is equally as important to understand how signaling events are terminated. Research performed by a graduate student in the Rogers Lab, Alyssa Manning, has made some headway into addressing these questions. The canonical view of receptor inactivation is that after a receptor has activated its effector $G\alpha$, a family of proteins, G protein receptor kinases (GRKs) phosphorylate a GPCR, causing recruitment of beta-arrestins and subsequent removal of receptors via clathrin coated pits⁴. There are three beta-arrestins encoded in the *Drosophila* genome, two visual arrestins (Arr 1 and 2) and one non-visual arrestin Kurtz, as well as two GRKs (GPRK 1 and 2). Preliminary experiments have found that depletion of GPRK1 or Kurtz in S2R+ cells increases the percentage of constricting cells in a population downstream of Fog application, unlike GPRK-2, Arr-1 or Arr-2. Co-immunoprecipitation experiments performed in our lab have also found that Kurtz directly interacts with Mist. These results suggest that GPRK-1 and Kurtz are important signaling components involved in the deactivation of the Fog signaling pathway.

Interestingly, research has shown that beta-arrestins are able to bind non-phosphorylated GPCRS, and recently it has been found that beta-arrestins are capable of activating downstream effectors in a $G\alpha$ independent manner⁴. Further, beta-arrestins have been implicated in the activation of the small GTPase Rho, to form stress fibers in mammalian cells⁵. Kurtz could play an, as yet, unidentified role in the Fog signaling

pathway in regulating the cytoskeleton. Overexpression and loss of function studies may yield interesting results in how Kurtz is not only involved in receptor deactivation but also force production or reorganization of the cytoskeleton.

We have shown in Chapter III that Mist is under the transcriptional activation of Snail in the ventral furrow. Snail is not expressed in the PMG⁶; so what then regulates Mist expression in presumptive endodermal cells? The formation of the ventral furrow and PMG utilize many of the same molecules, including Fog, Cta, RhoGEF2 and Rho. However, in the posterior midgut loss of Fog or Cta completely prevents invagination while in the ventral furrow *fog* or *cta* mutants have disorganized constriction of the presumptive mesoderm and delayed ventral furrow formation, but the furrow is still able to internalize⁷. This discrepancy in function highlights that while mechanically similar in function, there are different components necessary for pathway activation in each of these tissues. Overlapping patterns of zygotic transcription factors regulate gene expression prior to gastrulation. Snail expression is dependent on Twist, but Twist is expressed in the PMG while Snail is not. This is due to the anteriorly localized zygotic transcription factor Hucklebein, which acts as a transcriptional repressor for Snail. In *hucklebein* embryos the formation of the PMG is disrupted. Both Hucklebein and another zygotic transcription factor, Tailless, are expressed in the presumptive endodermal cells of the posterior midgut^{8,9}. Therefore, the best two candidates for Mist transcriptional regulation in the PMG are Tailless and Hucklebein. *in situ* analysis of Mist expression in *tailless* and *hucklebein* mutants could reveal if these potential regulators play a role in this process.

Chapter IV

An outstanding question involving Ric-8 in the Fog signaling pathway is whether it acts as a non-canonical GEF to activate Cta. While overexpression of Ric-8 does not drive constriction in S2 or S2R+ cells this may be due to overlapping GPCR and Ric-8 binding sites for $G\alpha$. Therefore to directly investigate GEF activity we wanted to perform GTPase exchange assays. We enlisted the help of Dr. David Siderovski's lab, where this procedure is routinely performed. Dr. Siderovski first suggested to us that Cta may not express solubly due to its "floppy, unstructured N-terminal sequence". He therefore provided us with an ideal sequence for an alternative N-terminally truncated (Δ amino acids 1-100) version of Cta. We made a tagged version of this construct in both *Drosophila* and *E. Coli* expression vectors. While a graduate student in the Siderovski lab, Dustin Bosch, had some success expressing this protein, we found that it did not pull down Ric-8 in immunoprecipitation experiments, and was therefore not useful for our study. The lack of binding in our system may have been due to the necessity of the N-terminal residues of Cta to create a binding interface with Ric-8 or due to misfolding of the protein. We therefore progressed with expression of full-length tagged Ric-8 and Cta in *E. coli* and found that upon protein expression Ric-8 and Cta were both insoluble. Previous methods used for $G\alpha$ expression and purification produced a very low abundance of soluble $G\alpha$. However, it was recently found that co-expression of Ric-8 and $G\alpha$ in insect cells using baculovirus dramatically increased the yield of purified, soluble $G\alpha$ ¹⁰. We therefore created Ric-8 and Cta vectors suitable for baculovirus expression in insect cells. Unfortunately, upon expression of these constructs we found that Cta and Ric-8 proteins were aggregated and insoluble. Thus, we found that even under ideal expression conditions *Drosophila* Ric-8 and Cta proteins were insoluble and were unable to perform GTPase assays and address the nature of Ric-8's GEF activity.

Investigation of Ric-8 in the *Drosophila* embryo has mostly focused on its role in aligning the mitotic spindle during asymmetric cell division of the neuroblast, and SOP cells¹¹⁻¹⁴. The G α involved in these processes is the *Drosophila* G α_{ii} . We have focused our attention on Ric-8's function during gastrulation signaling events within the Fog pathway. While examining Ric-8's role in the Fog signaling pathway in S2R+ cells fostered a more in-depth understanding of Ric-8/Cta dynamics, we would like to show that Ric-8 is functioning analogously in the *Drosophila* embryo. However, antibodies to Cta do not currently exist. We attempted to make two antibodies to two different peptides of Cta and upon testing both crude serum and affinity-purified antibody we found that neither one was specific for recognition of Cta. We also tried using commercially available antibodies that target other G $\alpha_{12/13}$ family members, these did not recognize Cta either. To overcome this issue we have two options 1) attempt to make another antibody, or revisit purification of the previously made antibodies, or 2) make transgenic flies expressing a tagged version of Cta.

Ric-8 is essential for Cta function in the Fog signaling pathway, and the data presented in Chapter IV presents a role for Ric-8 in binding and localizing Ric-8 to its site of function. We hypothesize that localization of Cta to the plasma membrane is dependent on Ric-8. This is supported by the fact that Fog pathway activation is suppressed when Ric-8 ectopically targets Cta to the mitochondria. Our attempts to visualize Cta's cellular localization using high-resolution scanning-disc confocal microscopy failed, as I was unable to differentiate the cytoplasmic and membrane bound pools of Cta and Ric-8 due to the small size of the cells. An alternative method we could use to address this question is to perform cellular fractionation experiments.

The research presented in Chapter IV provided a detailed understanding of the

functional relationship between Cta and Ric-8. However, there are additional inputs and effectors in this pathway that have not been as rigorously investigated. Ric-8 is unable to bind $G\alpha_i$ in *Drosophila* neuroblasts when $G\alpha_i$ is part of the heterotrimeric complex. This is most likely the case for Ric-8 and Cta, as Ric-8 potentiates Cta signaling downstream of Fog pathway activation, but does not activate the pathway when it is overexpressed. To directly test for interaction we can perform pulldowns with an anti-G β 13F antibody and probe for Ric-8. S2R+ cells depleted of G β 13F or G γ 1 do not respond to ectopic Fog application. An intact heterotrimer of G $\alpha\beta\gamma$ is needed for any of the subunits within the complex to localize to the plasma membrane¹⁵, thus it is probable that G $\beta\gamma$ RNAi prevents pathway activation due to mislocalization of Cta. However, G $\beta\gamma$ subunits are capable of activating effectors downstream of GPCR activation¹⁶. It is possible that G $\beta\gamma$ also drives signaling in a parallel or distinct pathway; overexpression studies would be informative to answer this question.

The RGS domain of RhoGEF2 binds to GTP-bound Cta, and catalyzes GTP to GDP hydrolysis. While several $G\alpha$ effectors have RGS domains, many do not¹⁷. How then is the RGS domain of RhoGEF2 regulating Cta behavior? Rapid GTP hydrolysis allows for quick turnover of Cta subunits, and provides a tightly spatially localized pool of inactive Cta. This temporal and spatial regulation of Cta localization by RhoGEF2 is ideal for the function of the Fog signaling pathway. In the *Drosophila* embryo gastrulation movements in the ventral furrow are completed in less than 20 minutes¹⁸. Therefore, a GEF containing an RGS domain would be advantageous to produce a localized pool of rapidly recycled Cta ready for reactivation, potentially by Ric-8.

Two $G\alpha$ binding GDIs in the *Drosophila* genome, Pins and Loco, have been found to function during *Drosophila* neuroblast spindle alignment to bind GDP- $G\alpha$ and GTP- $G\alpha$

respectively, acting as both a GDI and a GAP, respectively¹¹⁻¹⁴. No GDI has been implicated in regulating the behavior of Cta in the Fog signaling pathway. It is possible that Pins and/or Loco proteins are involved in modulating Cta behavior, in an intermediary step between GDP-Cta release from RhoGEF2 and binding of Ric-8. However, due to the rapid turnover of Cta it would be somewhat surprising that a GDI would bind during this intermediary time period, unless perhaps it is needed for Cta stabilization. Using anti-Pins and anti-LoCo antibodies we can test for interactions between Ric-8 and Cta and either of these GDIs using IP experiments.

While most research on Ric-8 has been preformed in *C.elegans*, it is obvious that Ric-8 plays very similar roles throughout different species. It has been shown repeatedly to bind and localize G α subunits, as well as regulate spindle positioning and neurotransmitter release in varying cell types and species investigated thus far¹⁹. All of these functions have been described in *Drosophila*, outside of neurotransmitter release. We therefore feel that *Drosophila* Ric-8 acts similarly during Fog pathway activation, and that the research we have performed is applicable to Ric-8 biology in all systems.

There is little information about the mechanistic regulation of Ric-8. Some of the first data provided have come from our structure/function study investigating the role of evolutionarily conserved amino acids necessary for productive Cta signaling and binding. Several residues have been identified in phosphoproteomic screens that may be potential targets for kinase activity in Ric-8²⁰⁻²². Performing a structure/function assay of Ric-8 based on mutating evolutionarily conserved electrostatic amino-acids, revealed insight into the structural components important for comprising the Cta/Ric8 binding interface as well as the minimal mutations necessary to abrogate Fog-induced pathway activation. Mutant 13,

strongly inhibited both binding and Fog induced cellular constriction. This mutant ectopically localized Cta_{GA} but failed to rescue constriction and had impaired binding to Cta_{GA}, but not wild-type or Cta_{QL}; indicating that this mutant may be important for regulating the activity of nucleotide specific GTP-free Cta, its preferred substrate. The location of the mutated residues within the C-terminal mutant 13 is proximal to an area previously identified as a phosphopeptide from a phospho-proteomics screen²². Additionally, in Ric-8-GFP IPs this cluster mutant appeared to have a slight band shift as compared to the molecular weights of all other cluster mutants. Based on the multiple sequence alignment of the mammalian residues comprising the phosphopeptide from the proteomics screen I will make both phospho-mimetic and non-phospho-mimetic mutants of potential phosphorylation sites. I will then use these in the same experiments used for cluster and point mutant immunoprecipitations and contractile assays to determine if this area regulates Ric-8 phosphorylation, and activation. Mutant 9, also found in the C-terminus and found to strongly inhibit both Cta binding and functionality in the Fog-induced contractile assay did not show any molecular weight shift, or appear nearby any phospho-peptide hits in previous studies²⁰⁻²². Therefore, while residues surrounding mutant 13 may be important for regulating the active/inactive state of Ric-8, mutant 9 may only function in nucleotide specific recognition of Cta.

Conclusions

Using S2 and S2R+ *Drosophila* tissue culture cells we have established a system to study signaling events and cytoskeletal regulation. This system has allowed us to identify a canonical and non-canonical regulator of the Ga, Cta; Mist and Ric-8, respectively. Future

use of this assay, and further investigation of Mist and Ric-8, will allow further advancement of our understanding of the dynamics of the Fog signaling pathway.

References

1. Seher, T. C., Narasimha, M., Vogelsang, E. & Leptin, M. Analysis and reconstitution of the genetic cascade controlling early mesoderm morphogenesis in the *Drosophila* embryo. *Mech. Dev.* **124**, 167–179 (2007).
2. Kolsch, V., Seher, T., Fernandez-Ballester, G. J., Serrano, L. & Leptin, M. Control of *Drosophila* Gastrulation by Apical Localization of Adherens Junctions and RhoGEF2. *Science* **315**, 384–386 (2007).
3. Dawes-Hoang, R. E. *et al.* folded gastrulation, cell shape change and the control of myosin localization. *Development* **132**, 4165–4178 (2005).
4. DeFea, K. A. Beta-arrestins as regulators of signal termination and transduction: how do they determine what to scaffold? *Cell. Signal.* **23**, 621–629 (2011).
5. Barnes, W. G. *et al.* beta-Arrestin 1 and Galphaq/11 coordinately activate RhoA and stress fiber formation following receptor stimulation. *J Biol Chem* **280**, 8041–8050 (2005).
6. Alberga, A., Boulay, J. L., Kempe, E., Dennefeld, C. & Haenlin, M. The snail gene required for mesoderm formation in *Drosophila* is expressed dynamically in derivatives of all three germ layers. *Development* **111**, 983–992 (1991).
7. Harris, T. J. C., Sawyer, J. K. & Peifer, M. How the cytoskeleton helps build the embryonic body plan: models of morphogenesis from *Drosophila*. *Curr. Top. Dev. Biol.* **89**, 55–85 (2009).
8. Leptin, M. Morphogenesis. Control of epithelial cell shape changes. *Curr. Biol.* **4**, 709–712 (1994).
9. Leptin, M. *Drosophila* gastrulation: from pattern formation to morphogenesis. *Annu. Rev. Cell Dev. Biol.* **11**, 189–212 (1995).
10. Chan, P., Gabay, M., Wright, F. A. & Tall, G. G. Ric-8B is a GTP-dependent G protein alpha guanine nucleotide exchange factor. *J Biol Chem* **286**, 19932–19942 (2011).
11. Wang, H. *et al.* Ric-8 controls *Drosophila* neural progenitor asymmetric division by regulating heterotrimeric G proteins. *Nat. Cell Biol.* **7**, 1091–1098 (2005).
12. Hampoelz, B., Hoeller, O., Bowman, S. K., Dunican, D. & Knoblich, J. A. *Drosophila* Ric-8 is essential for plasma-membrane localization of heterotrimeric G proteins. *Nat. Cell Biol.* **7**, 1099–1105 (2005).

13. David, N. B. *et al.* Drosophila Ric-8 regulates Galphai cortical localization to promote Galphai-dependent planar orientation of the mitotic spindle during asymmetric cell division. *Nat. Cell Biol.* **7**, 1083–1090 (2005).
14. Yu, F. *et al.* Locomotion defects, together with Pins, regulates heterotrimeric G-protein signaling during Drosophila neuroblast asymmetric divisions. *Genes Dev.* **19**, 1341–1353 (2005).
15. Takida, S. Heterotrimer Formation, Together with Isoprenylation, Is Required for Plasma Membrane Targeting of Gbeta gamma. *Journal of Biological Chemistry* **278**, 17284–17290 (2003).
16. Siderovski, D. P. & Willard, F. S. The GAPs, GEFs, and GDIs of heterotrimeric G-protein alpha subunits. *Int. J. Biol. Sci.* **1**, 51–66 (2005).
17. Rossman, K. L., Der, C. J. & Sondek, J. GEF means go: turning on RHO GTPases with guanine nucleotide-exchange factors. *Nat. Rev. Mol. Cell Biol.* **6**, 167–180 (2005).
18. Sweeton, D., Parks, S., Costa, M. & Wieschaus, E. Gastrulation in Drosophila: the formation of the ventral furrow and posterior midgut invaginations. *Development* **112**, 775–789 (1991).
19. Hinrichs, M., Torrejón, M., Montecino, M. & Olate, J. Ric-8: different cellular roles for a heterotrimeric G-protein GEF. *J Cell Biochem* (2012).doi:10.1002/jcb.24162
20. Dai, J., Jin, W. H., Sheng, Q. H. & Shieh, C. H. Protein Phosphorylation and Expression Profiling by Yin-Yang Multidimensional Liquid Chromatography (Yin-Yang MDLC) Mass Spectrometry - Journal of Proteome Research (ACS Publications). *Journal of proteome ...* (2007).
21. Yang, F. *et al.* Identification of a novel mitotic phosphorylation motif associated with protein localization to the mitotic apparatus. *J. Cell. Sci.* **120**, 4060–4070 (2007).
22. Mayya, V. *et al.* Quantitative phosphoproteomic analysis of T cell receptor signaling reveals system-wide modulation of protein-protein interactions. *Sci Signal* **2**, ra46 (2009).